PROPERTIES OF FORELIMB MUSCLE REPRESENTATIONS IN THE PRIMATE CEREBRAL CORTEX

By

Marie-Hélène Boudrias
B.S. (Physical Therapy), University of Montreal, 1997

Ph.D., University of Kansas, 2007
Submitted to the Program of Neuroscience
Faculty of the Graduate School of the University of Kansas
In partial fulfillment of the requirements for the degree of
Doctor of Philosophy

_____
Paul D. Cheney, Ph.D., Chairman

Committee members

_____
Thomas J. Imig, Ph.D.

_____
Randolph J. Nudo, Ph.D.

_____
Steven M. Barlow, Ph.D.

_____
Stephen C. Fowler, Ph.D.

Date defended: June 19th, 2007

The Dissertation Committee for Marie-Hélène Boudrias certifies that this is the approved version of the following dissertation:

PROPERTIES OF FORELIMB MUSCLE REPRESENTATIONS IN THE PRIMATE CEREBRAL CORTEX

Paul D. Cheney, Ph.D., Chairman

Committee members

Thomas J. Imig, Ph.D.

Randolph J. Nudo, Ph.D.

Steven M. Barlow, Ph.D.

Stephen C. Fowler, Ph.D.

Date approved: June 19th, 2007

*Adviser (if applicable, co-adviser) original signature(s) are required. Other committee members' signatures are optional **only** on Acceptance Page.

ABSTRACT

Labeling corticospinal neurons with retrograde tracers injected in the cervical segments of the spinal cord of macaque rhesus, has revealed multiple corticospinal output zones in both the lateral and the medial aspect of the hemisphere of the frontal lobe. Seven distinct forelimb motor representations have been identified including the primary motor cortex (M1) and six secondary motor areas. These include, the supplementary motor area (SMA), the dorsal, ventral and rostral cingulate motor areas (CMAd, CMAv, and CMAr), and the dorsal and the ventral premotor areas (PMd and PMv). Extensive data on the properties of M1 have already been published, and the direct linkage of its corticospinal neurons on motoneurons has been demonstrated. While the location and distribution of the corticospinal neurons from the secondary motor areas have been described in great detail, their specific roles in limb movement and the extent of their linkage on motoneurons remain much less understood. The broad objective of this study was to characterize the motor output properties of SMA, CMAd, PMd and PMv and to compare their roles in the control of forelimb movements to those from M1. Stimulus-triggered-averaging (StTA) of electromyography (EMG) activity was used to map and characterize their output properties in terms of sign (excitatory or inhibitory), latency, strength, and distribution of effects. Our results demonstrate that effects from SMA, CMAd, PMd and PMV have

longer latencies and are markedly weaker than those from M1, suggesting additional synapses in the anatomical pathway for their actions on motoneurons. Moreover, facilitation effects from SMA, CMAd, PMd and PMv did not follow the pattern of increased magnitudes of effects from proximal to distal muscles characteristic of M1. In terms of their organization, no clear segregated representations of proximal versus distal muscles were found in the secondary motor areas compared to M1, in which the existence of segregated proximal and distal muscle representations was demonstrated. Our results raise doubts about the role of the corticospinal neurons from SMA, CMAd, PMd and PMv in the direct control of forelimb motoneurons and suggest that their effects on muscular activity are most likely achieved indirectly through projections to M1 and/or to the intermediate zone of the spinal cord.

This body of work is dedicated to my parents,

Monique Hudon and Gervais Boudrias.

ACKNOWLEDGEMENTS

Completion of this dissertation would have not been possible without the support of numerous people. First, I would like to thank my mentor Dr. Paul D. Cheney for his full support and guidance during my doctoral work. His analytical view and broad knowledge in neurophysiology really inspired me to pursue a career in neuroscience and become an accomplished scientist.

I would also like to thank current and past members of the laboratory, especially Dr. Abderraouf Belhaj-Saïf who showed me the basis of laboratory work during the first months of my research. I would like to acknowledge Ted Gleason, Jim Rengel, and Ian Edwards for their crucial participation in the development, implantation and maintenance of experimental devices. Their technical supports have greatly influenced the success of the experiments reported in this dissertation.

Special thanks to Dr. Nathan Culley and Richard Smith from the Lab animal resources, who were always present to insure to wellbeing of the animals, to Dr. Kovac from the anesthesiology department for his assistance during surgeries, and to the staff of the Hoglund Brain Imaging Center for their technical assistance on the acquisition and processing of imaging data.

Many thanks to the staff from the physiology department and the MRRC core laboratory for their great support and constant assistance in proving my existence for enrollment and administrative purposes. Many thanks to my friends from the imaging center, Don Warn, Eric Grimes, Phil Shafer for their patience and assistance during the elaboration of my posters and illustrations for publication.

Special thanks to Dr. Shawn Frost for his contribution in the analysis of the histology data and to Rebecca L. McPherson for her contribution in reviewing the dissertation, in statistical and data analyses. Many thanks to all my KUMC/KU friends that made these past years enjoyable, especially to Ines Eisner-Janowicz who has been of tremendous help is the most difficult moments of my work.

I would also like to thank my student advisory committee who took valuable time to advice, direct and give me helpful feedback in my progress.

Finally, I thank my family and friends from Québec. Despite the distance, they always offered me constant support and encouragement throughout the years of my graduate school.

TABLE OF CONTENTS

LIST OF FIGURES

LIST OF TABLES

LIST OF ABBREVIATIONS

CMAd……	Cingulate Motor Area Dorsal
CMAr ……	Cingulate Motor Area Rostral
CMAv……	Cingulate Motor Area Ventral
EMG ……	Electromyography
ICMS ……	Intracortical Microstimulation
M1 ……	Primary Motor Cortex
PMd ……	Premotor Dorsal Area
PMv ……	Premotor Ventral Area
PStE ……	Poststimulus Effect
PStF ……	Poststimulus Facilitation
PStS ……	Poststimulus Suppression
SD……	Standard Deviation
SMA ……	Supplementary Motor Area
SpTA ……	Spike-Triggered Averaging
StTA ……	Stimulus-Triggered Averaging

CHAPTER 1

INTRODUCTION

The movements we initiate on a daily basis are the products of commands which come from the neurons located in the motor areas of the brain. The motor areas play a precise role in the organization of movement and can be studied based on their electrical activity. An important player in movement production is the corticospinal neuron which conveys motor information from the cerebral cortex to the spinal cord, where motoneurons for the limbs are located (Figure 1). Motoneurons are located in the ventral horn of the spinal cord and are directly involved in the control of muscular activity. The output properties of a corticospinal neuron and its role in movement production are critically related to the type of synaptic linkage that exists. The linkage can either be direct, referred as monosynaptic, or indirect through the presence of additional synapses in the pathway to a pool of interneurons in the spinal cord (Figure 1). Consequently, the shortest pathway by which a corticospinal neuron can participate in muscle activity is by a monosynaptic linkage with a motoneuron. The more direct the linkage between a corticospinal neuron and a motoneuron, the greater the magnitude of the effect produced on muscle activity and the shorter the time (latency) taken for the motor command to reach the muscle (Park *et al*., 2004). Because the appearance of monosynaptic connections with motoneurons and the ability to perform skillful hand movements are thought to have commonly evolved in parallel through the evolutionary process, these corticomotoneuronal (CM) connections are believed to play an important role

in the generation of independent finger movements (Kuypers, 1981; Porter and Lemon, 1993).

Seven forelimb motor representations have been identified in the frontal lobe of the macaque monkeys, each one with its own set of corticospinal neurons. On the lateral aspect of the hemisphere these include, the primary motor cortex (M1) and the dorsal and ventral premotor areas (PMd and PMv). On the mesial aspect of the hemisphere these include the supplementary motor area (SMA) and the dorsal, ventral and rostral cingulate motor areas (CMAd, CMAv, and CMAr) (Dum and Strick, 1991; He *et al*., 1993; 1995). Table 1 summarizes the properties of these cortical motor areas based on existing anatomical and physiological studies. The results of these studies are summarized in the following paragraphs.

The primary motor cortex (M1) was the first motor area to be discovered and has been studied for more than a century (Ferrier, 1875; Fritsch and Hitzig, 1870). Its role in motor execution, particularly in hand movements has been confirmed in a variety of studies. The other six motor areas, referred as secondary motor areas, have been more recently characterized, and their roles in the production of movement are consequently less well understood. Higher-order roles in motor control have generally been attributed to the secondary motor areas and were found to be highly related to the specific inputs each receives from other areas of the

brain. These inputs originate from many areas and carry a variety of information including visual, cutaneous and proprioceptive modalities (Figure 1). For example, PMv receives a substantial visual input via the parietal cortex and is thought to play an important role in the visually guided grasping (Luppino and Rizzolatti, 2000). SMA, receives large inputs from the basal ganglia, as well as from the contralateral SMA, and is thought to play a major role in self-initiated movements and bimanual coordination (Schell and Strick, 1984; Wiesendanger and Wiesendanger, 1985; Liu *et al*., 2002).

The belief that the secondary motor areas are mainly involved in higher-order of motor functions has been challenged by recent anatomical studies (Dum and Strick, 1991; Galea and Darian-Smith, 1994). Injections of retrograde tracers in the spinal cord, to define the origin of corticospinal neurons, have demonstrated that the neurons originating from the secondary motor areas share many of the same properties as the corticospinal neurons from M1 (Table 1). In fact, more than half of the total number of corticospinal neurons of the frontal lobe originates from the secondary motor areas. Of these neurons, 17% originate from PMd, 15% from SMA, 9% from CMAd, and 2% form PMv. Except for PMv and CMAr, the densities of the corticospinal neurons contained in each area are similar to the corticospinal neuron density in M1. Most significantly, these output zones contain large numbers of corticospinal neurons that project near motoneuronal pools suggesting a potential direct control of muscle activity paralleling that of M1. These results

suggest that corticospinal neurons from secondary motor areas make a greater contribution to motoneuronal excitation and movement execution than previously thought.

Monosynaptic linkages from M1 corticospinal neurons to motoneurons are known to exist and their output effects (including latencies and magnitudes of effects) on muscle activity have been quantified (Cheney and Fetz, 1980; Porter and Lemon, 1993; Maier *et al*., 2002; Rathelot and Strick, 2006). While the location and the distribution of the corticospinal neurons originating from the secondary motor areas have been described in great detail, their specific contributions to limb movement remain mostly unknown. Only a limited number of studies have investigated the linkage between secondary cortical motor areas and spinal motoneurons (Kuypers and Brinkman, 1970; Dum and Strick, 1996; Rouiller *et al*., 1996; Cerri *et al*., 2003; Shimazu *et al*., 2004). Therefore, the broad objective of this study was to assess the motor output capabilities of the secondary motor areas and to further investigate their contribution to movement production.

How corticospinal neurons are involved in producing limb movements is a question of great importance for a better understanding of mechanisms of recovery of motor function following injury. The results of the following studies could have important relevance and potential implications to the field of physical rehabilitation. For example, following a lesion of the spinal cord, a

partial or total disconnection between the brain and the motoneurons (thus with muscles) occurs. Similarly, damage to the cerebral cortex produces a loss of descending output from the brain to spinal motoneurons. An axonal disconnection or damage to primary motor cortex can induce a diversity of movement deficits, from muscular weakness to total paralysis. It has recently been demonstrated that functional recovery following a stroke correlates with the integrity of the corticospinal tract (Ward *et al*., 2006). Fully understanding the motor output role of corticospinal neurons originating from a specific motor area in the production of forelimb movements will consequently, contribute to a better understanding of that motor area in recovery following a stroke. The elaboration of exercise programs targeting specific joints or involving types of movement related to the spared motor areas could potentially help maximize the recovery of brain motor function. Therefore, for a better understanding of the contributions of corticospinal neurons originating from different secondary cortical motor areas in the production of forelimb movements, the primary goal of this study was to characterize the organization and output properties of these neurons in comparison to those in primary motor cortex (M1).

Table 1. Properties of the cortical motor areas

Cortical area	MI (F1)	SMA (F3, 6aβ)	CMAd (6c, 24d)	CMAv (23c, 24d)	CMAr (24c)	PMd (F2, 6aα)	PMv (F4–F5)
Total number of CS neurons:							
forelimb distal (LC[a])	15,918	5229	4629	2564	2186	6081	339
forelimb prox. (UC[a])	10,398	4970	1852	2310	2484	7214	2304
hindlimb (L6-S1)	23,870	5796	3740	2550	388	5164	6
% high density bins (cervical, upper 10%)	53	19	15	7	<1	5	<1
Cortical area occupied by forelimb CS neurons (mm^2)	84	44	22	14	24	45	18
% of total frontal lobe CS projection (frontal lobe = 70% of total)	46	15	9	7	4	17	2
Density of CS neurons (mean, cells/mm^2)	288	275	279	290	176	254	167
Electrical excitability (estimated average ICMS threshold, μA)	10	20	30	30	35	60	40
Functional activity:							
move execution	+++++	+++	–	++++	++	+++	+++
set related	++	+++	–	++	++++	++++	++
signal related	+	++	–	–	–	+	+++
Special functional role	move execution	♦ self-initiated ♦ selection ♦ sequence ♦ bilat. move	movement sequence from memory	–	reward based motor selection	visually guided reaching	visual grasp (F5)
Directional tuning	Y	Y	–	–	–	Y	–

Numbers of corticospinal neurons based on data from Dum and Strick (1991), He *et al*. (1993) and He *et al*. (1995). Reproduced from Cheney *et al*. (2000).

Figure 1. Pathways by which a corticospinal neuron can act a forelimb muscle. A) Direct pathway: a corticospinal neuron synapses directly on a motoneuron (monosynaptical linkage) that in tern synapses on a forelimb muscle. B) Indirect pathway: a corticospinal neuron synapses first on pool of interneurons which synapse on a motoneuron that in turn synapses on a forelimb muscle.

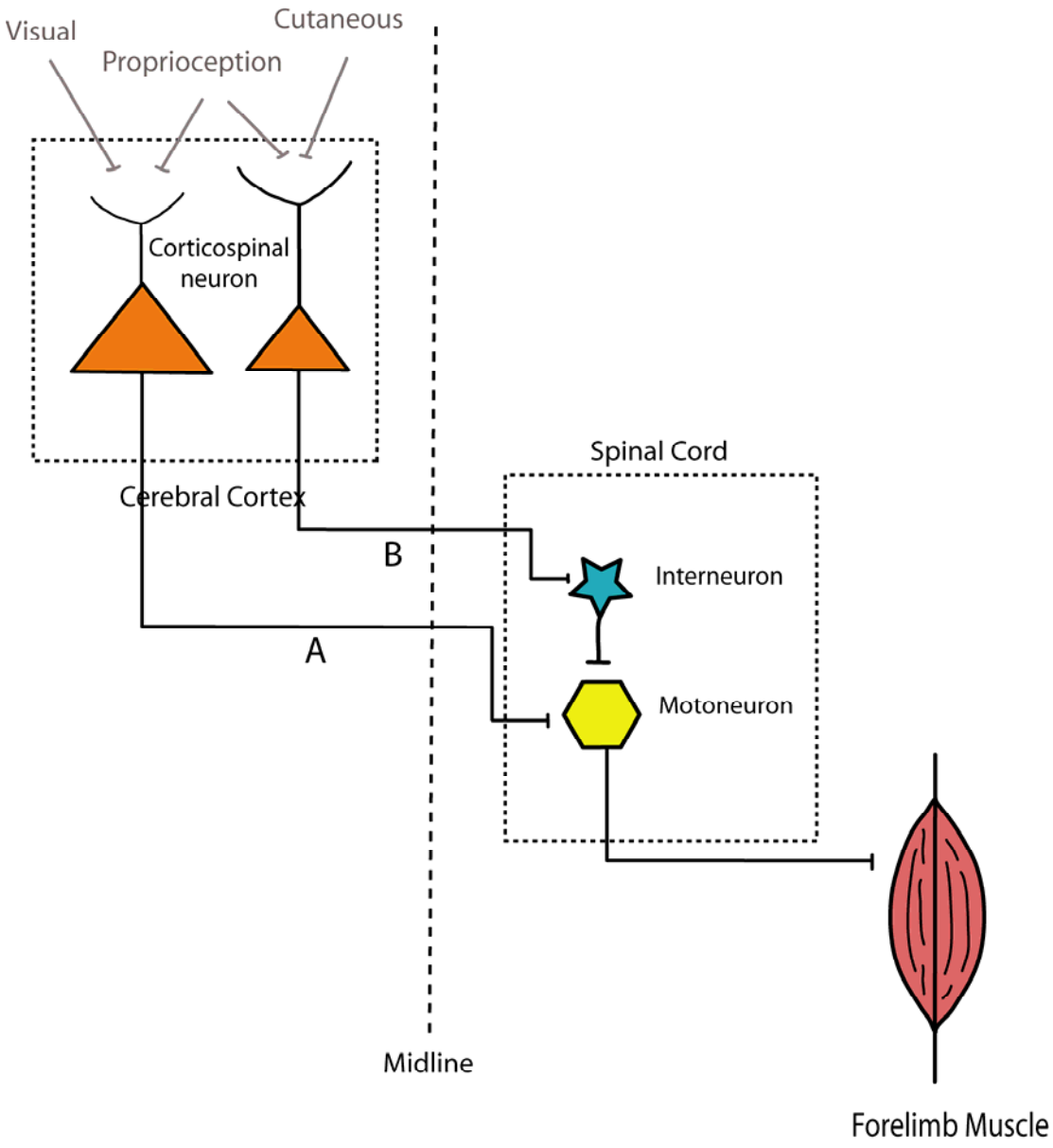
Visual
Cutaneous
Proprioception
Corticospinal neuron
Cerebral Cortex
Spinal Cord
B
Interneuron
A
Motoneuron
Midline
Forelimb Muscle

REFERENCES

Cerri G, Shimazu H, Maier MA, Lemon RN (2003) Facilitation from ventral premotor cortex of primary motor cortex outputs to macaque hand muscles. J Neurophysiol 90:832-842.

Cheney PD, Fetz EE (1980) Functional classes of primate corticomotoneuronal cells and their relation to active force. J Neurophysiol 44:773-791.

Cheney PD, Hill-Karrer J, Belhaj-Saif A, McKiernan BJ, Park MC, Marcario JK (2000) Cortical motor areas and their properties: implications for neuroprosthetics. Prog Brain Res 128:135-160.

Dum RP, Strick PL (1991) The origin of corticospinal projections from the premotor areas in the frontal lobe. J Neurosci 11:667-689.

Dum RP, Strick PL (1996) Spinal cord terminations of the medial wall motor areas in macaque monkeys. J Neurosci 16:6513-6525.

Ferrier D (1875) Experiments in the brain of monkeys. Proc R Soc Lon B Biol Sci 23:409-430.

Fritsch GT, Hitzig E (1870) Über die elektrische Erregbarkeit des Grosshirns. Arch Anat Physiol Med Wiss 300-332. Translation in G Von Bonin.

1960. Some papers on the cerebral cortex. Springfield (IL): Charles C Thomas:73-96.

Galea MP, Darian-Smith I (1994) Multiple corticospinal neuron populations in the macaque monkey are specified by their unique cortical origins, spinal terminations, and connections. Cereb Cortex 4:166-194.

He SQ, Dum RP, Strick PL (1993) Topographic organization of corticospinal projections from the frontal lobe: motor areas on the lateral surface of the hemisphere. J Neurosci 13:952-980.

He SQ, Dum RP, Strick PL (1995) Topographic organization of corticospinal projections from the frontal lobe: motor areas on the medial surface of the hemisphere. J Neurosci 15:3284-3306.

Kuypers HG, Brinkman J (1970) Precentral projections to different parts of the spinal intermediate zone in the rhesus monkey. Brain Res 24:29-48.

Kuypers HGJM (1981) Anatomy of the descending pathways. In: In: Handbook of physiology- the nervous system II (Brookhart J, Mountcastle V, eds), pp 597-666: Bethesda, MD: American Physiology Society.

Liu J, Morel A, Wannier T, Rouiller EM (2002) Origins of callosal projections to the supplementary motor area (SMA): a direct comparison between

pre-SMA and SMA-proper in macaque monkeys. J Comp Neurol 443:71-85.

Luppino G, Rizzolatti G (2000) The Organization of the Frontal Motor Cortex. News Physiol Sci 15:219-224.

Maier MA, Armand J, Kirkwood PA, Yang HW, Davis JN, Lemon RN (2002) Differences in the corticospinal projection from primary motor cortex and supplementary motor area to macaque upper limb motoneurons: an anatomical and electrophysiological study. Cereb Cortex 12:281-296.

Park MC, Belhaj-Saif A, Cheney PD (2004) Properties of primary motor cortex output to forelimb muscles in rhesus macaques. J Neurophysiol 92:2968-2984.

Porter R, Lemon RN (1993) Corticospinal function and voluntary movement. Oxford: Clarendon Press.

Rathelot JA, Strick PL (2006) Muscle representation in the macaque motor cortex: an anatomical perspective. Proc Natl Acad Sci U S A 103:8257-8262.

Rouiller EM, Moret V, Tanne J, Boussaoud D (1996) Evidence for direct connections between the hand region of the supplementary motor area

and cervical motoneurons in the macaque monkey. Eur J Neurosci 8:1055-1059.

Schell GR, Strick PL (1984) The origin of thalamic inputs to the arcuate premotor and supplementary motor areas. J Neurosci 4:539-560.

Shimazu H, Maier MA, Cerri G, Kirkwood PA, Lemon RN (2004) Macaque ventral premotor cortex exerts powerful facilitation of motor cortex outputs to upper limb motoneurons. J Neurosci 24:1200-1211.

Ward NS, Newton JM, Swayne OB, Lee L, Thompson AJ, Greenwood RJ, Rothwell JC, Frackowiak RS (2006) Motor system activation after subcortical stroke depends on corticospinal system integrity. Brain 129:809-819.

Wiesendanger R, Wiesendanger M (1985) The thalamic connections with medial area 6 (supplementary motor cortex) in the monkey (macaca fascicularis). Exp Brain Res 59:91-104.

CHAPTER 2

CONTRASTING PROPERTIES OF MOTOR OUTPUT FROM THE SUPPLEMENTARY MOTOR AREAS AND PRIMARY MOTOR CORTEX OF RHESUS MACAQUES

The studies described in the chapter have been published in *Cerebral Cortex*, 2006, volume 16, pages 632-638.

ABSTRACT

The goal of this study was to assess the motor output capabilities of the forelimb representation of the supplementary motor area (SMA) in terms of the sign, latency, and strength of effects on EMG activity. Stimulus triggered averages of EMG activity from 24 muscles of the forelimb were computed in SMA during a reach-to-grasp task. Poststimulus facilitation (PStF) from SMA had two distinct peaks (15.2 ms and 55.2 ms) and one poststimulus suppression (PStS) peak (32.4 ms). The short onset latency PStF and PStS of SMA were 5.5 ms and 16.8 ms longer than those of M1. The average magnitudes (peak increase or decrease above EMG baseline) of the short and long latency PStF and PStS from SMA at 60 μA were 13.8%, 11.3% and -11.9% respectively. In comparison, M1 PStF and PStS magnitudes at 15 μA were 50.2% and -23.8%. Extrapolating M1 PStF magnitude to 60 μA yields a mean effect that is nearly 15 times greater than the mean PStF from SMA. Moreover, unlike M1, the facilitation of distal muscles from SMA was not significantly greater than the facilitation of proximal muscles. We conclude that the output from SMA to motoneurons is markedly weaker compared to M1 raising doubts about the role of SMA corticospinal neurons in the direct control of muscle activity.

INTRODUCTION

The supplementary motor area (SMA) is located on the mesial wall of the hemisphere and is one of several secondary motor areas located in the primate frontal lobe that sends projections to the spinal cord (Dum and Strick, 1991; He *et al.*, 1995). SMA's overall termination pattern in the cervical enlargement of the spinal cord qualitatively resembles that from the primary motor cortex (M1) suggesting the generation of motor output from SMA via direct pathways independent of M1 (Dum and Strick, 1996; Rouiller *et al.*, 1996). Both M1 and SMA have terminations in the ventral horn where it has been shown that M1 neurons have powerful monosynaptic connections with motoneurons. Corticomotoneuronal synaptic connections provide a direct input to motoneurons, which is thought to be important for the generation of independent finger movements (Kuypers, 1981; Porter and Lemon, 1993). While the monosynaptic linkages from M1 to spinal motoneurons of the hand motor nuclei in primates are common and have been demonstrated in great detail, such a direct linkage from SMA has only recently been identified. Using intracellular recording from motoneurons in macaque monkeys, Maier *et al*. (2002) provided evidence that some SMA efferents make monosynaptic connections with motoneurons, although EPSPs (excitatory postsynaptic potentials) recorded from SMA stimulation were only half as common as

those from M1 stimulation. This suggests that SMA can act independently of M1 to influence the excitability of motorneurons in the control of movement.

Functionally, a variety of single unit recordings and brain imaging studies have demonstrated not only coactivation of SMA with M1 during various types of movement tasks, but also some unique functional properties of SMA and M1 (see Cheney *et al.,* 2004, for review). Despite the potential importance of SMA in the production of forelimb movement through its corticospinal projections, few functional output studies of SMA exist. The purpose of this study was to assess the motor output capabilities of SMA, relative to M1, in terms of the sign (excitatory or inhibitory), latency, and strength of poststimulus effects on EMG activity of 24 forelimb muscles including shoulder, elbow, wrist, digit and intrinsic hand muscles.

MATERIALS AND METHODS

Behavioral task and Surgical procedures

Data were collected from two male rhesus monkeys (*Macaca mulatta*, ~9 kg, 6 years of age) that were trained to perform a reach-to-grasp task as described previously (Belhaj-Saïf *et al.*, 1998; McKiernan *et al.*, 1998). On completion of training, each monkey was implanted over the forelimb area of SMA with a magnetic resonance imaging (MRI) compatible cortical chamber allowing the exploration of a 30 mm diameter area of the left hemisphere. The chambers were stereotaxically implanted at anterior 13.4 mm (Monkey B) and at anterior 12.9 mm (Monkey Y) with an angle of 15-degrees to the midsagittal plane. Chamber implantation and electrode placements were guided by structural MRIs obtained from a 3 Tesla Siemens Allegra system. Images were obtained with the monkey's head mounted in an MRI compatible stereotaxic apparatus so the orientation and location of the penetrations could be precisely estimated (Figure 1). The dura was opened during chamber implantation to confirm the location of the central sulcus. The location of the central sulcus also aided in matching the electrode penetrations to the MR images.

EMG activity was recorded from 24 muscles of the forelimb using a modular subcutaneous implant method in which a pair of multi-stranded stainless steel wires (Cooner Wire, Chatsworth, California) was implanted in

each muscle and the wires were led subcutaneously to connectors on the forearm. The monkeys wore jackets to protect the implants. These procedures are described in detail in a previous paper (Park *et al.*, 2000). EMGs were recorded from five shoulder muscles: pectoralis major (PEC), anterior deltoid (ADE), posterior deltoid (PDE), teres major (TMAJ) and latissimus dorsi (LAT); seven elbow muscles: biceps short head (BIS), biceps long head (BIL), brachialis (BRA), brachioradialis (BR), triceps long head (TLON), triceps lateral head (TLAT) and dorso-epitrochlearis (DE); five wrist muscles: extensor carpi radialis (ECR), extensor carpi ulnaris (ECU), flexor carpi radialis (FCR), flexor carpi ulnaris (FCU) and palmaris longus (PL); five digit muscles: extensor digitorum communis (EDC), extensor digitorum 2 and 3 (ED 2,3), extensor digitorum 4 and 5 (ED 4,5), flexor digitorum superficialis (FDS) and flexor digitorum profundus (FDP); and two intrinsic hand muscles: abductor pollicis brevis (APB) and first dorsal interosseus (FDI). All surgeries were performed under deep general anesthesia and aseptic conditions. Postoperatively, monkeys were given an analgesic (Buprenorphine 0.5 mg/kg every 12 hours for 3-4 days) and antibiotics (Penicillin G, Benzathaine/Procaine combination, 40,000 IU/kg every 3 days). All procedures were in accordance with the Association for Assessment and Accreditation of Laboratory Animal Care (AAALAC) and the Guide for the Care and Use of Laboratory Animals, published by the U.S. Department of Health and Human Services and the National Institutes of Health.

Data recording

Electrode penetrations were made broadly throughout the extent of the forelimb representation of SMA in each animal (He *et al.*, 1995; Luppino *et al.*, 1991). The chamber coordinates of forelimb SMA were estimated from MRI scans. For cortical recording and stimulation, we used glass and mylar insulated platinum-iridium electrodes with typical impedances between 0.7-2 MΩ (Frederick Haer & Co., Bowdoinham, Maine). The electrode was advanced with a manual hydraulic microdrive and stimulation was performed in all layers of the grey matter of SMA at 0.5 mm intervals, starting 0.5 mm below the first cortical electrical activity encountered. Sites below 6 mm were excluded of this analysis to avoid contamination from the dorsal cingulate motor area (CMAd) (Figure 1). Cortical electrical activity and EMG activity were simultaneously monitored along with task related signals. Stimulus triggered averages (60 μA at 7-15 Hz) of EMG activity were computed for 24 muscles of the forelimb from stimuli applied throughout all phases of the reach-to grasp task. The selection of 60 μA for SMA stimulation was based on an initial stimulus intensity study in which poststimulus effects at intensities from 15 to 60 μA were compared. Few effects were observed at 30 μA and below and effects remained largely weak at 40 μA. All StTAs were based on at least 2000 trigger events. Individual stimuli were symmetrical biphasic pulses (0.2 ms negative followed by 0.2 ms positive). EMGs were filtered from 30 Hz to 1 KHz, digitized at 4 kHz and full-wave rectified. Averages were

compiled using an epoch of 60 ms length, extending from 20 ms before the trigger to 40 ms after the trigger. Epoch duration was lengthened to 120 ms (30 ms pre-trigger to 90 ms post-trigger) when it was observed that a second, long latency facilitation peak was often present. The 60 ms epoch was used for 19 electrodes tracks in monkey Y. The remaining tracks in monkey Y and all the tracks in monkey B were performed using the 120 ms epoch.

Segments of EMG activity associated with each stimulus were evaluated and accepted for averaging only when the average of all EMG data points over the entire epoch was equal to or greater than 5% of full-scale input level (± 5 volt) on our data acquisition system (Power 1401, Cambridge Electronic Design ltd., Cambridge, UK). This prevented averaging segments where EMG activity was minimal or absent (McKiernan et al., 1998). EMG recordings were tested for cross-talk by computing EMG-triggered averages. Muscles showing cross-talk of 15% or greater were eliminated from the data base (Cheney and Fetz, 1980). Broad weak synchrony effects surrounding the trigger were observed but fell below our threshold for rejection.

When no poststimulus effects were detected at 60 μA, repetitive intracortical microstimulation (R-ICMS) was applied to determine if a motor output representation could be identified for that site. Using this method, the representation of muscles not implanted with electrodes (face, trunk, and hindlimb) could also be identified. R-ICMS consisted of a train of 10 symmetrical biphasic stimulus pulses (0.2 ms negative followed by 0.2 ms

positive) at a frequency of 330 Hz (Asanuma and Rosen, 1972) and an intensity of 30-100 μA. Evoked movements and muscle contractions detected visually and/or with palpation were noted. Mouth and hindlimb movements were evoked with ICMS in the most anterior and posterior track penetrations respectively. Tracks located more than 6 mm lateral to the midline did not show poststimulus effects. These results are in agreement with the SMA' forelimb boundaries reported by others (He *et al.*, 1995; Luppino *et al.*, 1991).

Comparison data for M1 output effects was obtained from two monkeys using the data set collected by Park *et al.* (2004). The task conditions for both the SMA and M1 data were the same. Data published by Park *et al.* (2004) was restricted to layer V sites in M1. For comparison purposes, in this paper we have expanded the analysis of M1 data to include sites in all layers of the grey matter. The M1 data were collected using an epoch of 60 ms (20 ms pre-trigger to 40 ms after the trigger), a minimum of 500 trigger events, and a stimulus intensity of 15 μA on animals of comparable size.

Data analysis

At each stimulation site, averages were obtained from all 24 muscles. Poststimulus facilitation (PStF) and suppression (PStS) effects were computer-measured as described in detail by Mewes and Cheney (1991). Non-stationary, ramping baseline activity was routinely subtracted from StTAs using custom analysis software. Mean baseline activity and standard

deviation (SD) were measured from EMG activity in the pre-trigger period (20-30 ms). StTAs were considered to have a significant PStF if the envelope of the StTA crossed a level equivalent to 2 SD of the mean of the baseline EMG for a period of time equal to or greater than 1.25 ms (5 points). Peaks that did not exceed 2 SD for at least 1.25 ms were considered insignificant. The magnitude of PStF and PStS was expressed as the percent increase or decrease in EMG activity above (facilitation) or below (suppression) baseline (Cheney and Fetz, 1985; Cheney *et al.*, 1991; Kasser and Cheney, 1985).

RESULTS

Poststimulus effects were obtained from all layers of the grey matter in the forelimb representation of the left SMA and M1 of four monkeys. Data from SMA were collected from 43 electrode tracks, 21 tracks in monkey B and 22 tracks in monkey Y (Table 1). StTA (60 μA) of rectified EMG activity from 24 forelimb muscles was performed at 397 sites, 170 sites in monkey B and 227 sites in monkey Y, yielding a total of 9,496 individual StTA records from which 897 individual poststimulus effects were obtained. Poststimulus effects included 450 (54%) PStF and 385 (46%) PStS. M1 StTA data used for comparison to SMA were collected from two additional monkeys that were part of a study that has been previously published (Park *et al.*, 2004). These data were based on 3,226 individual poststimulus effects including 1,971 (61%) PStF effects and 1,255 (39%) PStS effects obtained from two monkeys.

Figure 2 shows an example of poststimulus effects from one SMA site. This site was located in the mesial wall of SMA and is represented by an open circle on the brain surface map of monkey B (Figure 1). At this site, significant PStF effects were observed in several proximal and distal muscles as indicated by asterisks. In some cases, PStF was followed by suppression (Figure 2, ED 4,5). The suppression component of biphasic effects was not

measured because of uncertainty about its origin and exact onset. PStS, separate from facilitation, was also present at this site, for example, PDE.

Figure 3A shows the distribution of PStF and PStS onset latencies for effects obtained from SMA. The distribution for PStF was bimodal with an early peak containing onset latencies less than 40 ms (384 effects, 85% of PStF) and a late peak with onset latencies above 40 ms (66 effects, 15% of PStF). Early PStF from SMA had a mean latency of 15.2 ± 4.5 ms compared to an onset latency of 9.7 ± 2.1 ms for M1 PStF effects (Table 2). Late PStF from SMA had a mean latency of 55.2 ± 7.2 ms. Examples of short and long latency PStF are illustrated in Figure 4. Long latency PStF typically occurred without early PStF (EDC), but in some cases it was preceded by short latency facilitation (BIS) or by PStS. M1 has yet to be tested for late effects using a long analysis epoch.

Figure 3B shows the distribution of onset latencies for PStS from SMA. The distribution was unimodal with mean onset latency of 32.4 ± 9.2 ms. In comparison, the mean latency of M1 PStS was 15.6 ± 4.4 ms. The distribution of PStF and PStS latencies for SMA effects were broader than M1 effects as reflected in larger standard deviations (Table 2). Examples of PStS from SMA include PDE, ADE and PEC in Figure 2.

The latencies and magnitudes of PStF from SMA and M1 for muscles acting at different joints are given in Table 3. At all joints, SMA mean onset latencies were greater that those from M1 ($P < 0.001$, Mann-Whitney Rank

Sum test). The onset latencies from SMA averaged 5.5 ms longer than those from M1. Statistical comparison of mean PStF onset latency from SMA for different joints revealed that digit muscle onset latency was significantly longer than shoulder and elbow muscles latencies ($P < 0.01$, Holm-Sidak method). In comparison, except for PStF in intrinsic hand muscles, distal muscle onset latencies from M1 sites were shorter than proximal muscle onset latencies ($P \leq 0.001$, Holm-Sidak method). Proximal muscles PStF had the shortest onset latencies from SMA whereas the distal PStF had the shortest onset latency from M1.

Table 3 also gives the average magnitude of PStF for muscles acting at different joints. The average magnitudes of PStF from SMA were all statistically weaker than effects from M1 in the corresponding joints ($P < 0.001$, Mann-Whitney Rank Sum test). The magnitude of PStF from M1 sites was substantially greater for distal muscles compared to that of proximal muscles and there was a trend toward a progressive increase in magnitude the more distal the group of muscles. This difference was not evident in the data for SMA. In fact, the only significant differences that emerged in the data for SMA was that the magnitude of PStF from intrinsic hand muscles was weaker than that from elbow and wrist muscles ($P < 0.01$, Holm-Sidak method) and shoulder muscle PStF was weaker than that from elbow, wrist, and digit muscles ($P < 0.01$, Holm-Sidak method).

Figure 5 shows the distribution of PStF and PStS magnitudes for effects obtained from SMA. The average magnitudes of the PStF (early onset) and PStS from SMA at 60 μA expressed as peak-percent-increase (ppi) or decrease (ppd) relative to baseline were 13.8 ± 6.2% and -11.9 ± 4.1% respectively. Late onset PStF from SMA had an average magnitude of 11.3 ± 4.2%. In comparison, the magnitudes of PStF and PStS from sites in M1 at 15 μA were 50.2 ± 63.5% and -23.8 ± 8.8% respectively (Table 2). In previous work (Widener, 1989), we showed that the relationship between stimulus intensity applied to M1 cortex and ppi measured from spike triggered averages is linear. Accordantly, we performed a linear extrapolation of this relationship to estimate the magnitude of M1 PStF and PStS at 60 μA for more direct comparison to SMA magnitudes. M1 PStF magnitude extrapolated to 60 μA was 206.1%; M1 PStS magnitude was -97.7%. The extrapolation was based on data for stimulus sites in all cortical layers.

DISCUSSION

The goal of this paper was to analyze the magnitude and latency of effects from SMA to 24 muscles of the forelimb in rhesus macaques and compare these effects with those from M1. Our results show that StTA effects from SMA have longer onset latencies and are much weaker than those from M1. In addition, unlike M1, effects in distal muscles from SMA are not stronger than those in proximal muscles. The results also demonstrate a bimodal distribution of PStF onset latencies from SMA with clearly early and late effects. Early SMA effects had a mean onset latency that was 5.5 ms longer than the mean onset latency of PStF from M1. SMA onset latencies also exhibited greater variability than those from M1. The latency of poststimulus effects in stimulus triggered averages of EMG activity reflects a combination of conduction distance, conduction velocity, and synaptic transmission in the anatomical pathway from the stimulation site to the muscle. The longer latency and greater variability in latency of SMA effects may reflect a more indirect coupling to motoneurons and slower corticospinal conduction velocity than exists for M1 (Macpherson *et al.*, 1982; Maier *et al.*, 2002; Palmer *et al.*, 1981). In fact, SMA has only limited corticospinal projections to motor nuclei of the ventral horn; 11% in the cervical and upper thoracic segments compared to 28% for M1 (Dum and Strick, 1996). The majority of corticospinal terminations from SMA (87%) are confined to the

intermediate zone of the spinal cord (laminae V-VIII) where different populations of interneurons are located (Dum and Strick, 1996). This suggests that a major contribution of SMA to movement initiation and control is through its innervation of spinal interneurons influencing reflex and other spinal circuits rather than providing direct monosynaptic input to the motoneurons. This view is supported by the findings of the current study in which the magnitudes of PStF and PStS from SMA were vastly weaker than those from M1 and the onset latencies of PStF at all joints were substantially greater than for M1. This conclusion is also supported by the work of Maier *et al.* (2002) showing that the area of densest labeling from M1 in lamina IX motor nuclei supplying the hand muscles was about 13 times the area of labeling from SMA.

SMA's primary contribution to the control of movements might be achieved largely indirectly through its projections to M1 (Muakkassa and Strick, 1979). Tokuno and Nambu (2000) showed that stimulation of SMA evoked excitatory responses in 64% of the M1 pyramidal tract neurons tested. The mean latency of these responses was 4.3 ms. In our data, this is similar to the difference in mean latency of PStF from SMA compared to M1 of 5.5 ms (longer for SMA) consistent with a potential role of M1 in mediating SMA effects. While direct excitation of M1 corticospinal neurons is clearly a possibility, during volitional movement, SMA might also enhance M1 corticospinal output associated with other inputs (Cerri *et al.*, 2003). Tokuno

and Nambu (2000) also showed that 31% of the responses in M1 pyramidal tract neurons evoked by stimulation of SMA were pure inhibitory responses with a mean latency of 6.7 ms. Our PStS effects had latencies that averaged 16.8 ms longer than M1 PStS effects. While this latency difference is also compatible with the possibility that these effects might be mediated through M1, it is greater than would be expected for a simple relay in which M1 corticospinal neurons with inhibitory muscle effects are facilitated by SMA or M1 neurons with excitatory effects are suppressed. The mechanism of late PStF from SMA is unclear. The latency seems too long to be consistent with a relay through M1. In some cases, late PStF is preceded by suppression suggesting post-inhibitory rebound mechanism. However, late PStF was typically observed without any preceding PStS or early PStF in the same record so post-inhibitory rebound is an unlikely mechanism.

Effects from M1 were stronger than those from SMA even though the M1 stimulus intensity was 15 μA compared to 60 μA for SMA. Extrapolating the magnitudes of M1 PStF and PStS to 60 μA yielded facilitation and suppression effects from M1 that were vastly stronger (15 and 8 fold respectively) than those from SMA. These results again support the recent findings of Maier *et al*. (2002) showing that while both SMA and M1 evoke corticomotoneuronal EPSPs in forelimb motoneurons, those from M1 are far more numerous and much stronger than those from SMA.

We conclude that the corticospinal connections from SMA provide relatively weak direct input to spinal motoneurons compared to the robust effects from M1. The effects from SMA might be predominantly achieved indirectly. Innervation of interneurons in the intermediate zone of the spinal cord and/or projections to M1 might be the primary mechanisms by which SMA influences motoneurons.

Table 1. Summary and comparison of data collected from SMA

	SMA			M1
	Monkey B	Monkey Y	Total	Total
Electrode tracks	21	22	43	248
Sites stimulated	170 (43%)	227 (57%)	397	2477
StTA records	4,048	5,448	9,496	59,448
PStF effects (latency <40 ms)	103	281	384 (46%)	1971 (61%)
PStF effects (latency >40 ms)	38	28	66 (8%)	NT
PStS effects	242	143	385 (46%)	1255 (39%)
PStEs obtained	383	452	835	3226

SMA: Supplementary motor area; M1: Primary motor cortex; StTA: stimulus triggered average; PStE: poststimulus effect; PStF: poststimulus facilitation; PStS: poststimulus suppression; NT: not tested. M1 data were from a previously study some of which has been published (Park *et al.*, 2004). M1 and SMA data came from different monkeys.

Table 2. Comparison of the latency and magnitude of SMA and M1

	Early PStF Onset latency < 40 ms		Late PStF Onset latency > 40 ms		PStS All latencies	
	Onset Latency (ms)	Magnitude (ppi)	Onset Latency (ms)	Magnitude (ppi)	Onset Latency (ms)	Magnitude (ppd))
SMA (60 A)	15.2 ± 4.5	13.8 ± 6.2	55.2 ± 7.2	11.3 ± 4.2	32.4 ± 9.2	-11.9 ± 4.1
MI (15 μA)	9.7 ± 2.1	50.2 ± 63.5	NT	NT	15.6 ± 4.4	-23.8 ± 8.8
MI (60 μA) extrapolated	--	206.1	--	--	--	-97.7

NT: not tested; M1, primary motor cortex; SMA, supplementary motor area; Magnitude: peak increase or decrease expressed as a percent of baseline. M1 data come from the same data set used in previous paper (Park *et al.*, 2004). Extrapolation of M1 magnitudes to 60 μA is based on the work of G. Widener (1989) showing a linear relationship between stimulus intensity and magnitude of PStF and PStS. The magnitudes are expressed as peak percent increase (ppi) and peak percentage decrease (ppd).

Table 3. Comparison of the latency and magnitude of PStF from sites in SMA and M1 per joints

Joint	SMA			M1		
	No. of effects	Onset latency (ms)	Magnitude %	No. of effects	Onset latency (ms)	Magnitude %
Shoulder	68	14.0 ± 4.9	10.5 ± 4.8	230	9.9 ± 2.5	23.7 ± 10.5
Elbow	103	14.7 ± 4.1	14.8 ± 6.4	561	9.9 ± 2.2	31.9 ± 20.8
Wrist	85	15.3 ± 3.7	15.4 ± 5.4	500	9.3 ± 2.1	60.8 ± 74.6
Digit	102	16.3 ± 5.2	14.1 ± 5.7	477	9.3 ± 1.9	65.6 ± 85.8
Intrinsic Hand	26	15.7 ± 4.5	12.2 ± 9.4	203	10.4 ± 1.3	68.3 ± 63.2

Values are means and magnitudes ± SD. Data based on early PStF (onset latency < 40 ms). Stimulation at 60 μA for SMA and 15 μA for M1. % = peak percent increase above baseline. M1 data were collected from the same monkeys used in previous paper (Park *et al*., 2004). The average onset latencies and magnitudes of PStF from SMA were all statistically different than effects from M1 in the corresponding joints ($P < 0.001$, Mann-Whitney Rank Sum test). The mean onset latencies and magnitudes of PStF from SMA and M1 showed the following statistically significant differences. Onset latency differences ($P < 0.01$, Holm-Sidak method): SMA: digit versus shoulder and elbow; M1: all were different except digit versus wrist, and shoulder versus elbow. Magnitude differences ($P < 0.01$, Holm-Sidak method): SMA: shoulder versus digit, wrist and elbow, and intrinsic versus wrist and elbow muscles; M1: all were different except digit versus wrist and intrinsic hand.

Figure 1. Location and orientation of the penetrations in SMA. (A) Penetration maps of the left hemisphere for both monkeys. Sites where StTA produced poststimulus effects are marked by circles; the open circle in monkey B and figure 1B is the track from which the data shown in Figure 2 were obtained. Sites that produced no effects are marked by filled squares. (B) Orientation of the tracks based on MR images (MRI) and electrophysiological data. Doted line indicates the border between CMAd and SMA. Abbreviations: ARC, arcuate sulcus; CS, central sulcus: L, lateral; M, medial; MID, midline.

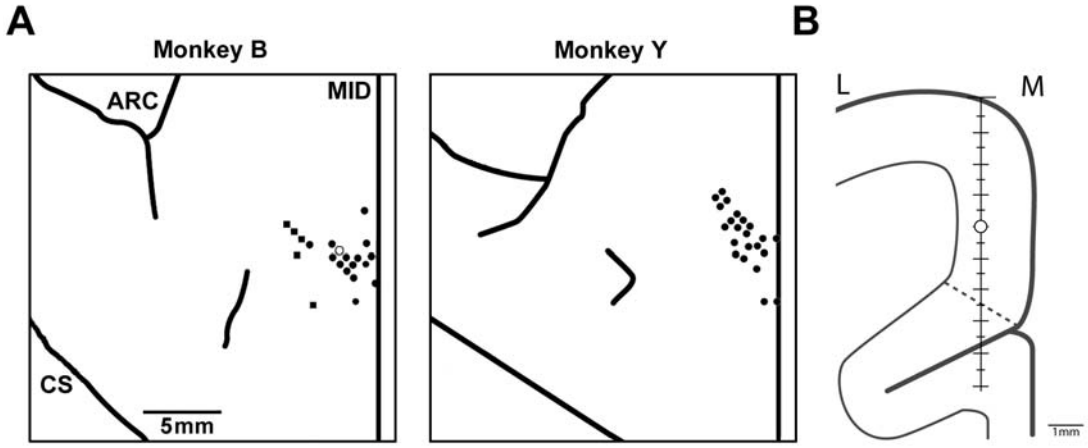
A
Monkey B
ARC
MID
CS
5mm
Monkey Y
B
L
M
1mm

Figure 2. Poststimulus facilitation (PStF) and suppression (PStS) of forelimb muscles from one SMA site (8B8). Time zero corresponds to the stimulus event used for the average. Stimulation was 60 μA at 10 Hz. Individual stimuli were symmetrical biphasic pulses (0.2 ms negative followed by 0.2 ms positive). PStF effects were observed in both proximal (BIL, BRA, BR, TLON) and distal (APB, FDI, FDS, FDP, ED 4,5, EDC, FCU) forelimb muscles. Pure PStS effects were observed in proximal (ADE, PEC, PDE, TLAT, DE) forelimb muscles. Individual records based on 3,074-4,074 trigger events. PStF are marked by an asterisk (*) and PStS by (**).

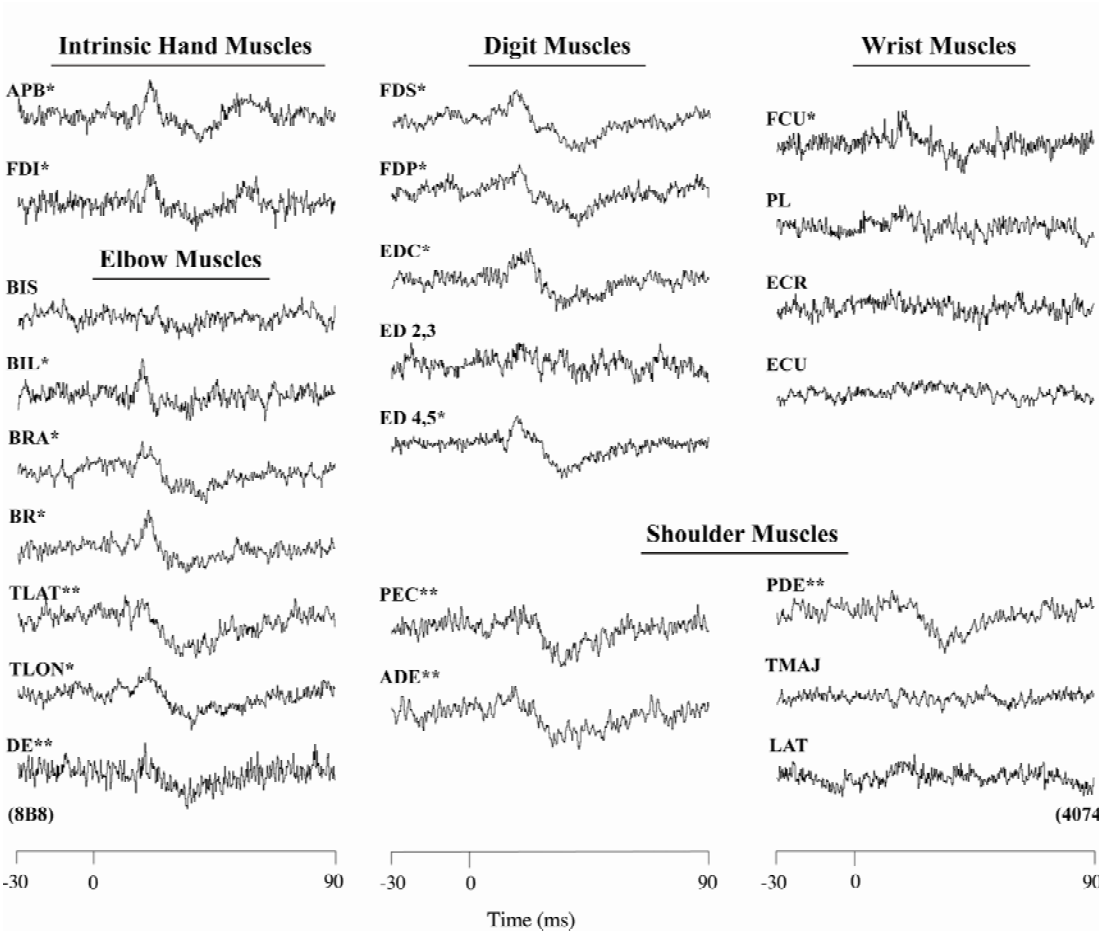
Intrinsic Hand Muscles
APB*
FDI*
Elbow Muscles
BIS
BIL*
BRA*
BR*
TLAT**
TLON*
DE**
(8B8)
Digit Muscles
FDS*
FDP*
EDC*
ED 2,3
ED 4,5*
Wrist Muscles
FCU*
PL
ECR
ECU
Shoulder Muscles
PEC**
ADE**
PDE**
TMAJ
LAT
(4074
-30
0
90
Time (ms)

Figure 3. (A) Distribution of SMA PStF onset latencies for muscles at all forelimb joints (n=450). (B) Distribution of PStS onset latencies for muscles at all forelimb joints (n=385).

A

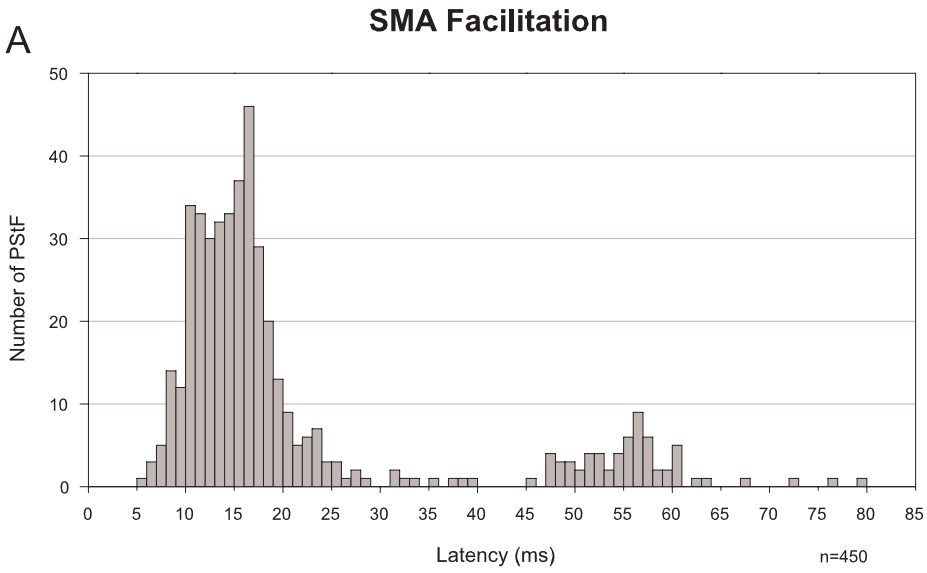
SMA Facilitation
Number of PStF
0
10
20
30
40
50
0 5 10 15 20 25 30 35 40 45 50 55 60 65 70 75 80 85
Latency (ms)
n=450

B

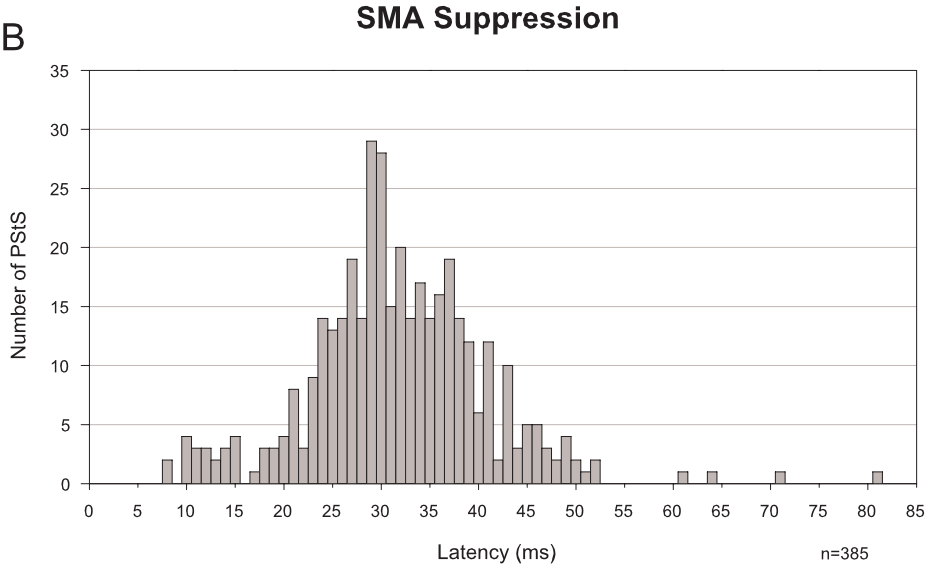
SMA Suppression
Number of PStS
0
5
10
15
20
25
30
35
0 5 10 15 20 25 30 35 40 45 50 55 60 65 70 75 80 85
Latency (ms)
n=385

Figure 4. Types of facilitation effects observed in stimulus triggered averages of EMG activity from sites in SMA. Time zero corresponds to the stimulus event used for the average. N, number of trigger events.

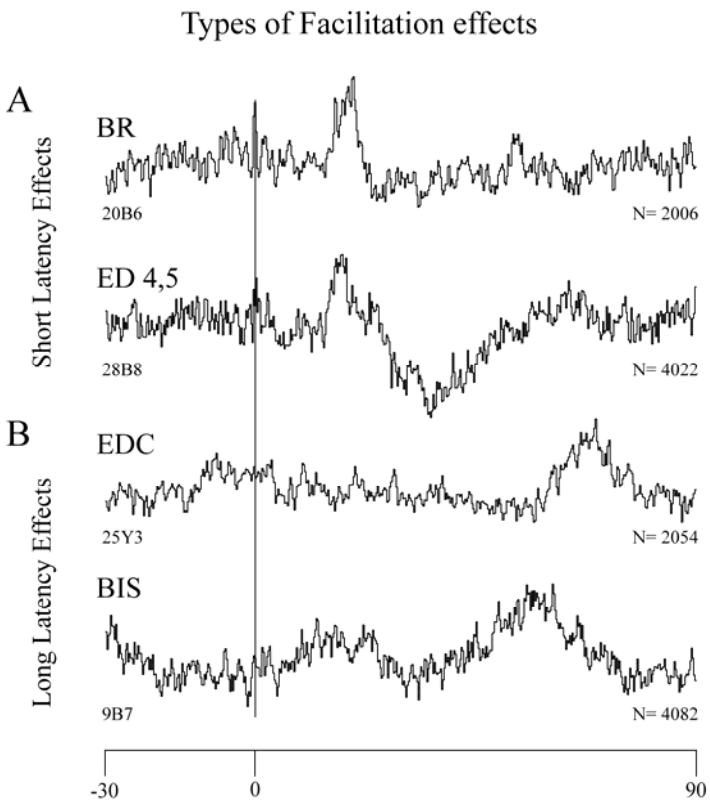
Types of Facilitation effects
A
Short Latency Effects
BR
20B6
N= 2006
ED 4,5
28B8
N= 4022
B
Long Latency Effects
EDC
25Y3
N= 2054
BIS
9B7
N= 4082
-30
0
90

Figure 5. (A) Distribution of SMA PStF magnitudes for muscles at all forelimb joints (n=450) and Black shading indicates long latency PStF (> 40 ms). The magnitudes are expressed as peak percent increase (ppi). Light shading indicates short latency PStF (< 40 ms). (B) Distribution of SMA PStS magnitudes for muscles at all forelimb joints (n=385). The magnitudes are expressed as peak percent decrease (ppd).

A

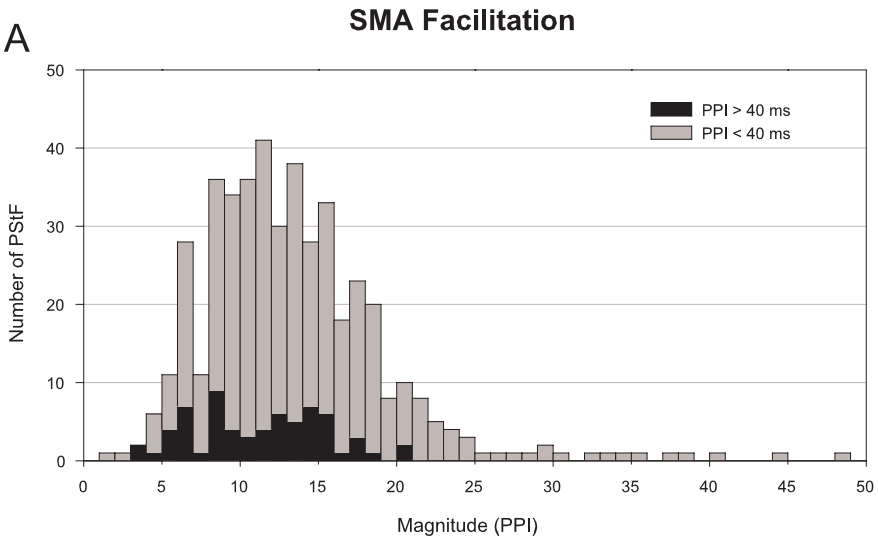
SMA Facilitation
PPI > 40 ms
PPI < 40 ms
Number of PStF
Magnitude (PPI)
0
10
20
30
40
50
0
5
10
15
20
25
30
35
40
45
50

B

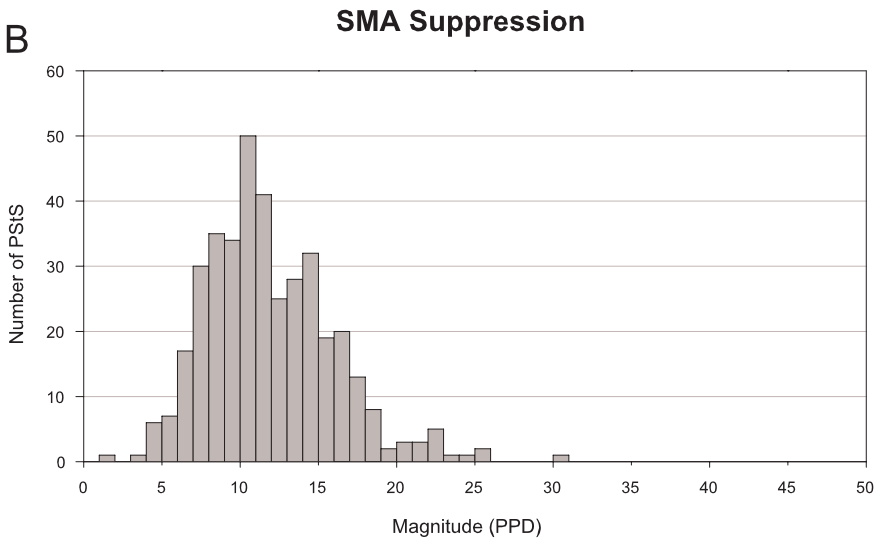
SMA Suppression
Number of PStS
Magnitude (PPD)
0
10
20
30
40
50
60
0
5
10
15
20
25
30
35
40
45
50

REFERENCES

Asanuma H, Rosen I (1972) Topographical organization of cortical efferent zones projecting to distal forelimb muscles in the monkey. Exp Brain Res 14: 243-256.

Belhaj-Saïf A, Karrer JH, Cheney PD (1998) Distribution and characteristics of poststimulus effects in proximal and distal forelimb muscles from red nucleus in the monkey. J Neurophysiol 79: 1777-1789.

Cerri G, Shimazu H, Maier MA, Lemon RN (2003) Facilitation from ventral premotor cortex of primary motor cortex outputs to macaque hand muscles. J Neurophysiol 90: 832-842.

Cheney PD, Belhaj-Saïf A, Boudrias M-H (2004) Principles of corticospinal system organization and function. In: Clinical Neurophysiology of Motor Neuron Diseases (Eisen A, editor), pp 59-96: Amsterdam, The Netherlands: Elsevier Science.

Cheney PD, Fetz EE (1980) Functional classes of primate corticomotoneuronal cells and their relation to active force. J Neurophysiol 44: 773-791.

Cheney PD, Fetz EE (1985) Comparable patterns of muscle facilitation evoked by individual corticomotoneuronal (CM) cells and by single

intracortical microstimuli in primates: evidence for functional groups of CM cells. J Neurophysiol 53: 786-804.

Cheney PD, Fetz EE, Mewes K (1991) Neural mechanisms underlying corticospinal and rubrospinal control of limb movements. Prog Brain Res 87: 213-252.

Dum RP, Strick PL (1991) The origin of corticospinal projections from the premotor areas in the frontal lobe. J Neurosci 11: 667-689.

Dum RP, Strick PL (1996) Spinal cord terminations of the medial wall motor areas in macaque monkeys. J Neurosci 16: 6513-6525.

He SQ, Dum RP, Strick PL (1995) Topographic organization of corticospinal projections from the frontal lobe: motor areas on the medial surface of the hemisphere. J Neurosci 15: 3284-3306.

Kasser RJ, Cheney PD (1985) Characteristics of corticomotoneuronal postspike facilitation and reciprocal suppression of EMG activity in the monkey. J Neurophysiol 53: 959-978.

Kuypers HGJM (1981) Anatomy of the descending pathways. In: Handbook of physiology- the nervous system II (Brookhart J, Mountcastle V, eds.), pp 597-666: Bethesda, MD: American Physiology Society.

Luppino G, Matelli M, Camarda RM, Gallese V, Rizzolatti G (1991) Multiple representations of body movements in mesial area 6 and the adjacent cingulate cortex: an intracortical microstimulation study in the macaque monkey. J Comp Neurol 311: 463-482.

Macpherson J, Wiesendanger M, Marangoz C, Miles TS (1982) Corticospinal neurones of the supplementary motor area of monkeys. A single unit study. Exp Brain Res 48: 81-88.

Maier MA, Armand J, Kirkwood PA, Yang HW, Davis JN, Lemon RN (2002) Differences in the corticospinal projection from primary motor cortex and supplementary motor area to macaque upper limb motoneurons: an anatomical and electrophysiological study. Cereb Cortex 12: 281-296.

McKiernan BJ, Marcario JK, Karrer JH, Cheney PD (1998) Corticomotoneuronal postspike effects in shoulder, elbow, wrist, digit, and intrinsic hand muscles during a reach and prehension task. J Neurophysiol 80: 1961-1980.

Mewes K, Cheney PD (1991) Facilitation and suppression of wrist and digit muscles from single rubromotoneuronal cells in the awake monkey. J Neurophysiol 66: 1965-1977.

Muakkassa KF, Strick PL (1979) Frontal lobe inputs to primate motor cortex: evidence for four somatotopically organized 'premotor' areas. Brain Res 177: 176-182.

Palmer C, Schmidt EM, McIntosh JS (1981) Corticospinal and corticorubral projections from the supplementary motor area in the monkey. Brain Res 209: 305-314.

Park MC, Belhaj-Saïf A, Cheney PD (2000) Chronic recording of EMG activity from large numbers of forelimb muscles in awake macaque monkeys. J Neurosci Methods 96: 153-160.

Park MC, Belhaj-Saïf A, Cheney PD (2004) Properties of primary motor cortex output to forelimb muscles in rhesus macaques. J Neurophysiol 92: 2968-2984.

Porter R, Lemon RN (1993) Corticospinal function and voluntary movement. Oxford: Clarendon Press.

Rouiller EM, Moret V, Tanne J, Boussaoud D (1996) Evidence for direct connections between the hand region of the supplementary motor area and cervical motoneurons in the macaque monkey. Eur J Neurosci 8: 1055-1059.

Widener GL (1989) Effects on muscle activity form somatosensory cortical areas 3a, 3b, 1 and 2 in the awake monkey. Doctoral dissertation.

Department of Molecular and Integrative Physiology: University of Kansas Medical Center. pp 1-234.

CHAPTER 3

FORELIMB MUSCLE REPRESENTATIONS AND OUTPUT PROPERTIES OF MOTOR AREAS ON THE MESIAL WALL OF RHESUS MACAQUES

ABSTRACT

The main goal of this study was to assess the forelimb organization and the output properties of the supplementary motor area (SMA) and the dorsal cingulate motor area (CMAd) relative to the primary motor cortex (M1). Stimulus-triggered averages of EMG activity from 19-24 muscles of the forelimb were computed from sites in layer V of SMA, CMAd and M1 of two rhesus monkeys performing a reach-to-grasp. A total of 1,014, 125 and 51 sites were stimulated in SMA, CMAd and M1 respectively. No segregation of the representations of proximal and distal muscles was found in SMA. In CMAd, a representation of distal muscles located rostrally to a smaller representation of proximal muscles was observed.

Our results demonstrate that at a stimulus intensity of 60 μA, effects from M1 were ~10 times greater than effects from CMAd and SMA. Latencies of poststimulus effects were 8-12.2 ms longer for SMA and CMAd respectively compared to those from M1. In SMA, facilitation represented 66% of all effects, with 64% occurring in distal muscles and 36% in proximal muscles. Of the PStF effects collected (72%) in CMAd, 79% came from distal muscles and 21% from proximal muscles. Our results suggest that corticospinal neurons in SMA and CMAd provide relatively weak direct input to spinal motoneurons compared to the robust effects from M1 and that their

forelimb representations are not discretely organized compared to the segregated representations of proximal and distal muscles observed in M1.

INTRODUCTION

Welch (1951) and Woosley *et al*. (1952), using electrical stimulation of the cortical surface, demonstrated the existence of a motor area on the medial wall of the hemisphere in monkeys, which they termed the supplementary motor area (SMA). Since its discovery, more recent studies have shown that the previously described SMA contains more than a single motor area, each one with its own set of corticospinal neurons. In addition to SMA, three cingulate motor areas have been identified in the cingulate sulcus including: the dorsal cingulate motor area (CMAd), the ventral cingulate motor area (CMAv) and the rostral cingulate motor area (CMAr) (Dum and Strick, 1991; Luppino *et al*., 1991; Matelli *et al*., 1991; Galea and Darian-Smith, 1994; He *et al*., 1995). More significantly, SMA and CMAd contain substantial numbers of corticospinal neurons projecting to the spinal cord where they can potentially influence motoneuronal pools via pathways independent of the primary motor cortex (M1) (Dum and Strick, 1991; Galea and Darian-Smith, 1994).

The pattern of termination of M1 corticospinal neurons was shown to partially end in portions of the ventral horn within the spinal cord; with some of the terminations making direct connections with spinal motoneurons (Kuypers, 1981). The direct connection of corticospinal neurons on motoneurons has been regarded as a prerequisite for the generation of

independent finger movements (Porter and Lemon, 1993). Using anterograde tracers to examine the spinal pattern of terminations of corticospinal neurons from SMA and CMAd, it was demonstrated that they both have terminations in the ventral horn, particularly on motoneuronal pools involved in the generation of finger and wrist movements (Dum and Strick, 1996). Additionally, SMA and CMAd were shown to have densities of corticospinal neurons similar to the density of corticospinal neurons in M1 (Dum and Strick, 1991; He *et al*., 1995). Consequently, this further suggests that the corticospinal neurons in SMA and CMAd share, in many respects, similarities with those from M1.

Despite the fact that the number and the location of the corticospinal neurons contained in SMA and CMAd have been described in detail, disparities exist in their forelimb organization. The topographic organization of SMA and CMAd examined by injecting retrograde tracers in cervical segments of the spinal cord, shows segregated zones of proximal and distal representation of corticospinal neurons in each area (Dum and Strick, 1991; He *et al*., 1995). In contrast, the few studies that used intracortical microstimulation (ICMS) to investigate forelimb movements from SMA reported no clear segregation between proximal and distal forelimb representations (Macpherson *et al*., 1982b; Mitz and Wise, 1987; Luppino *et al*., 1991). Hindlimb movements were reported to be mainly evoked with

ICMS in the upper bank of the cingulate sulcus with only a few sites producing forelimb movements (Luppino *et al*., 1991).

In comparison to ICMS and anatomical approaches, stimulus-triggered averaging (StTA) of electromyographic (EMG) activity gives the sign of synaptic output to motoneurons (excitation or inhibition) and provides quantification of the latency and magnitude of motor output from small clusters of corticospinal neurons to large numbers of muscles. Using this technique, the existence of segregated proximal and distal muscle representations were demonstrated in the forelimb area of M1 (Park *et al*., 2001). Therefore, one of the main goals of this study was to use StTA of EMG activity to further investigate their forelimb organizations in terms of proximal and distal muscle representations.

The data in this paper builds upon work presented in a previous report from our laboratory on SMA (Boudrias, *et al*., 2006). We have now studied a significantly larger number of sites in SMA to investigate in greater detail the forelimb organization. We used the same parameters of stimulation (current intensity of 60 μA) for sites in all three areas (SMA, CMAd and M1) for accurate comparison of their motor outputs. In our previous report, comparison data at 60 μA for M1 was based on extrapolation. We also restricted our data set to sites located in or near layer V of the cortical gray matter. The fact that SMA, CMAd and M1 contain comparable densities of corticospinal neurons suggests that the same parameters of stimulation

applied in each of these areas should activate a similar number of corticospinal neurons given the relatively limited effective current spread of a 60 μA stimulus of approximately 215 μm. Consequently, applying StTA of EMG activity to SMA, CMAd and M1 should have provided a comparable measure of the efficacy of motor output from a similar number of activated corticospinal neurons in each area.

MATERIALS AND METHODS

Behavioral task and surgical procedures

Data were collected from two male rhesus monkeys (*Macaca mulatta*, 8-10 kg, 5 and 8 years of age) trained to perform a reach-to-grasp task as described in previous studies (Belhaj-Saif *et al*., 1998; McKiernan *et al*., 1998). The animals were identified as monkey J and monkey Y and will be referred to as such throughout the report. On completion of training, a recording chamber was implanted over the left hemisphere of each monkey, allowing the exploration of a cortical area of 30 mm in diameter for fully accessing the forelimb areas of SMA, CMAd and M1 (Figures 1 & 2). The chambers were stereotaxically implanted at anterior 12.9 mm and lateral 9 mm (monkey Y) and at anterior 20.9 mm and lateral 12.9 mm (monkey J) with an angle of 15-degrees to the midsagittal plane.

EMG activity was recorded from 24 muscles of the forelimb, as described previously by (Park *et al*., 2000). Monkey J was implanted using a modular subcutaneous implant technique and monkey Y was implanted using a cranial subcutaneous implant technique. In the case of a modular implant method (monkey J), at all times other than recording sessions, the monkey wore a jacket reinforced with stainless steel mesh to protect the EMG implant. For each monkey, muscles were implanted with a pair of multi-stranded

stainless steel wires (Cooner Wire) and led subcutaneously to connectors on the forearm (modular implant), or to a connector anchored to the dental acrylic mound, next to the recording chamber (cranial implant). EMGs were recorded from five shoulder muscles: pectoralis major (PEC), anterior deltoid (ADE), posterior deltoid (PDE), teres major (TMAJ) and latissimus dorsi (LAT); seven elbow muscles: biceps short head (BIS), biceps long head (BIL), brachialis (BRA), brachioradialis (BR), triceps long head (TLON), triceps lateral head (TLAT) and dorso-epitrochlearis (DE); five wrist muscles: extensor carpi radialis (ECR), extensor carpi ulnaris (ECU), flexor carpi radialis (FCR), flexor carpi ulnaris (FCU) and palmaris longus (PL); five digit muscles: extensor digitorum communis (EDC), extensor digitorum 2 and 3 (ED 2,3), extensor digitorum 4 and 5 (ED 4,5), flexor digitorum superficialis (FDS) and flexor digitorum profundus (FDP); and two intrinsic hand muscles: abductor pollicis brevis (APB) and first dorsal interosseus (FDI). For monkey Y, one lead of TLON and TLAT were combined to form one triceps muscle (TRI) recording. One lead of APB and FDI were also combined to form an intrinsic hand muscle (Intrins.) recording. EMG recordings were tested for cross-talk by computing EMG-triggered averages. Muscles showing cross-talk were eliminated from the data base. Broad weak synchrony effects surrounding the trigger were observed but fell below our threshold for rejection. For monkey Y, BR, FCU and ED 4,5 and for monkey J, BR for one implant and FDS for another implant showed cross-talk and were rejected

from the analysis. For the calculation of a normalized number of muscles recorded at each joint, intrinsic hand (Intrins.) and triceps (TRI) muscles for monkey Y were considered to be two distinct muscles since either of the combined muscles could have been the origin of a poststimulus effects. All surgeries were performed under deep general anesthesia and sterile conditions. Analgesic and antibiotic drugs were given postoperatively in accordance with the Association for Assessment and Accreditation of Laboratory Animal Care (AAALAC) and the Guide for the Care and Use of Laboratory Animals, published by the U.S. Department of Health and Human Services and the National Institutes of Health.

Data recording

Stimuli were applied to SMA, CMAd and M1, and recorded together with EMG signals, while the monkey performed a reach-to-grasp task. Electrode penetrations are summarized and represented in Table 1 and Figure 1. Penetrations were made systematically using a 1 mm grid throughout the mesial wall of SMA's forelimb representation in each animal. In some areas, electrode tracks were placed 0.5 mm from each other or in the center of the 1 mm square formed by four adjacent tracks to achieve greater spatial resolution. Penetrations in CMAd were made using a 1 mm grid or less. In monkey J, the lateral boundary of SMA was sampled using 2 mm spacing. For SMA and CMAd, an area of up to 7 mm lateral to the midline and

13 mm along the antero-posterior axis of the lateral aspect of the hemisphere for each animal was covered with electrode penetrations. Sites located at or below 6.5 mm from the cortical surface were not included in the SMA data base; such sites were either rejected or considered to be part of CMAd. The bulk of the forelimb representation of SMA covered an area about 7-8 mm rostro-caudally.

Penetrations in M1 were randomly selected throughout its forelimb representation and systematically stimulated at two different intensities, 15 and 60 μA (Table 2 & Figure 1). The use of 15 μA is based on previous StTA of EMG activity studies in which it was found that this specific intensity of stimulation was optimal to map and assess M1 output properties (Park *et al*., 2001; Park *et al*., 2004). A total of 30 tracks were selected in M1 from the two monkeys. Half of the penetrations were performed on the anterior part of M1 (surface part) and the other half were performed on the posterior part of M1 (anterior bank of the precentral gyrus). Compared to a restricted number of muscles showing PStEs at a stimulation intensity of 15 μA, at 60 μA the number of PStEs in M1 expanded to include nearly all of the recorded muscles (Figure 4). However, for purposes of quantifying the change in magnitude and latency of PStEs at 15 and 60 μA, only effects present at both intensities were included in the final data set. This avoided distortion of the data set by additional PStEs produced at 60 μA which showed longer latencies and weaker magnitudes.

Glass and mylar insulated platinum-iridium electrodes with typical impedances between 0.7-2 MΩ (Frederick Haer & Co.) were used for cortical recording and stimulation. The electrode was advanced using a manual hydraulic microdrive and stimulation was performed at 0.5 mm intervals. Measurements of depth in the cortex were referenced to first activity. Only sites in or near the cortical gray matter of layer V of SMA, CMAd and M1 were included in this analysis. Sites corresponding to layer V were identified by using a combination of electrode depth, strength of effects and changes in background activity. White matter was identified by an abrupt decrease in background activity. Cortical unit activity and EMG activity were simultaneously monitored along with task related signals. Stimulus-triggered averages (StTA) of EMG activity (15 and 60 μA at 7-15 Hz) were computed for 19-24 muscles of the forelimb from stimuli applied throughout all phases of the reach-to-grasp task. EMGs were filtered from 30 Hz to 1 KHz, digitized at 4 kHz, and full-wave rectified. Individual stimuli were symmetrical biphasic pulses (0.2 ms negative followed by 0.2 ms positive). All StTAs were based on a minimum of 500 or a 1000 trigger events for M1 and SMA/CMAd respectively. The number of trigger events performed in SMA was increased in comparison to M1, in order to detect the weaker PStEs produced in SMA.

Data analysis

Averages were compiled using an epoch of 120 ms (30 ms pre-trigger to 90 ms post-trigger) for all sites in SMA in CMAd except for 15 tracks located most laterally in monkey J (Figure 1). For these tracks, a 60 ms length epoch, extending from 20 ms before the trigger to 40 ms after the trigger was used. The analysis period of 120 ms was also used in 16 tracks in M1 to evaluate the possible presence of long latency facilitation peaks, as previously observed in SMA (Boudrias *et al*., 2006). Segments of EMG activity associated with each stimulus were evaluated and accepted for averaging only when the average of all EMG data points over the entire epoch was equal to or greater than 5% of full-scale input level (± 5 volt) on our data acquisition system (Power 1401, Cambridge Electronic Design ltd). This prevented averaging segments where EMG activity was minimal or absent (McKiernan *et al*., 1998)

At each stimulation site, averages of EMG activity were obtained from 19-24 muscles. Mean baseline activity and standard deviation were measured from EMG activity in the pre-trigger period (20-30 ms). StTAs were considered to have a significant PStF if the envelope of the StTA crossed a level equivalent to 2 SD of the mean of the baseline EMG, for a period of time equal to or greater than 1.25 ms (5 points), otherwise they were considered insignificant. The magnitudes of PStF and PStS peaks were expressed as the percent increase (ppi) or decrease (ppd) in EMG activity above (facilitation) or below (suppression) baseline.

Statistical analysis of spatial representations in SMA

Pairwise comparisons were made for 5 data sets (shoulder, elbow, wrist, digit and intrinsic hand muscle) and for a proximal versus distal data set for SMA in each monkey. The Kolmogorov-Smirnov (K-S) test was used to establish whether two data sets (maps) were derived from the same population, regardless of their underlying distributions. We applied this nonparametric statistic to test the null hypothesis of no difference. The density of the data was established from the graphical interpretation, where each measured sample point was expressed in a Cartesian coordinate system. StatMost (Statistical Analysis and Graphics, v.2.50) software application was used to calculate K-S and probability values.

Intracortical microstimulation (ICMS)

Trains of repetitive intracortical microstimulation (ICMS) were performed in SMA and M1, at those sites where no previous poststimulus effects were detected, to identify the motor output representation of muscles not implanted with EMG electrodes (face, trunk and hindlimb). ICMS consisted of a train of symmetrical biphasic stimulus pulses (0.2 ms negative followed by 0.2 ms positive) at a frequency of 330 Hz (Asanuma and Rosen, 1972), a train duration of 100-500 ms and an intensity of 30-100 μA. Evoked

movements and muscle contractions detected visually were noted and recorded on video tape.

Data analysis of magnetic resonance imaging (MRI)

MR images were obtained from a 3 Tesla Siemens Allegra system with the monkey's head mounted in an MRI compatible stereotaxic apparatus. Structural MRIs and the reconstructed three dimensional image of the brain were used guiding the implantation of the recording chamber. The orientation and location of the penetrations (Figure 1) were matched to the MRI reconstruction of the brain as described previously (Boudrias *et al*., 2006). Based on the corresponding frontal sections of MRIs of the mesial wall, two dimensional maps of unfolded layer V were constructed for SMA and CMAd.

RESULTS

Poststimulus effects (PStEs) restricted to layer V of the forelimb representation of SMA, CMAd and M1 were recorded from the left hemisphere in two monkeys. There were a total of 240 electrodes tracks, 163 in SMA, 47 in CMAd (included in SMA tracks) and 30 in M1 (Table 1). StTA of EMG activity from 19-24 muscles were performed at 1014, 125 and 51 sites yielding a total of 513, 43 and 351 PStEs in SMA, CMAd and M1 respectively. Only a small number (6) of PStEs were obtained from CMAd in Monkey J. This can be explained by the smaller number of tracks performed on the dorsal aspect of the hemisphere, greater than 3 mm lateral to the midline. Therefore, most of CMAd PStEs were from monkey Y (Table 1 & Figure 1). ICMS was performed at sites where no PStEs were observed in order to establish the boundaries of the forelimb representations in SMA and M1. In SMA, movements of the mouth were evoked from the most anterior sites (monkey Y) and hindlimb movements were evoked from the most posterior sites (monkey J and monkey Y), in confirmation of SMA's general somatotopical organization described in other studies (Mitz and Wise, 1987; Luppino *et al*., 1991; Inase *et al*., 1996; Akazawa *et al*., 2000; Takada *et al*., 2001; Akkal *et al*., 2002). CMAd's location was extrapolated from SMA's boundaries as established previously (Dum and Strick, 1991; Luppino *et al*., 1991; Matelli *et al*., 1991; He *et al*., 1995). ICMS also revealed somatotopic

representation of the forelimb region of M1 comparable with that reported by Park *et al*. (2001).

Maps of SMA based on poststimulus effects

Digitally reconstructed images of the brain based on MRI and electrophysiological data were used to construct two-dimensional coordinates of unfolded maps of layer V for SMA and CMAd (Figure 1). Two-dimensional, unfolded layer V maps, of the mesial wall, showing the organization of PStF and PStS at each joint (shoulder, elbow, wrist, digit and intrinsic hand) based on StTA of EMG activities are shown in Figure 2 for each monkey. Comparison of the motor output maps for shoulder, elbow, wrist and digit muscles in SMA revealed no significant segregation in the representation of joint based muscle groups (K-S, $P > 0.05$; Figure 3). In both monkeys, we observed an area with a large number of PStEs from distal muscles. This area was localized in the posterior part of SMA at a particular depth in the mesial wall (Figures 2 & 3, row 8 in money J, row 6.5 in monkey Y). Stimulus-triggered averages of EMG of typical effects obtained in this area for monkey J are shown in Figure 4. However, statistical analysis of the spatial distribution of PStF effects between proximal and distal joints in SMA failed to fully corroborate this observation (K-S, $P > 0.05$).

For facilitation effects, distal muscles were predominantly represented in SMA (64% of all effects). They most represented muscles in order were

FDP, FDS, and ED 2,3. A large number of suppression effects were obtained from SMA (34%) and were found to be largely intermingled with the facilitation effects (Figures 2 & 3). Suppression effects from SMA were also observed predominantly in distal muscles (66%) compared to proximal muscles (34%). The muscles showing the largest number of suppression effects in SMA were in order: ED 2,3, FDP, EDC and ADE (Figure 7A).

Maps of CMAd based on poststimulus effects

Although our data was more limited than for SMA, motor output maps constructed for CMAd revealed a tendency for proximal muscles to be located more posterior to a core of distal muscles (monkey Y, Figures 2 & 3). For facilitation effects, as with SMA, distal muscles were predominately represented (79%), particularly the flexors FCR and FDS, and the intrinsic hand muscles APB and FDI (Figure 7B). Suppression effects were also more common in distal muscles, particularly in ED 2,3 and EDC, antagonists of muscles showing the most facilitation effects.

Examples of PStEs from SMA and M1

Figure 4 shows typical effects in shoulder, elbow, wrist, digit and intrinsic hand muscles from one SMA site stimulated at 60 μA. For comparison, effects from a site in M1 are shown at 15 and 60 μA. The SMA site produced facilitation in 9 of 12 distal muscles; including both flexors and

extensors and also showed a significant effect in the elbow muscle BRA. The M1 site produced PStF in both distal and proximal muscles at 15 μA and was selected because it yielded effects in many of the same muscles as the SMA site. The number next to each record gives the magnitude of the PStF effect. Note that the effects from M1 at 15 μA are greater in magnitude compared to the effects from SMA at 60 μA. At 60 μA, the number of effects from M1 has grown to include nearly all of the recorded muscles and the magnitude of effects has increased almost 10-fold in some muscles. At 60 μA, the strongest effect from SMA at the site illustrated was found to be 23 ppi in FDS and FCU. In contrast, the strongest effect at 60 μA from the M1 site was approximately 10 times greater (224 ppi in FDP).

Distribution of PStF latencies

The distribution of facilitation effects from SMA, CMAd and M1 at 60 μA, are compared in Table 2 and Figure 5A. Compared to SMA and CMAd, the onset latencies of PStF from M1 were shorter and less broadly distributed, as reflected by the smaller standard deviations. We observed a very narrow unimodal distribution of PStF latencies for effects from M1 (Figure 5A). PStF from M1 had an average onset latency of 7.7 ± 1.2 ms, which is shorter by 8 ms and 12.2 ms, respectively compared to effects from SMA (15.7 ± 5.0 ms) and CMAd (19.8 ± 8 ms) (One way ANOVA, $P < 0.001$). The PStF latencies from SMA were on average 4.1 ms shorter than those from CMAd ($P <$

0.001). A bimodal distribution of PStF, including a peak of long onset latency effects, was observed in SMA, as described previously (Boudrias *et al*., 2006), but was not included in this analysis. Long onset latencies effects were also present in effects from CMAd but were not included in this analysis. Significantly, long latency effects were not present in effects from M1. Only 35 PStF effects from SMA (10% of all SMA PStF effects) were encompassed by the standard deviation (SD) range of M1 latencies. Among those, 54% came from distal muscles and 46% from proximal muscles. However, it should be noted that the shortest PStF latencies from SMA were very similar to the shortest latency of effects obtained from M1 at 60 μA (6 ms for SMA and 5.75 ms for M1). The shortest latencies for SMA effects came from ED, 2 3 and from the intrinsic hand muscles.

For CMAd, 7 PStF effects (21% of all CMAd PStF effects) were encompassed by the SD range of M1 latencies, including 6 effects from distal muscles and one effect from a proximal muscle (LAT). The shortest PStF latency (5.75 ms) observed from CMAd came from LAT. In M1, 97% of the effects were facilitatory (Table 1) and were mainly from distal muscles (70%) confirming our previous findings (Park *et al*., 2001).

Comparison of PStF latencies at different joints

The latencies of facilitation effects from SMA, CMAd and M1 for different joints are compared to each other in Figure 6A. The average

latencies of PStF from SMA and CMAd were longer than those from M1 at 60 μA in the corresponding joints ($P < 0.001$). The comparison of the latencies in the corresponding joints revealed longer latencies in CMAd compared to SMA for elbow, wrist and digit muscles ($P < 0.001$). The comparison of the latencies between joints, among the same motor area, did not reveal differences in SMA or CMAd ($P > 0.05$). In comparison, among M1 PStF effects at 60 μA, most of the latencies at different joints were significantly different from one another ($P < 0.001$), except for wrist versus shoulder and digit muscles ($P > 0.05$). Only M1 PStF effects showed significantly shorter latencies in proximal muscles compared to those from distal muscles (Table 2, $P < 0.001$). Latencies of proximal versus distal joints in CMAd and SMA were not statistically different from each other ($P > 0.05$). With increased stimulation intensity from 15 to 60 μA, latencies of PStF effects from the same muscles became significantly shorter in M1 by an average of 1.2 ms ($P < 0.001$). Comparison of latencies of effects from M1 at 15 versus 60 μA also revealed shorter latencies for muscles lumped by joint and by muscle group (distal versus proximal) ($P < 0.001$), except for intrinsic hand muscles stimulated at 15 μA versus intrinsic hand muscles at 60 μA ($P = 0.26$).

Distribution of PStF magnitudes

The distribution of magnitudes expressed as peak percent increase (ppi) showed much stronger effects from M1 compared to SMA or CMAd ($P <$

0.001) (Figure 5B). Our results showed that the magnitudes of the effects were on average ~10-fold stronger in M1 (158.8 ± 140.1 ppi), compared to those from SMA (14.9 ± 5.2 ppi) or CMAd (15.6 ± 5.1 ppi) (Table 2). The PStF magnitudes from CMAd were not different than those from SMA ($P > 0.05$). In SMA, 51 effects had magnitudes above 20 ppi (15% of all effects), 3 effects had magnitudes above 30 ppi (PL, ppi=33; TMAJ; ppi=36, ADE, ppi=39), and one proximal muscle had PStF with a magnitude above 40 ppi (TMAJ, ppi=42). CMAd had 5 PStF effects (16% of all PStF) with magnitudes above 20 ppi, all originating from distal joints. The same M1 muscles stimulated at 15 and 60 μA showed an average increase in the PStF magnitude of ~4-fold (Table 2).

Comparison of PStF magnitudes at different joints

The average magnitudes of PStF from SMA and CMAd were all weaker than the effects from M1 at 60 μA in the corresponding joints ($P < 0.001$) (Figure 6C). There was no difference in the magnitudes in the corresponding joints between SMA and CMAd ($P > 0.05$). Additionally, no differences in the magnitudes of effects were observed between joints for CMAd or SMA ($P > 0.05$). In comparison, for M1 PStF effects at 60 μA, magnitudes between joints were significantly different from each other ($P < 0.001$), except for shoulder versus elbow, wrist versus digit and intrinsic hand muscles, and digit versus intrinsic hand muscles ($P > 0.05$). PStF effects from

distal muscles showed the strongest magnitudes in CMAd and M1 (P = 0.039 & P < 0.001). No difference was found between the magnitudes of distal and proximal joints in SMA (Table 2, P > 0.05). We observed the same progressive trend of increased magnitudes of M1 PStF effects from proximal to distal muscle groups at an intensity 60 μA as reported previously for 15 μA (Park *et al*., 2004). This increase in magnitude was not observed for SMA or CMAd (Figure 6D).

Distribution of the latencies and magnitudes of PStS effects

Latencies of PStS effects from SMA and CMAd were all longer (P < 0.001) than those from M1 at 60 μA in the corresponding joints (Table 2 and Figure 6B). PStS effects from M1, at 60 μA showed longer latencies with an average of 10.8 ± 1.9 ms compared to SMA and CMAd with latencies of 34.1 ± 9.3 ms and 35.3 ± 12.2 ms respectively (P < 0.001). PStS latencies from CMAd and SMA were not different from each other (P > 0.05). Comparing proximal and distal joints, the latencies of suppression effects were not different (P > 0.05) for any of the three areas (SMA, CMAd and M1). Whereas M1 PStF latencies became shorter at the higher intensity of stimulation, shortening of latency was not observed for PStS (P > 0.05) (Figure 6B). It should be emphasized that our analysis of M1 PStS data is based on a relatively small number of effects since most of the PStS effects changed sign and become excitatory at 60 μA. Out of 52 PStS effects obtained from M1

sites at 15 μA, only 11 PStS effects remained inhibitory at 60 μA. Our sample of PStS effects from CMAd was also relatively small. This may explain the irregular shape of the latencies plotted in Figure 6B, the broader standard deviation of mean (SEM) and the lack of PStEs for intrinsic hand muscles (Figure 6B & D).

The average magnitudes of PStS for SMA and CMAd respectively were -14.0 ± 3.8 and -12.2 ± 3.3 ppi, 2-fold weaker than those recorded from M1 (-28.6 ± 14.7 ppi) ($P < 0.001$). PStS magnitudes from CMAd and SMA were not different from each other ($P > 0.05$). Magnitudes of suppression effects at proximal and distal joints were also not different when compared within the same motor area (SMA, CMAd & M1) ($P > 0.05$). The strongest magnitude of PStS from M1 came from ED 2,3 (ppd=-65). SMA showed the greatest number of suppression effects (N= 172), with the majority occurring in distal joints (66%) compared to proximal joints (34%) (Table 2). The muscles showing the largest number of suppression effects were ED 2,3, FDP and EDC for SMA, and ED 2,3 and EDC for CMAd (Figure 7B). Among joints, SMA PStS effects were weaker for shoulder muscles than elbow, wrist and intrinsic hand muscles ($P < 0.0015$). The strongest suppression effects from SMA came from in order ECU, FCU, EDC and BRA with magnitudes between -22 and -27 ppd.

PStEs from the contralateral SMA

A total of 13 tracks were performed in SMA of the hemispheres of both monkeys ipsilateral to the recorded muscles. Nine PStEs were obtained, including 7 PStF and 2 PStS effects. These effects had average latencies of 10.1 ± 3.3 ms and 19.0 ± 3.2 ms, and magnitudes of 13.5 ± 4.1 ppi and -12.6 ± 1.1 ppd for PStF and PStS respectively. Latencies from the ipsilateral SMA were shorter than those observed for the contralateral SMA ($P < 0.004$). The magnitudes were similar to the means for effects from the contralateral SMA ($P > 0.05$). The majority of the facilitation effects came from distal muscles (N=6). The shortest latency and the strongest magnitude effects observed from the ipsilateral SMA were in ECU and ADE respectively. The two inhibitory effects were in distal muscles only.

DISCUSSION

The goals of this paper were to investigate the organization of SMA and CMAd in terms of their distal versus proximal forelimb muscle representations and compare their forelimb organization to that reported previously for M1 by Park *et al*. (2001). We also investigated the motor output properties from SMA and CMAd in comparison to M1 using the same parameters of stimulation. Finally, we also restricted our data analysis to sites where stimulation was performed in or near layer V of the cortical gray matter.

Forelimb organization of SMA

Figure 3 summarizes the organization of the forelimb representation of SMA. Proximal and distal representations were found not to be segregated in SMA in contrast to the M1 forelimb representation, which is organized into a segregated core of distal muscle representation surrounded by a horseshoe–shaped proximal muscle representation. In addition, these pure proximal and distal representations were separated by a large zone producing effects in both proximal and distal muscles (Park *et al*., 2001). This zone was termed the proximal-distal cofacilitation zone and was viewed as well suited to produce the patterns of distal and proximal muscle coactivation needed for coordinated multijoint movements. The lack of intra-areal (within limb)

topographic organization observed in SMA has also been noted in a number of previous studies in which ICMS was used to evoke movements (Macpherson *et al*., 1982a; Mitz and Wise, 1987; Luppino *et al*., 1991). In contrast, the forelimb representation of SMA, based on injections of retrograde tracers in the upper and lower segments of the spinal cord, showed that the corticospinal neurons involved in the control of distal muscles were largely located caudally in the mesial wall compared to those involved in the control of proximal muscles (He *et al*., 1995). A small overlapping area of neurons projecting to both proximal and distal cervical segments was found between these two segregated representations. The representations of proximal and distal muscles in SMA were interpreted to be largely separate from each other based on high density bins (200 μm) analysis of corticospinal neurons. The disparities existing in the forelimb organization of SMA between ICMS, including our StTA findings, and the anatomical studies mentioned above might be explained by spread of effective current with ICMS. We estimate the effective spread of current from a 60 μA stimulus to have a radius of 210 μm, which yields an area with a diameter of approximately ~420 μm (Stoney *et al*., 1968; Ranck, 1975; Tehovnik, 1996; Park *et al*., 2001). A spread of current of a radius of ~0.5 mm could potentially activate more than one of the high density bins of corticospinal neurons (200 μm) and/or activate cells belonging to a different muscle group not counted in these high density

bins, resulting in the cofacilitation of proximal and distal muscles observed in ICMS studies.

Discrepancies also exist regarding the muscles mainly represented in SMA. ICMS studies have reported that the proximal muscles are more presented in SMA (Mitz and Wise, 1987; Luppino *et al*., 1991). In contrast, the topographic organization of SMA examined by injecting retrograde tracers into the cervical segments of the spinal cord demonstrated that distal muscles were slighter more represented in SMA (He *et al*., 1995). Our results confirm this last finding as 64% of the PStF effects from SMA were distributed in distal joints. In addition, we also found that the muscles mainly represented in SMA came from distal joints (FDP, FDS, ED2 &3). Some ICMS studies have reported that distal forelimb movements were evoked from sites located in the lowest posterior part of the mesial surface of SMA (Macpherson *et al*., 1982b; Luppino *et al*., 1991). We also found an area where a large number of PStEs were produced in distal muscles (Figure 4) but this failed to achieve statistical significance.

Forelimb organization of CMAd

Only few studies have used ICMS to assess the distribution of evoked movements in the dorsal bank of the cingulate sulcus. The majority of these studies have reported a segregated forelimb representation located rostrally to a smaller hindlimb representation (Akazawa *et al*., 2000; Takada *et al*.,

2001; Akkal *et al*., 2002). However, these studies did not systemically characterize the proximal and distal forelimb representations of CMAd. Luppino *et al*. (1991) investigated in detail the organization of the dorsal bank of the cingulate sulcus, including the distribution of evoked movements in distal and proximal joints. They reported that hindlimb movements were mainly evoked in CMAd and that a small representation of forelimb movements was found caudally to the hindlimb representation. The majority of forelimb movements came from proximal joints. However, an area where wrist movements were evoked in isolation was found in the most caudal part in the dorsal bank of the cingulate sulcus (Luppino *et al*., 2001). Based on injections of retrograde tracers in upper and lower segments of the spinal cord, CMAd corticospinal neurons involved in the control of distal muscles were found to form two islands within the arm representation, a large one located rostrally on the dorsal bank of the cingulate sulcus and a smaller one located more caudally. Neurons involved in the control of proximal muscles were present rostrally within the larger distal arm representation of CMAd. The number of corticospinal neurons involved in the control of distal muscles was four times greater than those involved in the control of proximal muscles (He *et al*., 1995).

Although our data set consists of a relatively small number of PStEs from CMAd derived largely from one animal, our results do confirm that forelimb muscles are represented in CMAd and the effects are largely

distributed to distal muscles as reported previously in the anatomical studies of He *et al*. (1995). In contrast with the organization of Luppino *et al*. (1991) based on ICMS evoked movements, we found a larger representation of distal muscles extending rostro-caudally on the entire extent of the dorsal bank of the cingulate sulcus and the representation of proximal muscles was found to be located caudally to the representation of distal muscles. The forelimb organization of CMAd we found is in general agreement with the forelimb organization based on the anatomical studies of He *et al*. (1995), We were unable to adequately determine if a second segregated representation of distal muscles exists in the caudal part of CMAd because we did not perform tracks that far caudally.

Comparison of PStF effects from SMA, CMAd & M1

In a previous publication, we compared the output properties of SMA to extrapolated values of PStEs from M1 for a current intensity of 60 μA based on M1 PStEs obtained in previous studies at an intensity of 15 μA (Park *et al*., 2004; Boudrias *et al*., 2006). In the current study, stimulation at 15 and 60 μA were performed at the same sites in M1. The selection of the M1 data set stimulated at an intensity of 60 μA was based on the PStEs recorded in the same muscles at an intensity of 15 μA. The latencies of facilitation effects stimulated at 60 μA averaged 1.2 ms shorter than those at 15 μA. The presence of shorter latencies agrees with the reduced utilization time of ~0.8

ms reported when the somas or the axons of M1 corticospinal neurons are activated more directly (Cheney and Fetz, 1985). At 60 μA, the number of activated muscles enlarged to include almost all the recorded muscles (Figure 4). This can be explained at least partially by greater physical and physiological spread of effective stimulus current at 60 μA compared to 15 μA (Jankowska *et al*., 1975; Park *et al*., 2001).

At 60 μA, latencies of facilitation effects from SMA and CMAd were on average 8-12 ms longer that those observed for M1. As described in greater detail in a previous publication (Boudrias *et al*., 2006), the longer latency and the greater variability in the latency of SMA effects reflect a more indirect coupling with motoneurons and a slower corticospinal conduction velocity than that for M1. The magnitudes of the PStEs from M1 were on average 9-10 fold stronger than those from SMA and CMAd and no progressive increase in the magnitudes of the facilitation effects by muscle group, going from the most proximal to the most distal muscles, was found for SMA or CMAd. The magnitude difference is somewhat less than the 15-fold difference previously estimated based on extrapolated magnitudes of PStEs in M1 at a current intensity of 60 μA (Boudrias *et al*., 2006). However, the increase in the magnitude of effects in distal muscles was ~13-fold greater for M1 in comparison to CMAd and SMA, in agreement with our previous estimates. Output effects on EMG activity from CMAd were very similar to those from SMA. With few exceptions, no differences were observed between the

latencies and the magnitudes of their PStEs. This suggests that CMAd parallels SMA in terms of its capacity to influence muscle activity and movement. In fact, single unit recordings have also reported remarkable similarities between CMAd and SMA in the roles they seem to play in the production of visually-guided arm movements (Russo *et al*., 2002).

Our results are in agreement with the limited corticospinal projections of SMA (11%) and CMAd (4%) to motor nuclei in the spinal cord ventral horn compared to M1 (28%) (Dum and Strick, 1996; Maier *et al*., 2002). In fact, the majority of the corticospinal terminations from SMA (87%) and CMAd (90%) are confined to the intermediate zone of the spinal cord (laminae V-VIII) where different populations of interneurons are located. However, it should be noted that the dendrites of spinal motoneurons project into the intermediate zone so observing that the terminations of corticospinal neurons are restricted to the intermediate zone would not rule out the presence of direct synaptic connections with motoneurons. Nevertheless, as suggested previously, the major contribution of SMA and CMAd, to movement initiation and control might be achieved through cortico-cortical connections with M1 and/or innervation of spinal interneurons influencing reflex and other spinal circuits rather than providing direct input to motoneurons (Boudrias *et al*., 2006).

Stimulation restricted to layer V of the cortical gray matter of SMA did not significantly alter the latencies of facilitation and suppression effects when compared to our previous study based on effects collected in all layers of the

cortical gray matter of SMA ($P > 0.05$). However, the magnitudes of facilitation and suppression effects for sites in or near layer V showed were stronger than those based on all cortical layers of SMA ($P < 0.007$). This is consistent with more effective activation of corticospinal neurons when stimulation is applied close to layer V.

Distribution of suppression effects in SMA, CMAd & M1

The latencies PStS effects in M1 were ~3 ms longer than the latencies of its PStF effects reflecting a less direct coupling and/or the presence of an additional synapse, most likely on a spinal inhibitory neuron, interposed between the corticospinal neurons and the motoneurons (Kasser and Cheney, 1985). The distribution of PStS latencies in SMA and CMAd were broader as reflected by the larger values of standard deviations and had longer latencies (23 ms longer) that those from M1. As discussed in our previous paper, it has been reported that inhibitory effects produced in M1 pyramidal tract neurons evoked by stimulation of SMA had a mean latency of 6.7 ms (Tokuno and Nambu, 2000). Therefore, the average latencies of PStS observed from SMA and CMAd cannot be accounted for based on cortico-cortical connections producing disfacilitation of M1 corticospinal neurons (Boudrias *et al*., 2006). Longer latencies of suppression may reflect the different roles played by SMA and CMAd in specific aspects of movement production. For instance, the large number of suppression effects produced in

distal and proximal joints from SMA may be important for planning the temporal organization of movements, as reported in single unit recording studies (Mushiake *et al*., 1991; Tanji and Shima, 1994; Clower and Alexander, 1998; Shima and Tanji, 1998).

The majority of M1 PStS effects recorded at 15 μA changed sign to become facilitatory on at 60 μA so the number of effects that were present at both intensities was rather limited. Nevertheless, increasing the intensity of stimulation from 15 to 60 μA produced a 1.5-fold increase in the magnitude of PStS. We had previously estimated that this increase might be as high as 8-fold (Boudrias *et al*., 2006). In fact, the magnitudes of inhibitory effects at intensities of 15 and 60 μA were not statistically different from each other ($P > 0.05$). In addition, the magnitudes of inhibitory effects did not follow the large increase observed for facilitation effects in going from proximal to distal muscles, and did not show a preferential inhibition of the hand muscles. Moreover, latencies of suppression effects in M1 did not become significantly shorter at higher current intensities as observed for facilitation effects from M1. One interpretation of these results is that inhibition reaches a maximum at the spinal level at relatively low intensity of stimulation. However, an alternative explanation is that our estimate of the growth in magnitude of inhibition with stimulus intensity is too low because the true level of suppression is being masked by much more powerful facilitation that occurs at 60 μA.

The magnitudes of suppression effects in SMA and CMAd were 2-fold weaker that those from M1. As with the facilitation effects, this suggests a less efficient coupling with inhibitory interneurons in the spinal cord compared to M1.

PStEs from the contralateral SMA

PStEs were collected from SMA of the ipsilateral hemisphere, in agreement with the existence of a large number of corticospinal neurons originating from SMA (23%) with ipsilateral terminations in the cervical enlargement in the spinal cord (Dum and Strick, 1996). The facilitation and suppression effects showed latencies of 10.1 ± 3.3 ms and 19.0 ± 3.2 ms respectively. Interestingly, the average latencies of the facilitation effects from the ipsilateral SMA have very similar values to those encompassed by the SD range of M1 latencies.

Summary and Conclusion

Despite the fact that we quadrupled the number of tracks performed in SMA from our previous study (Boudrias *et al*., 2006), the resulting motor output maps of SMA did not reveal clear segregated representations of proximal and distal forelimb muscles compared to the segregated forelimb representations of M1. In CMAd we found a distal forelimb representation

located anterior to a smaller proximal muscle representation. We found that distal muscles are preferentially represented in SMA and CMAd in agreement with previous anatomical studies (Dum and Strick, 1991). Poststimulus effects (PStEs) from SMA and CMAd had latencies averaging 8-12 ms longer and magnitudes 9-10 fold weaker than those observed for M1. Moreover, unlike M1, no progressive increase in the magnitude of facilitation was observed for SMA or CMAd in going from the most proximal to the most distal muscles. Our results suggest that the typical corticospinal neuron in SMA and CMAd provides relatively weak direct input to spinal motoneurons compared to the robust synaptic effects from M1. The primary mechanisms by which SMA and CMAd influence motoneurons might be predominantly indirect through innervations of interneurons in the intermediate zone of the spinal cord and/or projections to M1.

Table 1. Summary of data collected from M1, SMA & CMAd

	M1			SMA			CMAd		
	Monkey Y	Monkey J	Total	Monkey Y	Monkey J	Total	Monkey Y	Monkey J	Total
Electrode tracks	18	12	30	97	66	163	28	19	47
Sites stimulated	29	22	51	574	440	1014	81	44	125
PStF effects	200	140	340	165	176	341	27	4	31
PStS effects	1	10	11	86	86	172	10	2	12
All PStEs	201	150	351	243	252	513	37	6	43

M1 data are based on effects that were present at both 15 and 60 μA. M1, SMA and CMAd data came from the same monkeys. CMAd, cingulate motor area dorsal; SMA, supplementary motor area; M1, primary motor cortex; PStE, poststimulus effect; PStF, poststimulus facilitation; PStS, poststimulus suppression.

Table 2. Latency and magnitude of PStF and PStS effects from M1, SMA & CMAd

	M1 @ 15 μA	M1 @ 60 μA	SMA @ 60 μA	CMAd @ 60 μA
Facilitation	N=340	N=340	N=341	N=31
Latencies (ms)				
Proximal	8.2 ± 1.4	7.1 ± 1.3	16.1 ± 5.1	18.6 ± 7.0
Distal	9.1 ± 1.5	8.0 ± 0.9	15.4 ± 4.9	20.4 ± 8.3
All	8.8 ± 1.6	7.7 ± 1.2	15.7 ± 5.0	19.8 ± 8.0
Magnitudes (ppi)				
Proximal	24.1 ± 16.3	90.8 ± 63.2	14.6 ± 5.9	12.5 ± 4.3
Distal	51.7 ± 59.4	196.8 ± 155.7	15.2 ± 4.5	16.9 ± 4.9
All	41.8 ± 50.4	158.8 ± 140.1	14.9 ± 5.2	15.6 ± 5.1
Distribution				
Proximal	30%	30%	36%	21 %
Distal	70%	70 %	64%	79 %
All PStF *	97 %	97 %	66%	72%
Inhibition	N=11	N=11	N=172	N=12
Latencies (ms)				
Proximal	8.2 ± 0.8	8.8 ± 0.8	33.3 ± 8.8	35.2 ± 14.3
Distal	11.3 ± 1.2	11.6 ± 1.5	32.3 ± 8.9	35.3 ± 10.5
All	10.5 ± 1.9	10.9 ± 2.0	32.7 ± 8.9	35.3 ± 12.2
Magnitudes (ppd)				
Proximal	-19.3 ± 9.4	-28.9 ± 15.0	-12.5 ± 3.5	-10.6 ± 2.4
Distal	-16.4 ± 9.7	-27.9 ± 13.6	-18.8 ± 3.5	-13.4 ± 3.3
All	-17.2 ± 9.7	-28.6 ± 15.4	-13.3 ± 3.6	-12.2 ± 3.3
Distribution				
Proximal	20%	20%	34%	39%
Distal	80%	80%	66%	61%
All PStS *	3%	3%	34%	28%

M1 data are based on effects that were present at both 15 and 60 μA. CMAd, SMA and M1 data came from the same monkeys. Magnitudes are expressed as peak percent increase (ppi) and peak percent decrease (ppd). CMAd, cingulate motor area dorsal: M1, primary motor cortex; PStF, poststimulus facilitation; PStS, poststimulus suppression; SMA, supplementary motor area.
* All PStF and all PStS as a percent of the total number of PStEs obtained.

Figure 1. Reconstruction procedures of the mesial wall based on MR images and electrophysiological data. (A) Surface view of the penetration maps of the left hemisphere for both monkeys. Sites where ICMS produced face and mouth movements in M1 and ventral premotor area (PMv) are marked by pink circles; Sites where ICMS produced hindlimb movements in M1 are marked by yellow circles; Sites randomly selected in M1 forelimb areas stimulated at both intensities of 15 and 60 μA are marked by orange circles: Sites where StTA yielded poststimulus effects (PStEs) in SMA are marked by red circles; Sites where StTA yielded no PStEs in SMA and when StTA was performed in CMAd are marked by blue circles; Sites where StTA yielded PStEs in SMA and where StTA was applied to sites in CMAd are marked by green circles; Sites where StTA did not produce PStEs in SMA are marked by black circles; Sites used for surface reconstruction of the brain but where data collected were not included in this analysis are marked by small gray circles. Numbers 1-11 are 1 mm apart and refer to the coronal section represented on the unfolded layer V map in (C). (B) Coronal section (Monkey J, section 1) of the mesial wall and the cortical dorsal surface in SMA based on MRI image; (C) Map of unfolded layer V of the gray matter of SMA and CMAd represented in two-dimensional coordinates. Doted lines indicate the anatomical markers. Abbreviations: A, Anterior; ArS, arcuate sulcus; CS, central sulcus; M, medial; MID, midline; SPS, superior precentral sulcus.

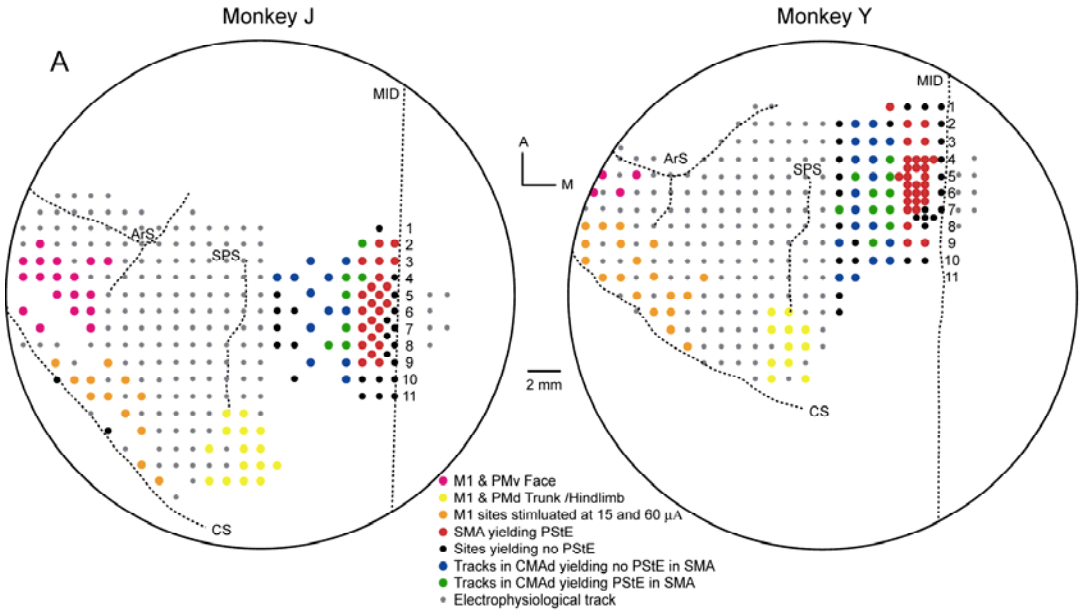
Monkey J
Monkey Y
A
MID
ArS
SPS
CS
1
2
3
4
5
6
7
8
9
10
11
A
M
2 mm
M1 & PMv Face
M1 & PMd Trunk /Hindlimb
M1 sites stimluated at 15 and 60 µA
SMA yielding PStE
Sites yielding no PStE
Tracks in CMAd yielding no PStE in SMA
Tracks in CMAd yielding PStE in SMA
Electrophysiological track

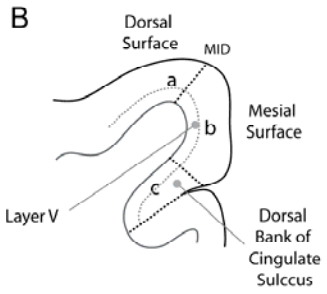
B
Dorsal Surface
MID
a
b
c
Mesial Surface
Layer V
Dorsal Bank of Cingulate Sulccus

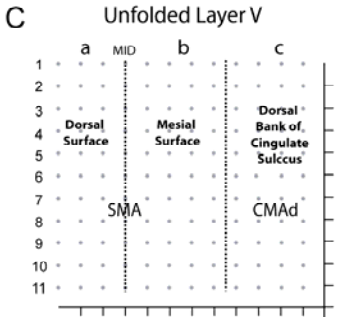
C
Unfolded Layer V
a
MID
b
c
1
2
3
4
5
6
7
8
9
10
11
Dorsal Surface
Mesial Surface
Dorsal Bank of Cingulate Sulccus
SMA
CMAd

Figure 2. Two-dimensional unfolded layer V maps of the mesial wall showing the organization of PStF and PStS at each joint (shoulder, elbow, wrist, digit and intrinsic hand) based on StTA of EMG activities for each monkey. The color-shaded motor representation for each joint is explained in the legend. Unfolded map procedures are explained in Figure 1.

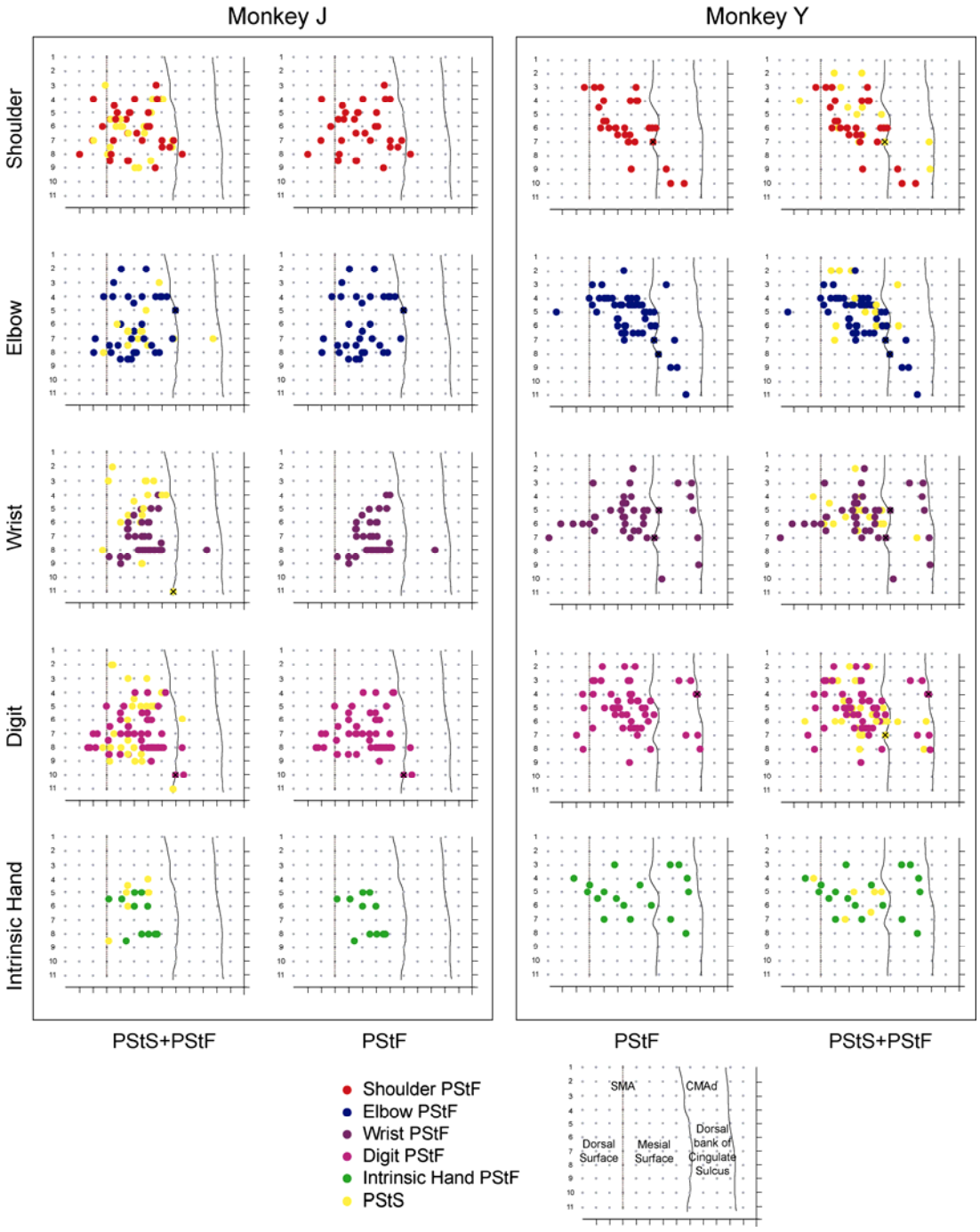
Monkey J
Monkey Y
Shoulder
Elbow
Wrist
Digit
Intrinsic Hand
PStS+PStF
PStF
PStF
PStS+PStF
Shoulder PStF
Elbow PStF
Wrist PStF
Digit PStF
Intrinsic Hand PStF
PStS
SMA
CMAd
Dorsal Surface
Mesial Surface
Dorsal bank of Cingulate Sulcus

Figure 3. Maps of SMA and CMAd for two monkeys represented in two-dimensional coordinates after unfolding the mesial wall of the cortex. Maps are based on PStF and PStS effects at proximal and distal joints. Effects marked with an X were not included in SMA or CMAd data set.

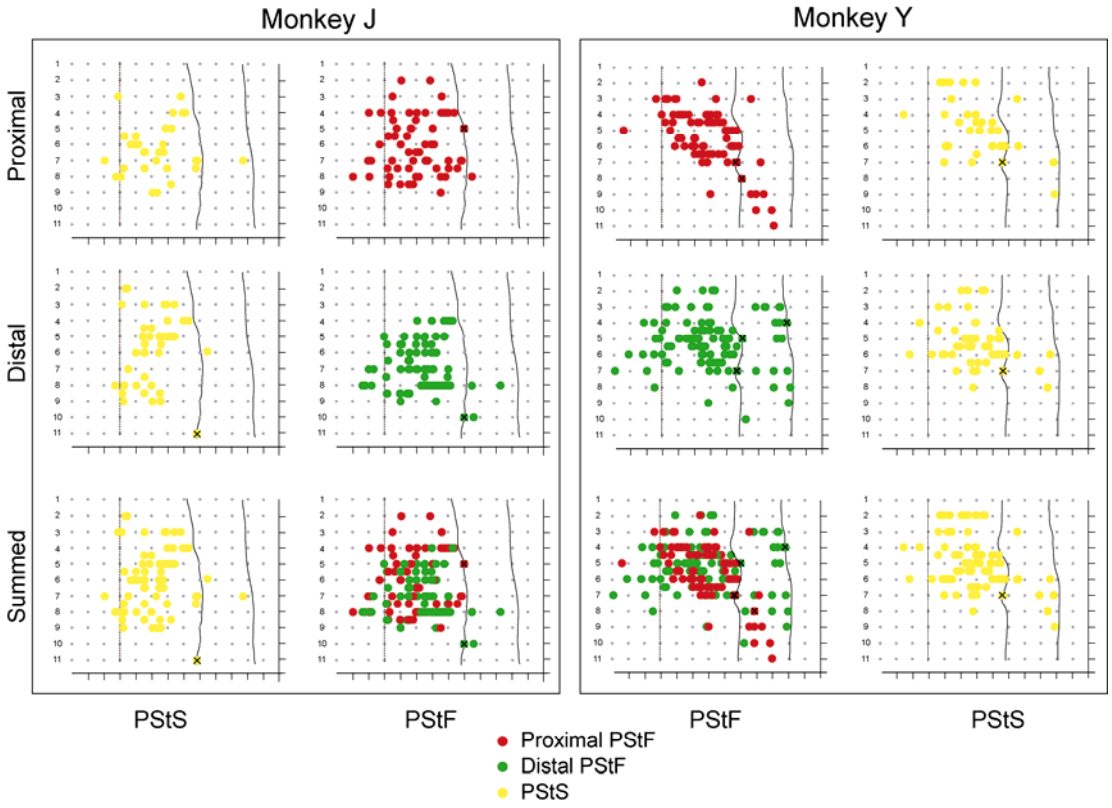
Monkey J
Monkey Y
Proximal
Distal
Summed
PStS
PStF
PStF
PStS
Proximal PStF
Distal PStF
PStS

Figure 4. Stimulus-triggered averages (StTA) of forelimb muscles from one SMA site (188J11) at 60 μA and one M1 site (267J9) at two different intensities, 15 and 60 μA. Time zero corresponds to the stimulus event used for constructing the average. Poststimulus facilitation (PStF) effects were observed in muscles shown in bold and no poststimulus effects in lighter gray. The range of the number of trigger events for different muscles is given in parenthesis.

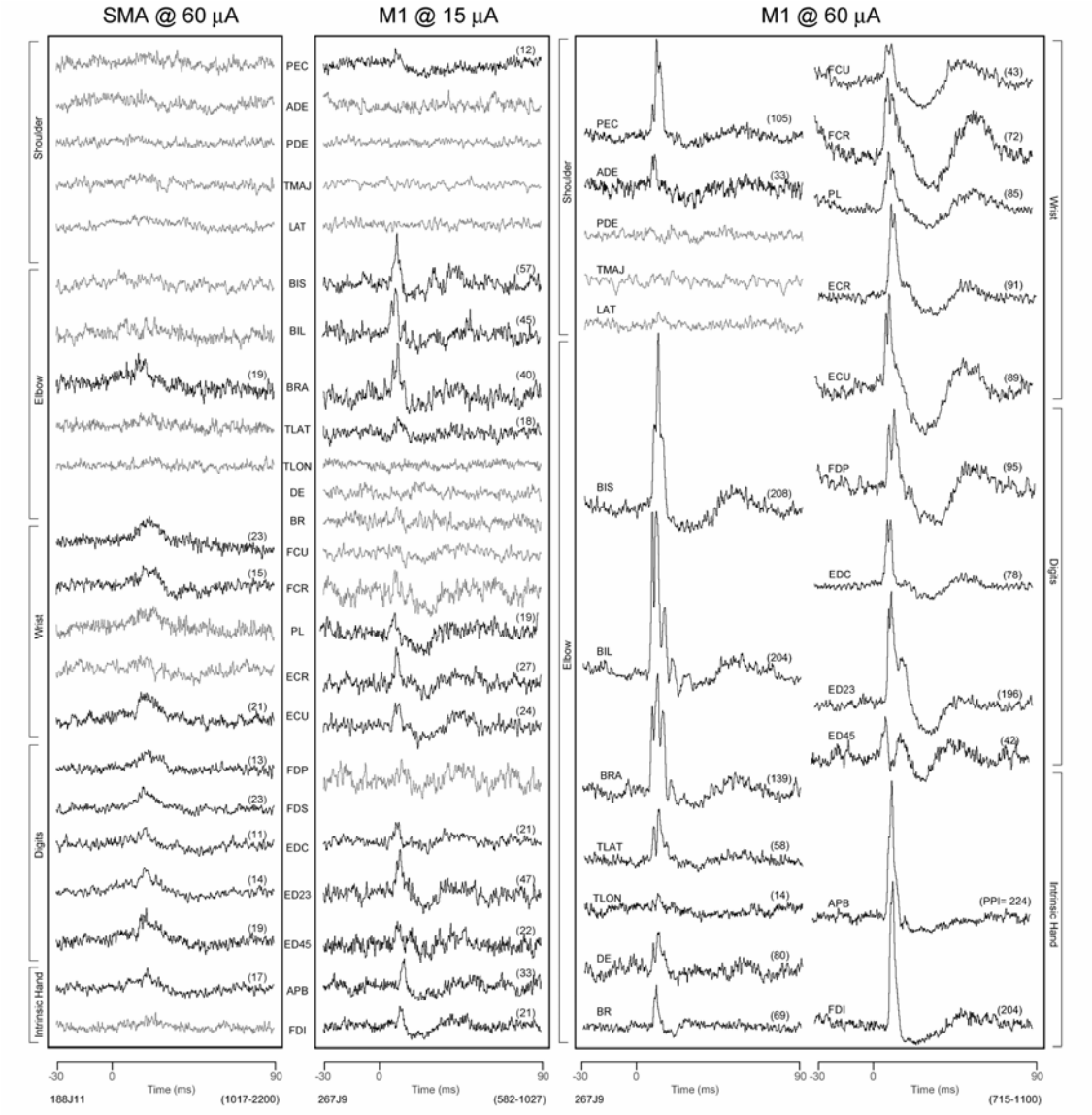
SMA @ 60 µA
M1 @ 15 µA
M1 @ 60 µA
Shoulder
Elbow
Wrist
Digits
Intrinsic Hand
PEC
ADE
PDE
TMAJ
LAT
BIS
BIL
BRA
TLAT
TLON
DE
BR
FCU
FCR
PL
ECR
ECU
FDP
FDS
EDC
ED23
ED45
APB
FDI
(12)
(57)
(45)
(40)
(18)
(23)
(15)
(19)
(27)
(24)
(21)
(47)
(22)
(33)
(105)
(33)
(208)
(204)
(139)
(58)
(14)
(80)
(69)
(43)
(72)
(85)
(91)
(89)
(95)
(78)
(196)
(42)
(PPI= 224)
(204)
-30
0
90
Time (ms)
188J11
(1017-2200)
267J9
(582-1027)
267J9
(715-1100)

Figure 5. (A) Distribution of poststimulus facilitation (PStF) onset latencies for SMA, CMAd and M1 for muscles at all forelimb joints (N=341 for SMA, N=33 for CMAd, and N=340 for M1). (B) Distribution of PStF magnitudes for SMA, CMAd and M1 for muscles at all forelimb joints. Plots have different magnitudes scale. The magnitudes are expressed as a peak percent increase (ppi). The asterisk (*) in the graph of magnitudes for M1 corresponds to the highest magnitude value on the axis scale of SMA and CMAd.

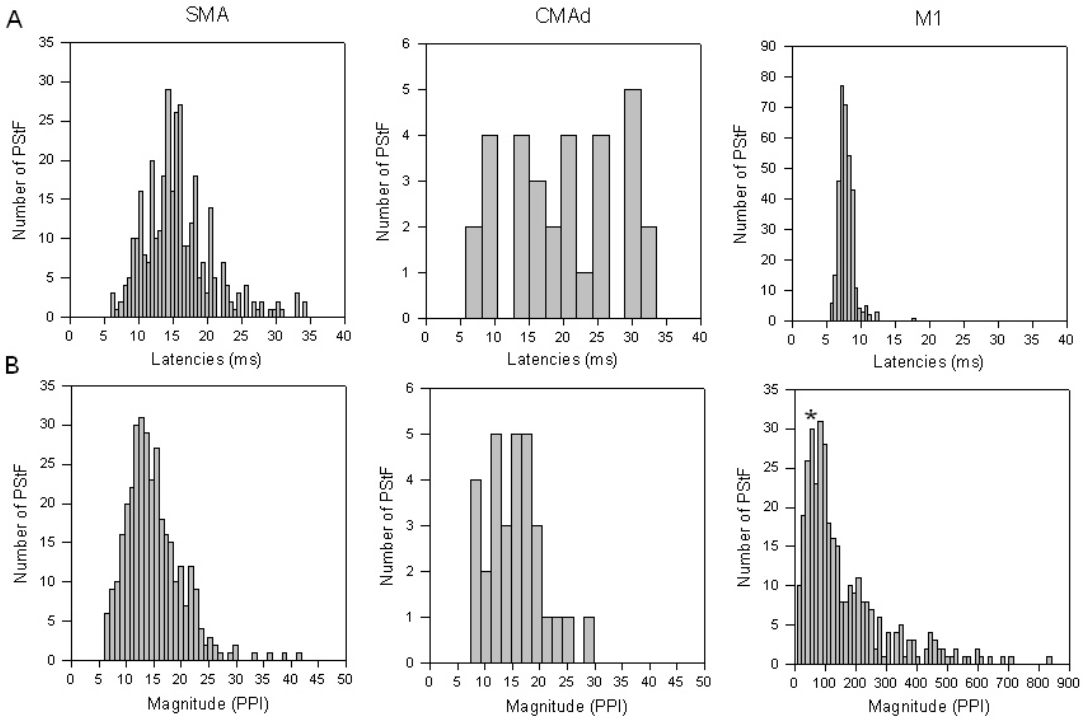
A
SMA
CMAd
M1
Number of PStF
Latencies (ms)
B
Magnitude (PPI)
*

Figure 6. Comparison of the latencies and magnitudes of the poststimulus effects from SMA, CMAd and M1 at different joints (shoulder, elbow, wrist, digit and intrinsic hand muscles). Two different stimulation intensities were used for M1 (15 and 60 μA). (A & B) Summed latencies of facilitation and inhibition of PStEs at each joint of two monkeys. For facilitation effects, N=341 for SMA, N=31 for CMAd, N=350 for M1 at 15 and 60 μA. For inhibition effects, N=172 for SMA, N=12 for CMAd, N=11 for M1 at 15 and 60 μA. (B & D) Summed magnitudes of facilitation and inhibition of PStEs at each joint of two monkeys. No PStS were present in CMAd for intrinsic hand muscles. The bars represent the standard error of the mean (SEM).

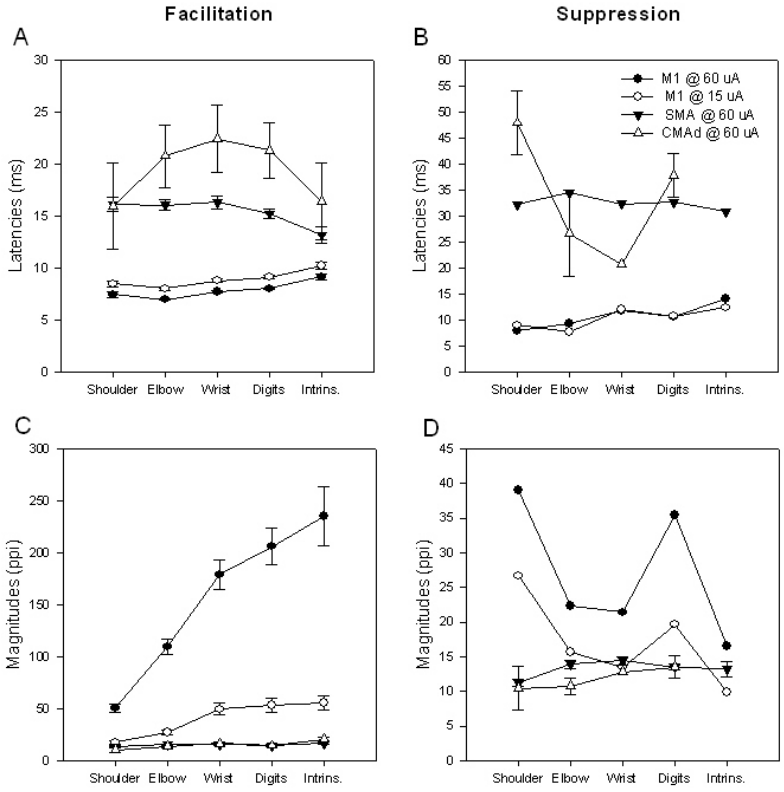
Facilitation
Suppression
A
B
C
D
Latencies (ms)
Magnitudes (ppi)
Shoulder
Elbow
Wrist
Digits
Intrins.
M1 @ 60 uA
M1 @ 15 uA
SMA @ 60 uA
CMAd @ 60 uA

Figure 7. Distribution of PStF (right) and PStS (left) obtained from 19-23 muscles of the forelimb for A) SMA & B) CMAd. The discontinuous lines separate muscles belonging to different joints. Pectoralis major (PEC), anterior deltoid (ADE), posterior deltoid (PDE), teres major (TMAJ) and latissimus dorsi (LAT), biceps short head (BIS), biceps long head (BIL), brachialis (BRA), triceps long head (TLON), triceps lateral head (TLAT) and dorso-epitrochlearis (DE), extensor carpi radialis (ECR), extensor carpi ulnaris (ECU), flexor carpi radialis (FCR), flexor carpi ulnaris (FCU) and palmaris longus (PL), extensor digitorum communis (EDC), extensor digitorum 2 and 3 (ED 2, 3), extensor digitorum 4 and 5 (ED 4, 5), flexor digitorum superficialis (FDS) and flexor digitorum profundus (FDP), abductor pollicis brevis (APB) and first dorsal interosseus (FDI). The asterisk (*) in muscles FCU and ED 4, 5 indicates effects from monkey J only. Because of the combination of muscles formed to produce TRI and Intrins. in monkey Y, the total number of effects in these muscles were divided by two and distributed equally in muscles labeled TLON and TLAT and in muscles labeled FDI and APB.

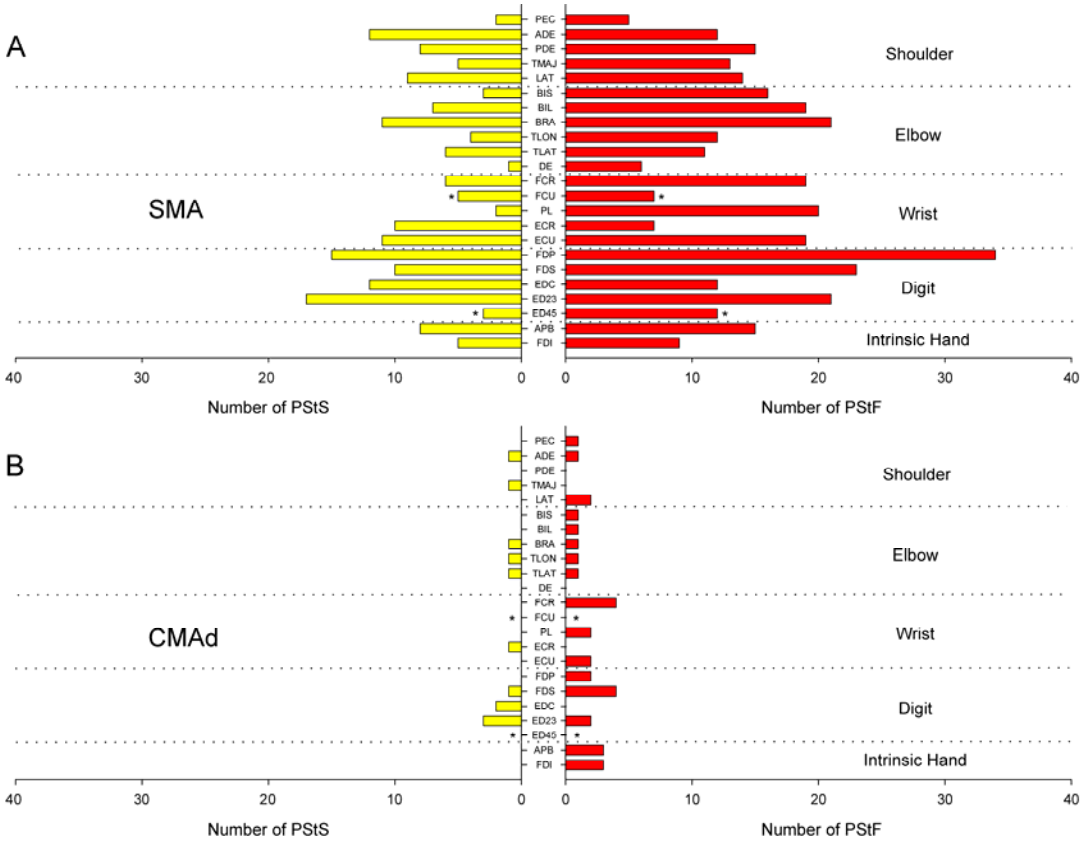
A
SMA
PEC
ADE
PDE
TMAJ
LAT
BIS
BIL
BRA
TLON
TLAT
DE
FCR
FCU
PL
ECR
ECU
FDP
FDS
EDC
ED23
ED45
APB
FDI
Shoulder
Elbow
Wrist
Digit
Intrinsic Hand
40
30
20
10
0
Number of PStS
Number of PStF
B
CMAd

REFERENCES

Akazawa T, Tokuno H, Nambu A, Hamada I, Ito Y, Ikeuchi Y, Imanishi M, Hasegawa N, Hatanaka N, Takada M (2000) A cortical motor region that represents the cutaneous back muscles in the macaque monkey. Neurosci Lett 282:125-128.

Akkal D, Bioulac B, Audin J, Burbaud P (2002) Comparison of neuronal activity in the rostral supplementary and cingulate motor areas during a task with cognitive and motor demands. Eur J Neurosci 15:887-904.

Asanuma H, Rosen I (1972) Topographical organization of cortical efferent zones projecting to distal forelimb muscles in the monkey. Exp Brain Res 14:243-256.

Belhaj-Saif A, Karrer JH, Cheney PD (1998) Distribution and characteristics of poststimulus effects in proximal and distal forelimb muscles from red nucleus in the monkey. J Neurophysiol 79:1777-1789.

Boudrias MH, Belhaj-Saif A, Park MC, Cheney PD (2006) Contrasting properties of motor output from the supplementary motor area and primary motor cortex in rhesus macaques. Cereb Cortex 16:632-638.

Cheney PD, Fetz EE (1985) Comparable patterns of muscle facilitation evoked by individual corticomotoneuronal (CM) cells and by single intracortical microstimuli in primates: evidence for functional groups of CM cells. J Neurophysiol 53:786-804.

Clower WT, Alexander GE (1998) Movement sequence-related activity reflecting numerical order of components in supplementary and presupplementary motor areas. J Neurophysiol 80:1562-1566.

Dum RP, Strick PL (1991) The origin of corticospinal projections from the premotor areas in the frontal lobe. J Neurosci 11:667-689.

Dum RP, Strick PL (1996) Spinal cord terminations of the medial wall motor areas in macaque monkeys. J Neurosci 16:6513-6525.

Galea MP, Darian-Smith I (1994) Multiple corticospinal neuron populations in the macaque monkey are specified by their unique cortical origins, spinal terminations, and connections. Cereb Cortex 4:166-194.

He SQ, Dum RP, Strick PL (1995) Topographic organization of corticospinal projections from the frontal lobe: motor areas on the medial surface of the hemisphere. J Neurosci 15:3284-3306.

Inase M, Sakai ST, Tanji J (1996) Overlapping corticostriatal projections from the supplementary motor area and the primary motor cortex in the

macaque monkey: an anterograde double labeling study. J Comp Neurol 373:283-296.

Jankowska E, Padel Y, Tanaka R (1975) The mode of activation of pyramidal tract cells by intracortical stimuli. J Physiol 249:617-636.

Kasser RJ, Cheney PD (1985) Characteristics of corticomotoneuronal postspike facilitation and reciprocal suppression of EMG activity in the monkey. J Neurophysiol 53:959-978.

Kuypers HGJM (1981) Anatomy of the descending pathways. In: In: Handbook of physiology- the nervous system II (Brookhart J, Mountcastle V, eds), pp 597-666: Bethesda, MD: American Physiology Society.

Luppino G, Matelli M, Camarda RM, Gallese V, Rizzolatti G (1991) Multiple representations of body movements in mesial area 6 and the adjacent cingulate cortex: an intracortical microstimulation study in the macaque monkey. J Comp Neurol 311:463-482.

Macpherson J, Wiesendanger M, Marangoz C, Miles TS (1982a) Corticospinal neurones of the supplementary motor area of monkeys. A single unit study. Exp Brain Res 48:81-88.

Macpherson JM, Marangoz C, Miles TS, Wiesendanger M (1982b) Microstimulation of the supplementary motor area (SMA) in the awake monkey. Exp Brain Res 45:410-416.

Maier MA, Armand J, Kirkwood PA, Yang HW, Davis JN, Lemon RN (2002) Differences in the corticospinal projection from primary motor cortex and supplementary motor area to macaque upper limb motoneurons: an anatomical and electrophysiological study. Cereb Cortex 12:281-296.

Matelli M, Luppino G, Rizzolatti G (1991) Architecture of superior and mesial area 6 and the adjacent cingulate cortex in the macaque monkey. J Comp Neurol 311:445-462.

McKiernan BJ, Marcario JK, Karrer JH, Cheney PD (1998) Corticomotoneuronal postspike effects in shoulder, elbow, wrist, digit, and intrinsic hand muscles during a reach and prehension task. J Neurophysiol 80:1961-1980.

Mitz AR, Wise SP (1987) The somatotopic organization of the supplementary motor area: intracortical microstimulation mapping. J Neurosci 7:1010-1021.

Mushiake H, Inase M, Tanji J (1991) Neuronal activity in the primate premotor, supplementary, and precentral motor cortex during visually

guided and internally determined sequential movements. J Neurophysiol 66:705-718.

Park MC, Belhaj-Saif A, Cheney PD (2000) Chronic recording of EMG activity from large numbers of forelimb muscles in awake macaque monkeys. J Neurosci Methods 96:153-160.

Park MC, Belhaj-Saif A, Cheney PD (2004) Properties of primary motor cortex output to forelimb muscles in rhesus macaques. J Neurophysiol 92:2968-2984.

Park MC, Belhaj-Saif A, Gordon M, Cheney PD (2001) Consistent features in the forelimb representation of primary motor cortex in rhesus macaques. J Neurosci 21:2784-2792.

Porter R, Lemon RN (1993) Corticospinal function and voluntary movement. Oxford: Clarendon Press.

Ranck JB, Jr. (1975) Which elements are excited in electrical stimulation of mammalian central nervous system: a review. Brain Res 98:417-440.

Russo GS, Backus DA, Ye S, Crutcher MD (2002) Neural activity in monkey dorsal and ventral cingulate motor areas: comparison with the supplementary motor area. J Neurophysiol 88:2612-2629.

Shima K, Tanji J (1998) Both supplementary and presupplementary motor areas are crucial for the temporal organization of multiple movements. J Neurophysiol 80:3247-3260.

Stoney SD, Jr., Thompson WD, Asanuma H (1968) Excitation of pyramidal tract cells by intracortical microstimulation: effective extent of stimulating current. J Neurophysiol 31:659-669.

Takada M, Tokuno H, Hamada I, Inase M, Ito Y, Imanishi M, Hasegawa N, Akazawa T, Hatanaka N, Nambu A (2001) Organization of inputs from cingulate motor areas to basal ganglia in macaque monkey. Eur J Neurosci 14:1633-1650.

Tanji J, Shima K (1994) Role for supplementary motor area cells in planning several movements ahead. Nature 371:413-416.

Tehovnik EJ (1996) Electrical stimulation of neural tissue to evoke behavioral responses. J Neurosci Methods 65:1-17.

Tokuno H, Nambu A (2000) Organization of nonprimary motor cortical inputs on pyramidal and nonpyramidal tract neurons of primary motor cortex: An electrophysiological study in the macaque monkey. Cereb Cortex 10:58-68.

CHAPTER 4

OUTPUT PROPERTIES AND ORGANIZATION OF THE FORELIMB REPRESENTATION OF MOTOR AREAS ON THE LATERAL ASPECT OF THE HEMISPHERE OF RHESUS MACAQUES

ABSTRACT

The goal of this study was to assess the motor output capabilities of the forelimb representation of dorsal premotor (PMd) and ventral premotor (PMv) areas relative to the primary motor cortex (M1) in terms of latency, strength, sign, and distribution of effects. Stimulus-triggered averages (60 μA) of EMG activity collected from 19-24 forelimb muscles were computed at 458 tracks in layer V of the gray matter on the lateral aspect of the left hemisphere of two monkeys trained to perform a reach-to-grasp task. Poststimulus facilitation (PStF) showed significantly longer latencies from PMd and PMv compared to the PStF effects from M1 (2 ms and 2.5 ms respectively). Magnitudes of the effects were 7 to 9-fold greater in M1 compared to those from PMd and PMv. Facilitation effects from PMd and PMv did not follow the pattern of increased magnitudes of effects from proximal to distal muscles characteristic of M1. Latencies of poststimulus suppression (PStS) effects from M1 were 5 ms shorter and the magnitudes were 2-fold greater than the PStS effects recorded in PMd and PMv. Proximal muscles were mostly represented in PMd, whereas equal amounts of proximal and distal muscles were represented in PMv. A gradual increase in latency and decrease in magnitude was observed for facilitation and suppression effects in moving from M1 surface sites toward more anterior sites in PMd. Distal muscle representations were completely intermingled within the proximal

presentations of PMd and PMv. However, for many muscles, segregated areas producing suppression effects were found along the medial portion of PMd and adjacent M1. We conclude that motor output effects from PMd and PMv are inconsistent with a model of motor output typical of M1 corticospinal neurons. Our results suggest that effects on muscle activity from PMd and PMv are most likely achieved indirectly through cortico-cortical connections with M1 and/or comparatively weak interneuronal linkages in the spinal cord.

INTRODUCTION

The premotor cortex corresponds to the superior aspect of Brodmann's area 6 in primates and is located on lateral aspect of the hemisphere of the frontal cortex (Brodmann, 1909). The premotor cortex is composed of two functional representations, the dorsal motor area (PMd) and the ventral motor area (PMv). PMd and PMv are two of seven separable motor areas contained within the frontal lobe. Each of these areas contains corticospinal neurons and are involved in the control of forelimb movements (Dum and Strick, 1991; Galea and Darian-Smith, 1994). More significantly, corticospinal neurons from PMd and PMv project into and near motoneuronal pools suggesting a potential monosynaptic control over motoneurons, paralleling that from the primary motor cortex (M1) (Kuypers and Brinkman, 1970; Galea and Darian-Smith, 1994; He *et al*., 1995). Whereas the existence of monosynaptic M1 corticomotoneuronal linkages have been well characterized, the nature of the linkage from PMd and PMv corticospinal neurons to spinal motoneurons and the efficacy of effects from these areas on motor output remain largely unknown (Cheney and Fetz, 1980; Porter and Lemon, 1993; Maier *et al*., 2002; Shimazu *et al*., 2004).

Using intracortical microstimulation (ICMS), proximal and distal movements can be evoked in PMd and PMv (Godschalk *et al*., 1995; Graziano *et al*., 2002; Raos *et al*., 2003; Stark *et al*., 2007). The extent to

which segregated proximal and distal forelimb representations exist in PMd and PMv is debatable. Anatomical studies of PMd based on high density bins of labeled corticospinal neurons show a segregated forelimb representation of proximal muscles located laterally to a representation of distal muscles (He *et al*., 1993). The opposite organization was reported with evoked movements in ICMS studies in which a proximal forelimb representation was found to be located medially to a distal representation (Raos *et al*., 2003). Whereas segregated representations of proximal versus distal muscles were reported in the above studies, others studies have reported that proximal and distal movements in PMd are largely overlapping (Godschalk *et al*., 1995). In the case of PMv, recent studies have shown that its effects on muscular activity are mainly achieved indirectly through M1, suggesting a weak contribution of the corticospinal neurons on muscular activity (Cerri *et al*., 2003; Shimazu *et al*., 2004).

In comparison to ICMS and anatomical approaches, stimulus-triggered averaging (StTA) of electromyographic (EMG) activity has the advantage that both excitatory and inhibitory output effects to large number of individual muscles can be quantified in terms of magnitude, latency and distribution. Using this technique, the forelimb representation of M1 was mapped and the existence of segregated proximal and distal muscle representations were demonstrated (Park *et al*., 2000). Therefore, using StTA of EMG activity, the broad objective of this study was to assess the motor output capabilities of

PMd and PMv in producing forelimb movements in terms of sign (excitatory or inhibitory), latency and strength of output effects. We also systematically mapped the representation of PMd and PMv relative to 19-24 muscles of the forelimb, including the identification of the border between M1 and PMd, in an effort to further investigate their proximal, distal, and individual muscle representations. The same parameters of stimulation (60 μA) were used in PMd, PMv and M1 for direct comparison of their poststimulus effects on muscle activity.

MATERIALS AND METHODS

Behavioral task and Surgical procedures

Two male rhesus monkeys (*Macaca mulatta*, ~9 kg, 5 and 8 years of age) were trained to perform a reach-to-grasp task requiring coactivation of multiple proximal and distal forelimb muscles in natural synergies. The animals were identified as monkey J and monkey Y and will be referred as such throughout the report. On completion of training, each monkey was stereotaxically implanted with a 30 mm diameter cortical chamber over the left hemisphere at an angle of 15-degrees to the midsagittal plane. The specific coordinates of the chambers were anterior 20.9 mm and lateral 12.9 mm for monkey J and anterior 12.9 mm and lateral 9 mm for monkey Y. The location of the chamber allowed us to have full access to the forelimb representations of M1 and PMd, and to most medial portion of PMv in both monkeys. Chamber implantation and electrode placements were guided by a structural MRI obtained from a 3 Tesla Siemens Allegra system. The images were acquired with the monkey's head mounted in an MRI compatible stereotaxic apparatus. The orientation and location of the penetrations (Figure 1) were matched to the MRI reconstruction of the brain as described previously (Boudrias *et al*., 2006).

Each forelimb muscle was implanted with a pair of multi-stranded stainless steel wires (Cooner Wire, Chatsworth, California) which were led subcutaneously to connectors on the forearm (subcutaneous implant) or to a cranial connector attached to the acrylic surrounding the recording chamber (Park *et al*., 2000). While the monkeys were performing the task, EMG activity was recorded from 19-24 muscles of the forelimb including five shoulder muscles: pectoralis major (PEC), anterior deltoid (ADE), posterior deltoid (PDE), teres major (TMAJ) and latissimus dorsi (LAT); seven elbow muscles: biceps short head (BIS), biceps long head (BIL), brachialis (BRA), brachioradialis (BR), triceps long head (TLON), triceps lateral head (TLAT) and dorso-epitrochlearis (DE); five wrist muscles: extensor carpi radialis (ECR), extensor carpi ulnaris (ECU), flexor carpi radialis (FCR), flexor carpi ulnaris (FCU) and palmaris longus (PL); five digit muscles: extensor digitorum communis (EDC), extensor digitorum 2 and 3 (ED 2, 3), extensor digitorum 4 and 5 (ED 4, 5), flexor digitorum superficialis (FDS) and flexor digitorum profundus (FDP); and two intrinsic hand muscles: abductor pollicis brevis (APB) and first dorsal interosseus (FDI). In monkey Y, we recorded across FDI and APB because one wire in each muscle had high impedance. The combined FDI/APB recording was referred to as the intrinsic hand muscle (Intrins.). For similar reasons, one wire from TLAT and another one from TLON were combined to form a triceps muscle (TRI).

All surgeries were performed under deep general anesthesia and sterile conditions in accordance with the Association for Assessment and Accreditation of Laboratory Animal Care (AAALAC) and the Guide for the Care and Use of Laboratory Animals, published by the U.S. Department of Health and Human Services and the National Institutes of Health.

Data recording

Glass and mylar insulated platinum-iridium electrodes with typical initial impedances between 0.7-2 MΩ were used for cortical recording and stimulation (Frederick Haer & Co., Bowdoinham). The electrode was advanced with a manual hydraulic microdrive (Frederick Haer & Co., Bowdoinham) and stimulation was performed at 0.5 mm intervals in all layers of the gray matter. Only effects recorded near or in layer V of the gray matter were included in this study. Layer V was identified by calculating the depth of the penetration according to the first cortical electrical activity encountered and by the presence of increased background activity and spike amplitude typical of layer V. Electrode penetrations were made 1 mm apart over the full extent of the forelimb representation of M1, PMd, and on the most medial portion of PMv, except for a few sites that were made 2 mm apart in the forelimb representation of M1 in monkey J (Figure 1). Stimulus-triggered averages (15 and 60 μA at 7-15 Hz) of EMG activity were computed for 19-24 muscles of the forelimb from stimuli applied throughout all phases of the

reach-to-grasp task. StTAs were based on at least 500 trigger events. Individual stimuli were symmetrical biphasic pulses (0.2 ms negative followed by 0.2 ms positive). EMGs were filtered from 30 Hz to 1 KHz, digitized at 4 kHz and full-wave rectified. To prevent averaging periods where EMG activity was minimal or absent, segments of EMG activity associated with each stimulus were evaluated and accepted for averaging only when the data points over the entire epoch was equal to or > 5% of the full-scale input voltage level (± 5 Volt) of the CED Power 1401 (Cambridge Electronic Design ltd., Cambridge, UK). EMG recordings were tested for cross-talk by computing EMG-triggered averages and muscles were eliminated from the data set when cross-talk was observed (Cheney and Fetz, 1980).

Data analysis

Averages were compiled using an epoch of 60 ms in length, extending from 20 ms before the trigger to 40 ms after the trigger. Epoch duration was lengthened to 120 ms (30 ms pre-trigger to 90 ms post-trigger) for all sites in PMd of monkey Y and in randomly selected sites in PMv and M1 for both monkeys in order to evaluate the presence of a second long latency peak as previously observed in the supplementary motor area (SMA) (Boudrias *et al*., 2006). At each stimulation site, averages were obtained from all 19-24 muscles. Mean baseline EMG level and standard deviation (SD) were measured during the pre-trigger period. Poststimulus facilitation (PStF) and

suppression (PStS) effects were computer-measured. PStF effects were only considered significant if the envelope of the StTA crossed a level equivalent to 2 SD of the mean of the baseline EMG for a period of time equal to or greater than 1.25 ms (5 points). Peaks less than 2 SD of the baseline and peaks that remained above 2 SD for less than 1.25 ms period were not included in our data set. The magnitude of PStF and PStS was expressed as the percent increase or decrease (ppi & ppd) in EMG activity above (facilitation) or below (suppression) baseline.

M1 data base

A total of 174 tracks were performed in the different representations of M1 and along its borders with PMd and PMv. Effects collected from these tracks were used to form two different M1 data sets. For the comparison of the distribution of magnitudes and latencies of effects, penetrations in M1 were randomly selected throughout the forelimb and the data collected were at two different intensities, 15 and 60 μA (Tables 1, 2 & 3 and Figure 2). The use of 15 μA was based on previous StTA of EMG activity studies (Park *et al*., 2001; Park *et al*., 2004). A total of 30 tracks were selected in M1 from the two monkeys. Half of the penetrations were performed on the anterior part of M1 (cortical surface) and the other half were performed on the buried posterior part of M1 (wall of the precentral gyrus). Compared to a restricted number of muscles showing PStF effects at a stimulation intensity of 15 μA in M1, at 60

μA, the number of PStF effects at the same sites enlarged to include nearly all of the recorded muscles (Figure 7). For comparison of effects at 15 μA and 60 μA, only muscles with effects at both intensities from a particular cortical site were included.

An additional M1 data set was established for the study of the transition of the magnitude and latency of poststimulus effects (PStEs) in moving forward from the anterior part of M1 on the surface of the hemisphere into PMd (Figures 4, 5 & 6). For this analysis, only sites located on the anterior part of M1 and located medial to a line extending from the spur of arcuate sulcus were included in the data set. In other words, the line extending from the spur of the arcuate meets the curvature of central sulcus at a perpendicular angle; only effects from tracks located medial to this line were included in this M1 data set. All the PStEs produced at a stimulation intensity of 60 μA were included in these analyses**.**

Intracortical microstimulation to evoke movements

Motor output to body regions not implanted with EMG electrodes (face, trunk, hindlimb) were identified using repetitive intracortical microstimulation (ICMS) to evoke movements. ICMS consisted of a train of symmetrical biphasic stimulus pulses at a frequency of 330 Hz and intensity of 30-100 μA (Asanuma and Rosen, 1972). Train duration was 100-500 ms (Graziano *et al*., 2002). Hindlimb and facial movements were evoked respectively in the

most medial and lateral parts of M1 as described previously (Gentilucci *et al*., 1988; Park *et al*., 2001).

Boundary between M1 and PMd

We established the boundary between M1 and PMd based on a combination of criteria including: the number of PStEs, the density and the size of the cells assessed histologically, and the latency and the magnitude of PStF. Our placement of the boundary was consistent with previous studies (Dum and Strick, 1991; He *et al*., 1993; Kurata and Hoffman, 1994; Raos *et al*., 2003; Raos *et al*., 2004; Hoshi and Tanji, 2006; Stark *et al*., 2007).

Histology procedures

At the completion of neurophysiological testing, one monkey (monkey Y) underwent a final procedure in which ink tracks were placed stereotaxically into the forebrain as reference marks for reconstructing the location of motor area and for subsequent histological analysis. The monkey was then given a lethal dose of sodium pentobarbital (Euthasol, 100 mg per kg of body weight) and perfused transcardially with 0.1 M phosphate buffered saline, followed by 10% buffered formalin fixative. The brain was removed, cryoprotected, and cut in coronal sections on a freezing microtome at 50 μm. Alternate sections were mounted on clean, subbed slides and stained for Nissl substance (cresyl violet acetate) and myelin (Gallyas, 1979).

A neuroanatomical reconstruction system, consisting of a computer-interfaced microscope (Carl Zeiss, Inc.) and associated software (Neurolucida: Microbrightfield, Inc.), was used to record the location and diameter of layer V pyramidal cell bodies. One set of 12 cresyl violet-stained sections, 300 μm apart, was used to analyze pyramidal cell density and pyramidal cell size in relation to the M1/PMd border. Each large pyramidal neuron found on every sixth 50 μm section through the central M1/PMd border area was counted and measured for diameter. All measured cells contained a complete nucleus and/or had prominent apical and basal dendrites.

Soma diameters of pyramidal neurons in layer V were measured by averaging the length of the cell in the long axis and the width measured along a perpendicular through a point of the length at the maximum width. Using this criterion, we have defined “large pyramidal cells” as those with average maximal (length and width) diameters of greater than 25 μm. These large pyramidal cells were counted and measured in 1 mm distances from both sides of the M1/PMd border. No corrections were made for tissue shrinkage.

RESULTS

Poststimulus effects for this study were selected from layer V of the gray matter in the motor areas of the left hemisphere in two rhesus monkeys. Data were collected from PMd, PMv and M1 for a total of 458 electrode tracks performed on the dorsal aspect of the hemisphere of the frontal lobe and in the anterior bank of the central gyrus (Table 1 & Figure 1). ICMS was performed at sites where no PStEs in forelimb muscles were obtained to identify motor output to the trunk, hindlimb and face.

Boundary between M1 and PMd

We established the boundary between PMd and M1 to be ~5 mm anterior to the central sulcus (gray zone in Figure 1). This was based on a combination of criteria including: latencies, magnitudes, number of PStEs, density and cell count as well as from the boundaries established in previous studies (Dum and Strick, 1991; He *et al*., 1993; Kurata and Hoffman, 1994; Raos *et al*., 2003; Raos *et al*., 2004; Hoshi and Tanji, 2006; Stark *et al*., 2007). A large number of muscles showed a substantial decrease in the number of PStEs recorded before and after what we established to be the border between M1 and PMd and represented as the gray zone in Figure 1. This was particularly observable in distal joints in both monkeys.

Figures 4, 5 and 6 show the transition in latencies and magnitudes of PStEs in moving from sites on the surface of M1 toward more anterior sites in PMd. Negative distance values on the axis correspond to sites in M1 and the gray bar at zero corresponds to the boundary between M1 and PMd indicated as the gray zone of Figure 1. Note that PStEs in the gray zone were not included in the PMd or M1 data analysis. Positive distance values correspond to sites recorded in PMd. A gradual increase in latency and gradual decrease in magnitude of facilitation effects was observed in moving from sites in M1 toward sites in PMd (Figures 3 & 4). Some variability in PStEs in the M1 forelimb representation existed between the monkeys (Figure 5). For example, the M1 representation of monkey Y was 1 mm longer in the anterior-posterior axis and was located more laterally in relation to the spur of the arcuate sulcus compared to monkey J (Figure 1). Stronger magnitudes of effects, particularly in distal muscles, were obtained from the surface portion of M1 in monkey Y compared to those for monkey J (Figure 5A & B). In order to see the transition of effects in greater detail around the border, we re-plotted the data in Figure 5 E & F with a different vertical axis after eliminating data in M1 that was greater than 2.12 mm from the border with PMd (Figure 5G & H). The latencies of effects in moving from M1 sites toward more anterior sites in PMd increased in both monkeys (Figure 4) following a polynomial relationship (linear, $f = yo + ax$, $P < 0.0001$). A strong decreasing relationship (exponential decay, $f = a^{(-bx)}$, $P < 0.0001$) between the

magnitudes of effects and the distances from M1 sites toward PMd sites was also observed (Figure 5).

Figure 3A shows the histological results of cresyl violet staining in a coronal section through the M1/PMd border area. Hodological analysis of the large pyramidal cell densities in 1 mm increments demonstrated a decrease in density of large pyramidal cells in PMd approaching the M1 border (14 cells/mm to 8 cells/mm) and an increased density of large pyramidal cells across the border area from PMd into M1 (Figure 3B). A relatively small number of large pyramidal cells in the PMd area bordering M1 was followed by a gradual increase in the number of large pyramidal cells across M1. This increased density reached a maximum at the caudal region of M1 approaching the central sulcus.

Figure 3C shows the mean soma diameters of large pyramidal cells across the M1/PMd border. A total of 274 large pyramidal cells were measured. The mean maximal soma diameters are shown to increase at the immediate border area, and increase further across M1, reaching a maximum mean diameter 5 mm from the M1/PMd border. Soma diameters were significantly larger at 3 mm and beyond from the M1/PMd border compared to PMd pyramidal cell diameters at ~1 mm (ANOVA using Fisher's PLSD, $P < 0.05$).

The boundary between M1 and PMd was further compared to those established by previous anatomical and electrophysiological studies (Dum

and Strick, 1991; He *et al*., 1993; Kurata and Hoffman, 1994; Raos *et al*., 2003; Raos *et al*., 2004; Hoshi and Tanji, 2006; Stark *et al*., 2007). In these previous studies, the boundary between M1 and PMd was estimated to be 2 mm posterior to the end of the spur of the arcuate sulcus and/or 5 mm anterior to the central sulcus; this is in good agreement with the boundary established in our study and correlates well with transitions in the latency and magnitude of PStEs.

Properties of poststimulus effects (PStE) from M1

Figure 2A shows the distribution of PStF onset latencies for effects obtained in PMd, PMv and M1. PStF in M1 showed a narrow distribution compared to PMd and PMv with a peak in onset latency of 7.7 ± 1.2 ms (Table 3). Latencies from PMd and PMv were an average of 2.5 and 2 ms longer than respectively than those recorded in M1 (one-way ANOVA, $P < 0.0001$). At 60 μA, the vast majority of effects obtained from M1 was facilitation effects (97%) and distributed in distal muscles (70%). This can be explained by the fact that most of the inhibitory effects present at 15 μA changed sign to become facilitation effects when stimulation was applied at 60 μA.

The magnitudes of effects from M1 (Figure 2B) covered a broader range and were vastly stronger than those observed for PMd and PMv ($P < 0.0001$). M1 magnitudes had a mean ppi of 159 ± 140 and were 7 to 9-fold

stronger than those for PMd and PMv (Table 3 & Figure 2B). As described previously, M1 showed an increase in magnitude for each muscle group going from the most proximal to the most distal muscles (Park *et al*., 2004). This progressive trend was not present in PMd and PMv. All M1 PStF effects (46 effects) with magnitudes above 300 ppi were in distal muscles. Only 33 PStF effects from proximal joints had magnitudes above 105 ppi and they all came from elbow flexor muscles (16 for BRA, 13 for BIL, 2 for BIS, and 2 for BR).

Figure 7 shows typical effects found in shoulder, elbow, wrist, digit and intrinsic hand muscles from a given site in M1 at intensities of 15 and 60 μA. At 60 μA, the number of effects in M1 enlarged to include nearly all of the recorded muscles and the magnitude of effects increased by approximately 10-fold in some muscles. In comparison, typical effects found within PMd and PMv at 60 μA produced facilitation in only a few muscles (7 and 6 muscles respectively). In Figure 7, the strongest facilitation effects observed in PMd and PMv were 50 ppi (TRI) and 16 ppi (BRA) respectively.

Properties of Poststimulus facilitation (PStF) effects from PMd

Poststimulus effects from PMd included 256 PStF (74%) and 91 PStS (26%) (Table 2 & Figure 9A). Among the PStF effects, 71% were from proximal muscles and 29% from distal muscles. PStF from PMd had a mean latency of 10.2 ± 4.1 ms, 0.5 ms and 2.5 ms longer than those from PMv and

M1 (P = 0.0137 & P < 0.0001) (Table 3). The distribution of PStF latencies for PMd effects (Figure 2A) was broader than the distributions for PMv and M1 as reflected in the larger standard deviations (Table 3). Comparison across joints showed shorter latencies for shoulder muscles than distal muscles (P < 0.0002) (Table 3). Additionally, latencies for elbow muscles were shorter than those for digit muscles (P < 0.0007). PMd was the only area where onset latencies above 20 ms were observed (Figure 2A). When these effects were analyzed as a separate group, the average latency was 25.8 ± 2.8 ms. In previous work (Boudrias *et al*., 2006), we reported that the distribution of onset latencies for PStF effects from SMA contained both short and long latency peaks. However, only three late PStF effects with a mean latency of 52.1 ms were observed from PMd in this study and these were all from one monkey (monkey Y). These three effects were excluded from the final data analysis.

The average magnitude of PStF from PMd was 17.3 ± 7.6 ppi (Table 3). There was no difference in the magnitudes between muscle groups in PMd and no difference when compared to effects from PMv (P = 0.90 and P = 0.55 respectively). The strongest effects (> 27.5 ppi) all came from the proximal joints (strongest 22 effects). TRI was the muscle showing the strongest PStF from PMd (ppi = 52). Additionally, there was a strong correlation between onset latency and magnitude of PStF effects in PMd (polynomial quadratic, $f = yo + ax + bx^2$, P < 0.0001).

Properties of PStF effects from PMv

Poststimulus effects from PMv included 327 PStF (94%) and 20 PStS (6%) effects (Table 2 & Figure 3). Among the PStF effects, 52% came from proximal muscles and 48% from distal muscles (Figure 9B). PStF from PMv had a mean latency of 9.7 ± 1.8 ms (Table 3). The distribution of PStF latencies for PMv effects was narrower when compared to those for PMd, as reflected in the smaller standard deviations. Across joints, latencies for proximal muscles were shorter than those for distal muscles ($P < 0.0001$). Intrinsic hand muscle latencies were significantly longer than any other muscle group ($P < 0.0001$).

The average magnitude of PStF from PMv was 21.6 ± 15.2 ppi (Table 3). Elbow muscles in PMv had stronger magnitudes than shoulder, wrist, or digit muscles ($P < 0.0001$). Of the 11 strongest effects obtained from PMv, nine came from BRA and two from APB. These muscles had the strongest magnitudes observed among the secondary motor areas and were between 65 and 115 ppi. There was a strong correlation between onset latency and magnitude of PStF effects from PMv (exponential, $f = a^{(-bx)}$, $P < 0.0001$)

Properties of inhibitory effects

We compared suppression effects from PMd and PMv to M1 surface sites on the convexity of the precentral gyrus and to a random selection of M1 sites taken from both the surface and buried in the wall of the precentral

gyrus. The data base of randomly selected sites throughout the forelimb M1 representation included 30 tracks (Tables 1 & 2). In M1, the majority of suppression effects obtained at 15 μA became facilitatory (earliest effect) for stimulation at the higher intensity of 60 μA. In many of these cases, the effects were biphasic with strong early facilitation followed by later suppression. However, because of the difficulty in quantifying late suppression in biphasic effects, these effects were not measured. Only 11 PStS effects remained inhibitory at 60 μA (Table 2) and, though the sample was small, these effects were used for the comparisons that follow. The mean latency of PStS effects from M1 was 10.9 ± 1.9 ms, about 5 ms shorter than the mean latency from PMd and PMv ($P < 0.03$ & $P < 0.008$) (Table 3). The mean PStS magnitude from M1 (-28.6 ± 14.7, ppd) was about 2-fold greater than the magnitude of PStS from PMd and PMv ($P < 0.03$). No differences in PStS latency or magnitude were observed when comparing PMd PStS effects to those from PMv ($P = 0.96$ and $P = 0.37$ respectively).

As noted above, we also compared PMd and PMv effects to all M1 PStS effects obtained from at 60 μA from sites on the surface convexity of the precentral gyrus. The majority of these suppression effects were located near the medial boundary of M1 and PMd. Once again, decreased magnitudes and increased latencies were observed for PStS effects in moving from sites in M1 toward more anterior sites in PMd (linear regression, $f = yo + ax$, $P < 0.0005$) (Figure 5). The mean latencies and magnitudes of these M1 surface

PStS effects were 11.3 ± 2.1 ms and -19.5 ± 8.1 ppd for monkey J (N=123), and 13.1 ± 4.7 ms and -22.1 ± 8.1 ppd for monkey Y (N=46). Typical suppression effects found in elbow, wrist, digit and intrinsic hand muscles from sites located in the most medial portion of PMd and 1-3 mm anterior to the boundary with M1 are illustrated in Figure 8. Although a few facilitation effects in the shoulder muscles were observed, these sites and numerous others yielded predominantly inhibitory output effects.

Proximal and distal forelimb representations in PMd, PMv & M1

Motor output maps based on all PStEs at layer V sites revealed no clear segregation of proximal and distal muscle representations in PMd (Figures 10 & 11). Proximal muscles were the predominant representation in PMd (71% of all PStF effects) particularly in Monkey J, which showed 87% of poststimulus effects from proximal muscles (Table 2 and Figures 9A & 10). In comparison, there were merely three sites where only distal muscle effects were evoked (monkey Y, Figure 11B). A larger number of sites (N=30 total from both monkeys) evoked only proximal muscle effects in PMd.

Motor output maps based on PStEs from PMv did not reveal a clear segregation of proximal and distal representations (Figures 10 & 11). Proximal and distal muscles were almost equally represented in PMv, 52% and 48% respectively. At most sites, proximal and distal muscles were cofacilitated (Table 2 and Figures 9B & 10). Only one site showed facilitation

limited to distal muscles (monkey J, Figure 11B). As in PMd, a larger number of sites in both monkeys evoked effects limited to proximal muscles.

All sites stimulated at an intensity of 60 μA on the surface of M1 showed cofacilitation of proximal and distal muscles with the exception of a few sites where only distal or only proximal muscles were facilitated (monkey Y, Figure 11B). As shown in Figure 7, this is due to the fact that at 60 μA, the number of effects expanded to include nearly all of the recorded muscles.

Representation of individual forelimb muscles in PMd and PMv

Motor output maps for individual forelimb muscles were constructed for PMd and PMv. Figures 12 and 13 show the individual muscle maps based on PStF and PStS effects for monkeys J and Y. We found no observable evidence from either monkey of a difference in the area represented by different individual muscles or muscle groups. However, it was apparent that many muscles were suppressed from a core region located medially and/or rostrally to a core facilitatory region and spanning the M1/PMd boundary (Figures 12 & 13). This core suppression region was present in both monkeys and applied to muscles at all joints except the shoulder (monkey Y = EDC, ED 2, 3, ECR, ECU, BIL, BRA & monkey J = APB, FDS, ED 2, 3 & ED 4, 5, EDC, FCR, ECU, ECR, BIS, BRA).

Some variations existed in the representations of individual muscles between monkeys. For example, PEC and PDE were strongly represented in

monkey J compared to monkey Y. Variations between monkeys also existed in the number of facilitation effects obtained from PMd. Monkey Y had more than twice the number of PStF effects obtained from PMd (182 effects) compared to monkey J (74 effects). Differences were especially evident for the number of facilitation effects obtained from distal joints. We obtained only 9 facilitation effects in muscles of distal joints for monkey J compared to 57 effects obtained in monkey Y. However, proximal muscles were predominantly represented in PMd in both monkeys, with ADE showing the largest number of facilitation effects in both monkeys (Figure 9A). Additionally, TRI, TMAJ and DE in monkey Y, and PEC, PDE and LAT in monkey J were additional proximal muscles showing large numbers of facilitation effects (Figures 12 & 13).

A larger number of PStEs were recorded in PMv of monkey J because of the larger surface area covered laterally by the recording chamber (Figure 1). However the distribution of effects was very similar between monkeys with 52% and 54% of proximal muscles represented in PMv of monkeys J and Y respectively. Combinations of proximal and distal muscles were cofacilitated at the majority of sites in PMv. Only one site in monkey Y showed a PStF effect limited to a distal muscle (Figure 11B). More sites in both monkeys showed effects limited to proximal muscles. Flexors muscles were preferentially represented in PMv with the largest number of effects in the

elbow flexors (BRA, BIL and BIS), followed by a wrist flexor (FRC), a shoulder flexor (ADE) and a digit flexor (FDS) (Figure 9B).

DISCUSSION

General conclusion

Our results show that StTA effects from PMd and PMv have longer onset latencies and are vastly weaker than those from M1 (Table 3 & Figure 2) despite similar densities of corticospinal neurons for PMd and M1 (Dum and Strick, 1991; He *et al*. 1993, 1995). In fact, effects from M1 were stronger than those from PMd and PMv even when 15 μA effects from M1 were compared to 60 μA effects from PMd and PMv (Figure 7). In addition, while there is a progressive increase in the magnitude of PStF from M1 for each muscle group from the most proximal to the most distal muscles, this phenomenon was not evident for PMd or PMv. Our results suggest that the bulk of corticospinal output from PMd and PMv differs fundamentally from M1 corticospinal output. Our results are inconsistent with a model in which the typical corticospinal neuron from PMd or PMv makes monosynaptic connections with motoneurons. Even disynaptic linkages to motoneurons would be expected to produce stronger effects than we obtained from PMv and PMd. For example, there is evidence from virus labeling of corticospinal neurons after injections into distal muscles that only neurons buried in the wall of the precentral gyrus make monosynaptic connections with motoneurons (Rathelot and Strick, 2006). The linkage for neurons on the surface or convexity of the precentral gyrus is not monosynaptic. However,

sites on the surface of the precentral gyrus also produced much stronger effects than the effects from PMd and PMv. Also supporting this view are the results of lesion studies of PMd and PMv showing few degenerating elements present in the cervical motoneuron pools and a terminal distribution located mainly in the intermediate zone (dorsolateral portion) of the spinal cord (Kuypers and Brinkman, 1970).

Properties and organization of effects from PMd

PMd onset latencies were longer and exhibited greater variability than those from M1. The latency of poststimulus effects in stimulus triggered averages of EMG activity reflects a combination of conduction distance, conduction velocity and synaptic transmission in the anatomical pathway from the stimulation site to the muscle. Therefore, the latencies of PMd effects reflect a more indirect coupling to motoneurons and/or slower corticospinal conduction velocity than that for M1. This suggests that a major contribution of PMd corticospinal neurons to movement initiation and control is achieved through its innervation of spinal interneurons influencing reflex and other spinal circuits rather than providing direct input to the motoneurons. This view is also supported by the fact that the magnitudes of PStF effects from PMd were significantly weaker than those from M1 ($P < 0.0001$). As with SMA (Boudrias *et al*., 2006), a few late PStF effects were also observed in PMd. Although the mechanism of late PStF effects is unclear, their onset latencies

seem too long to be consistent with a simple relay through M1 (Cerri *et al*., 2003; Shimazu *et al*., 2004).

The majority of the effects from PMd were distributed to proximal muscles. In particular, PMd effects were preferentially facilitatory to extensors of the elbow, further supporting its role in reaching movements which mainly involves muscles at the proximal joints (Kurata and Hoffman, 1994; Luppino and Rizzolatti, 2000) (Table 2, Figures 9 & 10). Proximal muscles were represented in the entire extent of PMd and showed a greater number of sites where only poststimulus effects in proximal muscles were obtained (Figures 9, 10A & B). The majority of the sites located more rostrally in PMd predominantly influenced muscles of proximal joints as reported in previous anatomical studies (He *et al*., 1993). Our results are also consistent with a recent extensive ICMS study (Stark *et al.*, 2007) reporting a predominance of proximal muscle representation in what they considered to be the dorsal region of PMd. However, in contrast to the Stark *et al*. (2007) study, which also reported a limited number of sites where distal movements could be evoked, we found a substantial number of PStF effects from PMd in muscles of distal joints.

The presence of poststimulus effects in both proximal and distal joints agrees with anatomical data showing that corticospinal neurons in the forelimb area of PMd project to both upper and lower cervical segments of the spinal cord (He *et al*., 1993; Galea and Darian-Smith, 1994). However, our

data does not support a segregated representation of distal and proximal muscles in PMd as suggested by previous ICMS and anatomical studies (Dum and Strick, 1991; He *et al*., 1993; Raos *et al*., 2003). We found that nearly all PMd sites cofacilitated distal and proximal muscles. This is agreement with the extensive overlap of proximal and distal evoked movements reported by Golschalk *et al*. (1995).

Properties and organization of effects from PMv

Almost half of PMv effects obtained in our study came from distal muscles with APB showing magnitudes of effects that were among the strongest ones we observed from PMv. Based on the results of Cerri *et al*. (2003) and Shimazu *et al*. (2004), PMv produces robust facilitation of output from M1 corticospinal neurons, particularly to hand and digit muscles. This is further supported by anatomical studies showing that PMv corticospinal neurons do not project sufficiently caudally in the cervical enlargement to reach the motor nuclei supplying hand muscles (He *et al*., 1993; Galea and Darian-Smith, 1994). Therefore, the effects produced from PMv on distal muscles in our study are most likely to be achieved predominantly through the heavy cortico-cortical connections existing between the PMv and M1 forelimb representations (Muakkassa and Strick, 1979; Dum and Strick, 2005; Dancause *et al*., 2006)

PMv contains only 2% of the total number of corticospinal projections in the frontal lobe and the density of its corticospinal neurons is the lowest among the secondary motor areas although still 63% of the density found in M1 (Dum and Strick, 1991). This seems contradictory to the fact that PMv had the strongest effects observed among all the secondary motor areas, particularly in elbow muscles. Therefore, our results suggest the presence of an effective linkage through M1 and that to the facilitation of M1 output from PMv reported for hand muscles might be even more powerful for proximal muscles. In fact, PMv output to forelimb muscles had features that resembled M1 output including the existence of a very narrow peak of latencies with less variability than any of the other secondary cortical motor areas (Figure 2). Onset latencies in PMv were on average 2 ms longer than those from M1; this is agreement with the conduction time of 1-3 ms from PMv to M1 reported in previous studies (Godschalk *et al*., 1984; Tokuno and Nambu, 2000; Cerri *et al*., 2003).

Detailed muscle and joint-based maps did not show clear segregated representations of distal and proximal muscles. Neither was there a significant difference in the representations of individual muscles. This result is in agreement with the recent ICMS study of Stark *et al*. (2007) which showed a nearly equal representation of proximal and distal movements throughout what they considered to be PMv.

PMv is part of a cortico-cortical circuit that is essential for hand movements required for the manipulation of objects (Jeannerod *et al*., 1995; Rizzolatti *et al*., 1998). Our results support this functional role, as the muscles involved in grasping movements are clearly represented within PMv. We found that flexor muscles of the elbow, wrist, digit as well as intrinsic hand muscles were mainly represented in PMv and were among the muscles showing the strongest magnitudes of effects. However, it is also clear that effects on proximal muscles were just as common as those on distal muscles and that proximal muscles, particularly muscles of the elbow, yielded some of the strongest effects from PMv. Moreover, cofacilitation of proximal and distal muscles was the predominant result at nearly all sites in PMv (Figures 10, 11A & B). Therefore, our data support a role for PMv in aspects of grasping that require multi-joint coordination (Luppino and Rizzolatti, 2000; Graziano *et al*., 2002), including both proximal and distal joints, rather than a role focused solely on distal muscles and strictly limited to grasp (Davare *et al*., 2006).

Inhibitory effects

For many distal and elbow muscles, our maps based on individual muscle representations demonstrate the presence of a concentration of PStS effects around the boundary between M1 and PMd (Figures 12 & 13). This organization was particularly pronounced in monkey J (Figure 12). To our knowledge, this is the first evidence of a potential segregated core region

producing inhibitory effects in relative isolation from facilitatory effects. This fact that this representation was not found in a previous study from our laboratory based on StTA data (Park *et al*., 2001) can be explained by the use of higher intensity of stimulation in the present study. The location of this inhibitory representation may correspond to the separate island of distal corticospinal neurons located medially on M1 surface and to the segregated distal representation of corticospinal neurons located in PMd reported in anatomical studies of He *et al*. (1993).

Inhibitory effects involve at least one additional synapse, most likely on a spinal inhibitory neuron, interposed between the corticospinal neurons and the motoneurons. Latencies of PStS effects were on average 3 ms longer than PStF latencies from M1 reflecting a less direct coupling than PStF effects (Table 3). The magnitude of suppression effects from M1, selected from effects present at both stimulation intensities of 15 and 60 μA, did not follow the pattern observed for PStF from M1 with steadily increasing magnitudes in going from the most proximal to the most distal muscles. In addition, latencies of these inhibitory effects were not significantly different from each other. This suggests that a maximum amount of inhibition is reached, with possibly, a maximum number of interneurons activated in the spinal cord. The functional role of segregated inhibitory zones on muscle activity is unknown. However, it might be linked to the control of excitability of the motoneurons during the holding period of delayed movement tasks and/or

the preparation for movements as reported in previous studies showing elevated activity of PMd neurons during these specific aspects of motor tasks (Weinrich and Wise, 1982; Weinrich *et al*., 1984).

PStS latencies were longer in PMd and PMv compared to M1. This can be partially explained by the smaller size of their corticospinal neurons, thus their slower conduction velocity compared to those from M1. The magnitude of suppression effects from PMd and PMv were half those observed from M1. As for their facilitation effects on muscle activity, this suggests a more indirect coupling to inhibitory interneurons in the spinal cord and/or weaker direct input on interneurons compared to the more robust effects from M1. Alternatively, inhibitory effects from PMv might also be mediated largely through connections with M1.

Boundary between PMd and M1

The boundary established between M1 and PMd was based on a variety of parameters including the transition of poststimulus effects in terms of latency and magnitude. A gradual decrease in magnitude and a gradual increase in latency were observed in moving from sites in M1 toward sites in PMd. This was observed for both facilitation and suppression effects and provided an additional means to localize a border region separating PMd and M1.

Histological results showed a gradual decrease in the density of large pyramidal cells in M1 approaching the PMd border, and a gradual, though smaller, increase in density across PMd, approaching the superior precentral sulcus. The greatest number of large pyramidal (presumably corticospinal) neurons was shown to be in the M1 area adjacent to the central sulcus, in agreement with the previous findings that the greatest number of large corticospinal neurons is located in the arm area of M1 compared to other motor areas (Dum RP and PL Strick, 1991). Furthermore, while variation in mean soma diameter of pyramidal cells was observed across both motor areas, average soma diameters were significantly larger in M1 adjacent to the central sulcus, compared to the lateral area of PMd.

Our observations are in agreement with previous anatomical studies showing that the number and the density of retrogradely labeled giant pyramidal cells contributing to the corticospinal tract, do not end abruptly, but rather decreases gradually across the M1/PMd border (Dum and Strick, 1991; Galea and Darian-Smith, 1994). Based on our data, the boundary between M1 and PMd was estimated to be ~5 mm anterior to the central sulcus, matching the boundary location established in previous studies (Dum and Strick, 1991; He *et al*., 1993; Kurata and Hoffman, 1994; Raos *et al*., 2003; Raos *et al*., 2004; Hoshi and Tanji, 2006; Stark *et al*., 2007).

Conclusion

Our results raise doubts about the role of the corticospinal neurons from PMv and PMd in the direct control of forelimb motoneurons. Poststimulus effects from PMd and PMV have longer latencies and vastly weaker magnitudes than those from M1 suggesting the presence of additional synapses in the anatomical pathway for their actions on the motoneurons. For PMv, our results and the results from others, suggest that its effects on distal muscles are most likely achieved through projections to M1 (Cerri *et al*., 2003; Shimazu *et al*., 2004). We further suggest that PMv output effects on proximal muscles are also predominantly achieved through a cortico-cortical linkage, facilitating M1 corticospinal neurons with terminations on proximal motoneurons. For PMd, our results suggest that the effects of its corticospinal neurons on muscle activity are mainly achieved through innervation of interneurons in the intermediate zone of the spinal cord.

Table 1. Summary of data collected from PMd, PMv & M1

	PMd			PMv			M1		
	Monkey J	Monkey Y	Total	Monkey J	Monkey Y	Total	Monkey J	Monkey Y	Total
Electrode tracks	103	102	205	54	25	79	12	18	30
PStF effects	74	182	256	188	139	327	140	200	340
PStS effects	50	41	91	18	2	20	10	1	11
PStEs obtained	124	223	347	206	141	347	150	201	351

PMd, PMv and M1 data came from two monkeys. M1 data are based on PStEs that were present at both 15 & 60 μA only. A total of 174 tracks were performed in M1 and only a portion of these tracks (N=30) are represented in this table (see M1 data base, in methods section). PMd, dorsal premotor area; PMv, ventral premotor area; M1, primary motor cortex; PStE, poststimulus effect; PStF, poststimulus facilitation; PStS, poststimulus suppression.

Table 2. Summary and comparison of data collected from PMd, PMv & M1

	Number of muscles with effects and percent of total effects		
Joint	**PMd**	**PMv**	**M1**
Shoulder	107	67	39
Elbow	83	128	83
Wrist	25	64	103
Digit	36	50	88
Intrinsic Hand	5	18	27
PStF Proximal %	71%	52%	30%
PStF Distal %	29%	48%	70%
Total PStF	256	327	340
Total PStS	91	20	11
Total PStF effects %	74%	94%	97%

M1 data are based on effects that were present at both 15 & 60 μA. Percentages of proximal (shoulder and elbow muscles) and distal (wrist, digit and intrinsic hand muscles) effects were adjusted to equalize the number of muscles recorded. M1, primary motor cortex; PMd, premotor dorsal area; PMv, premotor ventral area; PStE, poststimulus effect; PStF, poststimulus facilitation; PStS, poststimulus suppression.

Table 3. Latency and magnitude of PStF and PStS effects from PMd, PMv & M1

	PMd	PMv	M1
Facilitation	N=256	N=327	N=340
Latencies (ms)			
Shoulder	8.5 ± 1.8	8.9 ± 1.5	7.5 ± 1.9
Elbow	10.6 ± 4.2	9.1 ± 1.6	7.0 ± 0.8
Wrist	11.8 ± 5.6	10.5 ± 1.6	7.7 ± 0.7
Digit	13.3 ± 5.6	10.5 ± 1.3	8.0 ± 0.8
Intrinsic H.	10.4 ± 2.4	12.1 ± 1.6	9.2 ± 1.3
All	10.2 ± 4.1	9.7 ± 1.8	7.7 ± 1.2
Magnitudes (ppi)			
Shoulder	17.6 ± 8.0	15.9 ± 7.3	50.5 ± 25.8
Elbow	16.9 ± 9.0	28.3 ± 19.6	109.7 ± 66.6
Wrist	18.3 ± 4.6	17.1 ± 6.6	178.9 ± 145.0
Digit	16.7 ± 4.4	17.5 ± 7.7	206.0 ± 167.5
Intrinsic H.	17.7 ± 5.7	22.0 ± 21.1	235.2 ± 145.3
All	17.3 ± 7.6	21.6 ± 15.2	158.8 ± 139.9
Inhibition	N=91	N=20	N=11
Latencies (ms)			
Shoulder	15.0 ± 6.0	15.1 ± 2.2	8.0
Elbow	14.1 ± 6.9	18.1 ± 2.0	9.3 ± 0.8
Wrist	17.0 ± 5.7	16.0 ± 1.1	11.8
Digit	16.7 ± 7.0	15.5 ± 2.5	10.6 ± 0.4
Intrinsic H.	17.3 ± 6.3	13.8 ± 0.5	14.1 ± 0.4
All	15.8 ± 6.4	15.9 ± 2.4	10.9 ± 1.9
Magnitudes (ppd)			
Shoulder	-12.5 ± 3.8	-17.6 ± 12.1	-39.0
Elbow	-16.5 ± 6.0	-16.4 ± 3.5	-22.3 ± 13.6
Wrist	-14.1 ± 3.2	-16.5 ± 4.0	-21.4
Digit	-13.9 ± 4.2	-13.9 ± 1.3	-35.4 ± 15.7
Intrinsic H.	-12.4 ± 2.9	-11.1 ± 4.2	-16.5 ± 0.9
All	-14.4. ± 4.6	-15.9 ± 7.9	-28.6 ± 14.7

M1 data are based on effects that were present at both 15 & 60 μA only. Magnitudes are expressed as peak percent increase (ppi) and peak percent decrease (ppd) compared to baseline. Magnitude data are for 60 μA stimuli. Values are means of latencies or magnitudes ± SD. M1, primary motor cortex; PMd, premotor dorsal area; PMv, premotor ventral area; PStE, poststimulus effect; PStF, poststimulus facilitation; PStS, poststimulus suppression.

Figure 1. Dorsal view of the electrode penetration maps of the left hemisphere in two monkeys. Red area corresponds to tracks in M1 where StTA yielded poststimulus effects (PStE); blue area corresponds to tracks where StTA yielded PStE in PMd; green area correspond to tracks where StTA yielded PStE in PMv; gray area indicates boundary zone between M1 and lateral premotor areas; tracks where StTA produced PStE are marked by small black circles; tracks where StTA did not produce PStE are marked by small gray circles; tracks where ICMS produced hindlimb movements in M1 and PMd are marked in yellow; tracks where ICMS produced oral-facial movements in M1 and PMv are enclosed by fine dotted lines. Course dotted lines indicate the fundus (curvature) of the central sulcus. Tracks were performed 1 mm apart. Abbreviations: A, Anterior; ArS, arcuate sulcus; CS, central sulcus; M, medial; SPS, superior precentral sulcus.

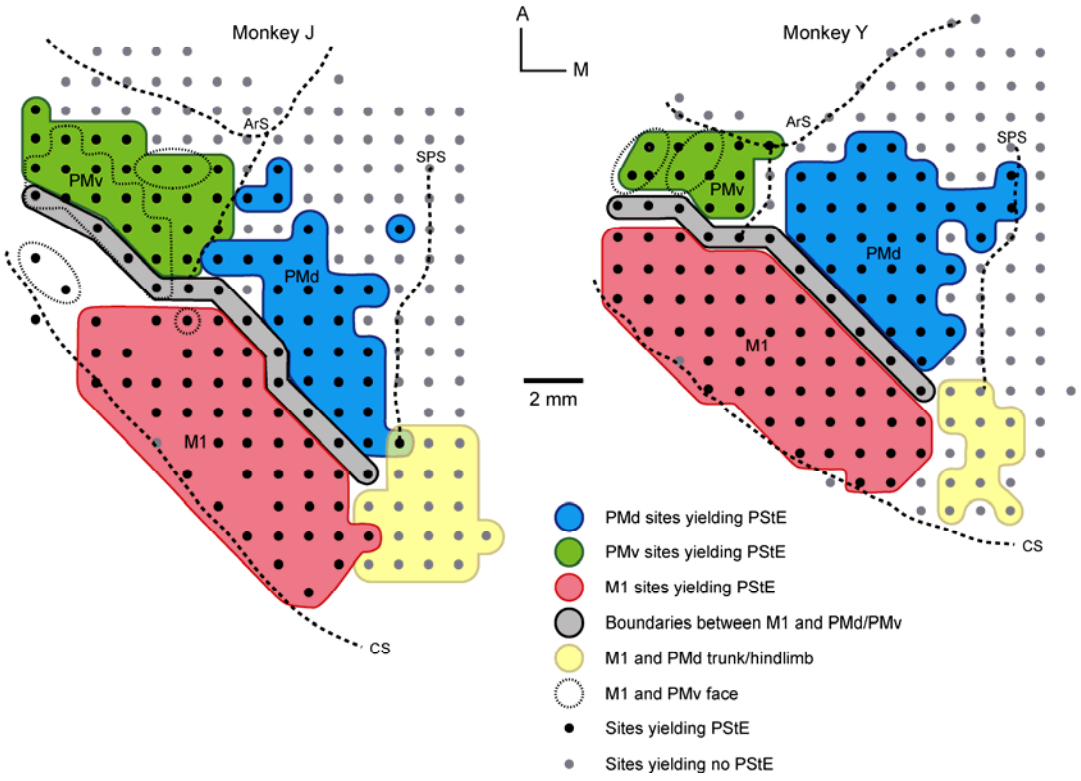
Monkey J
ArS
SPS
PMv
PMd
M1
CS
A
M
Monkey Y
ArS
SPS
PMv
PMd
M1
CS
2 mm
PMd sites yielding PStE
PMv sites yielding PStE
M1 sites yielding PStE
Boundaries between M1 and PMd/PMv
M1 and PMd trunk/hindlimb
M1 and PMv face
Sites yielding PStE
Sites yielding no PStE

Figure 2. Distribution of onset latencies and magnitudes of poststimulus effects (PStEs) obtained from the forelimb representations of PMd, PMv & M1. M1 data are based on PStF and PStS effects that were present at both stimulation intensity of 15 & 60 μA only (Figure 1). Magnitudes are expressed as peak percent increase (ppi) as a percent of baseline. Note the difference in magnitude scales for M1 versus the graphs for PMd and PMv. N=327 for PMd, N=357 for PMv, and N=340 for M1.

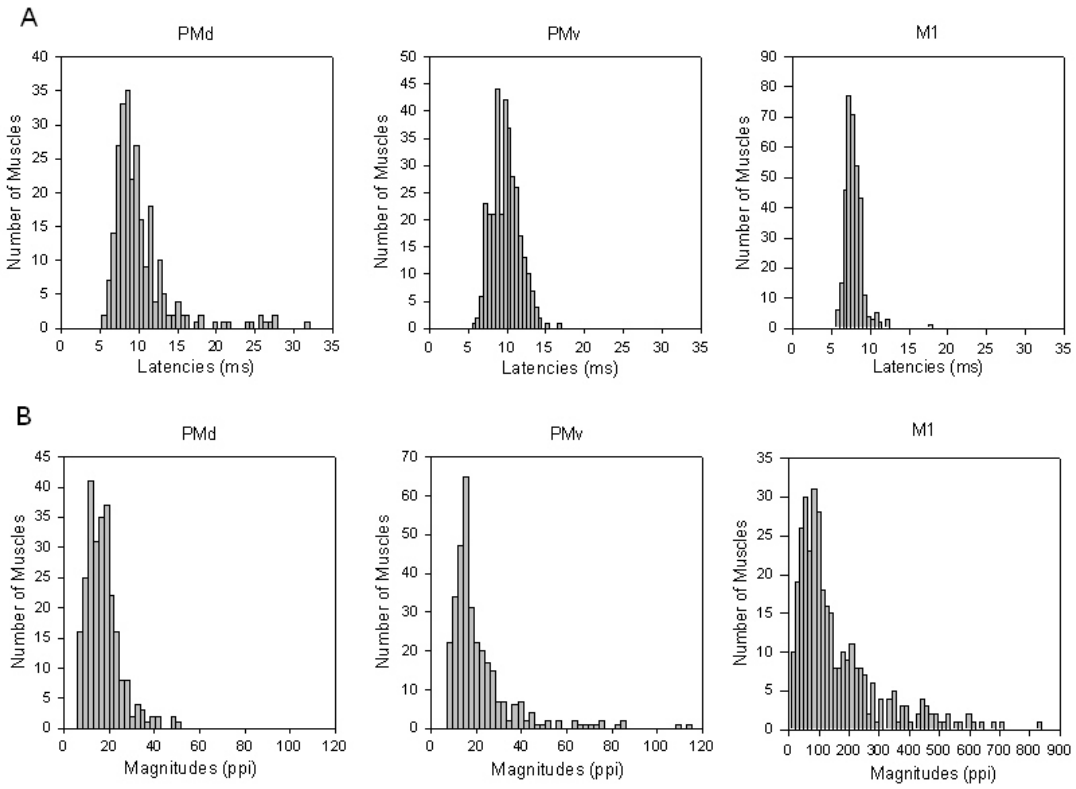
A
PMd
PMv
M1
Number of Muscles
Latencies (ms)
B
PMd
PMv
M1
Number of Muscles
Magnitudes (ppi)

Figure 3. Histology results. A & B) Photomicrographs of a coronal section from the M1/PMd border area in Monkey Y. A) Section stained with cresyl violet for histological analysis of pyramidal cells. One set of 12 cresyl violet-stained sections, 300 μm apart, was used to analyze pyramidal cell density and pyramidal cell size in relation to the M1/PMd border. The M1/PMd border is indicated by the black line. The area outlined in the black box is shown at higher magnification in. Calibration bar = 1 mm. B) Higher magnification of the same section in A (box). Pyramidal cells are indicated by black arrows. Calibration bar=250 μm. Abbreviations: A, Anterior; M, medial; SPS, superior precentral sulcus. C) The number of large layer V pyramidal cells on each side of the M1/PMd border in 1 mm increments. The number for the border zone (0) is the average for 1 mm on each side of the border as indicated by the electrophysiological results. A relatively small number of large pyramidal cells in the PMd area bordering M1 was followed by a gradual increase in the number of large pyramidal cells across the border area and continuing through M1. D) Mean soma diameter of large layer V pyramidal cells per mm on each side of the M1/PMd border in 1 mm increments. Soma diameters of pyramidal neurons in layer V were measured by averaging the length of the cell in the long axis and the width measured along a perpendicular through a point of the length at the maximum width. The mean maximal soma diameters are shown to increase at the immediate border area, and increase further across M1, reaching a maximum mean diameter 5 mm from the M1/PMd border. Abbreviations: A, Anterior; M, medial; SPS, superior precentral sulcus. Negative values on the axis correspond to sites located on the surface of the forelimb representation of M1; zero corresponds to the boundary between PMd and M1 as represented in Figure 1; positive values correspond to sites in PMd.

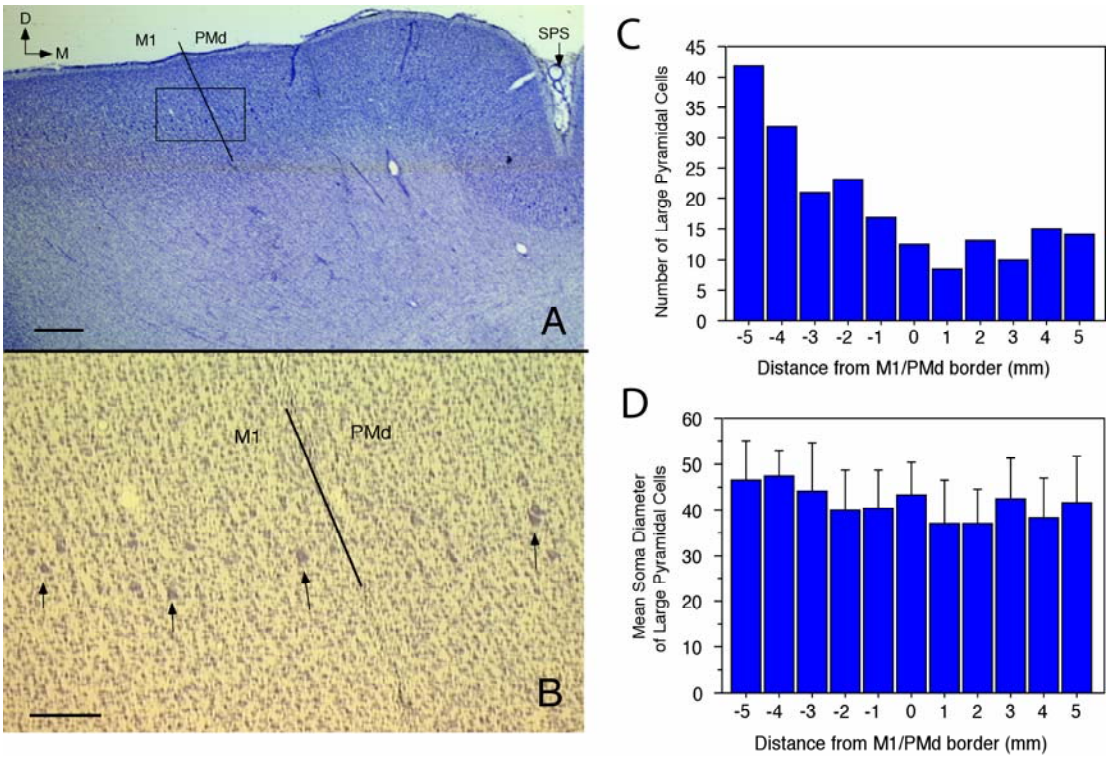
D
M
M1
PMd
SPS
A
M1
PMd
B
C
Number of Large Pyramidal Cells
0
5
10
15
20
25
30
35
40
45
-5 -4 -3 -2 -1 0 1 2 3 4 5
Distance from M1/PMd border (mm)
D
Mean Soma Diameter of Large Pyramidal Cells
0
10
20
30
40
50
60
-5 -4 -3 -2 -1 0 1 2 3 4 5
Distance from M1/PMd border (mm)

Figure 4. Increased latencies of facilitation effects from sites in M1 toward more anterior sites in PMd for distal joints (A & B), proximal joints (C & D), and all joints (E & F) of two monkeys. A) Polynomial, linear, f = 9.9937 + 0.3194x, r^2 = 0.0883, *P* < 0.0001. B) Polynomial, linear, f = 10.7699 + 0.7807x, r^2 = 0.236, *P* < 0.0001. C) Polynomial, quadratic, f = 8.0352 + 0.4860x + 0.1126x^2, r^2 = 0.1713, *P* < 0.0001. D) Polynomial, quadratic, f = 8.3061 + 0.4147x + 0.0444x^2, r^2 = 0.1939, *P* < 0.0001. E) Polynomial, linear, f = 8.9547 + 0.2265x, r^2 = 0.0446, *P* < 0.0001. F) Polynomial, linear, f = 9.3798 + 0.4697x, r^2 = 0.1458, *P* < 0.0001. Negative values on the axis correspond to sites located on the surface of the forelimb representation of M1, dotted lines at zero corresponds to the boundary between PMd and M1 as represented in Figure 1; positive values correspond to sites in PMd. M1 data included all effects obtained at 60 μA in layer V on the surface of the cortex. For monkey J, N=520 (N=311 for proximal joints; N=209 for distal joints). For Monkey Y, N=724 (N=391 for proximal joints; N=333 for distal joints).

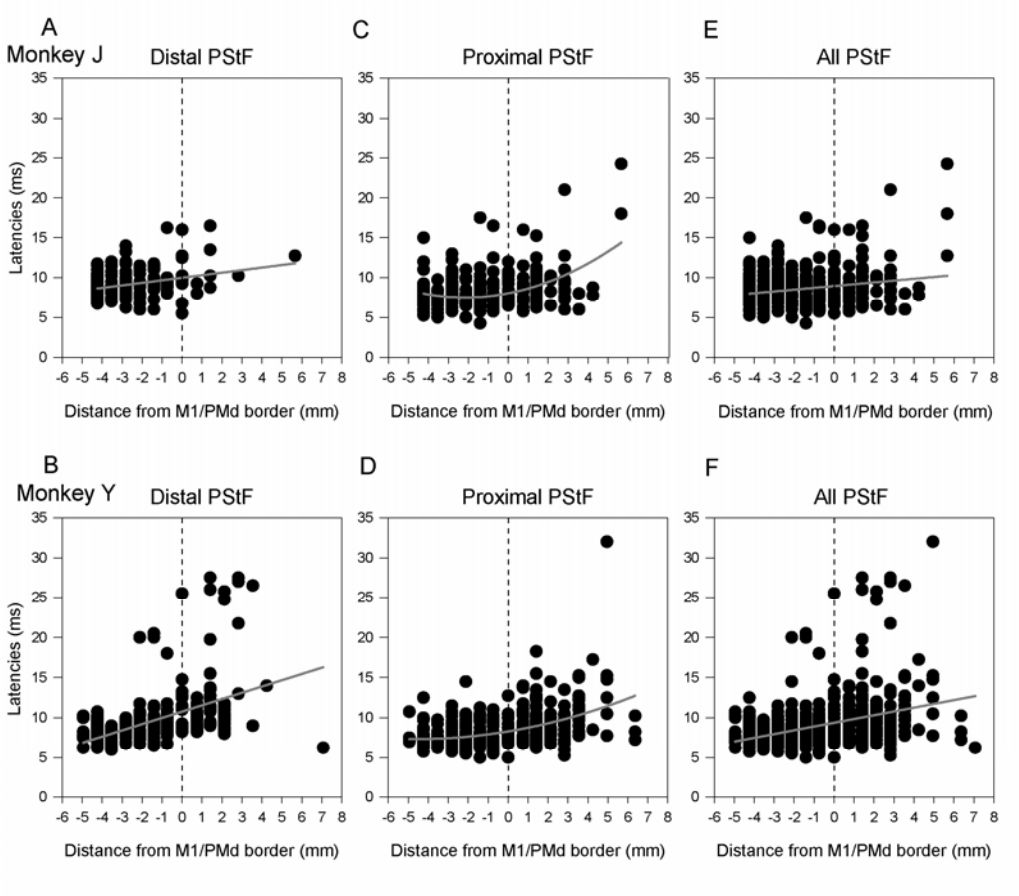
A
Monkey J
Distal PStF
C
Proximal PStF
E
All PStF
B
Monkey Y
Distal PStF
D
Proximal PStF
F
All PStF
Latencies (ms)
Distance from M1/PMd border (mm)

Figure 5. Decreased magnitudes of facilitation effects in M1 and PMd for muscles at proximal joints, distal joints, and all joints in two monkeys (all exponential decay). (A, B, C & D) Effects from all sites on M1 surface and PMd (E & F). Same data as E &F but restricting the M1 data to sites within 2.12 mm of the PMd border and expanding the vertical axis (G & H). A) $f = 12.47^{(-0.39x)}$, $r^2 = 0.1774$. B) $f = 25.936^{(-0.40x)}$, $r^2 = 0.2799$. C) $f = 26.6195^{(-0.14x)}$, $r^2 = 0.1234$. D) $f = 20.8038^{(-0.16x)}$, $r^2 = 0.1988$. E) $f = 22.0038^{(-0.21x)}$, $r^2 = 0.1336$. F) $f = 20.8987^{(-0.37x)}$, $r^2 = 0.2119$. G) $f = 23.7816^{(-0.13x)}$, $r^2 = 0.1139$. H) $f = 23.2591^{(-0.18x)}$, $r^2 = 0.2135$. Magnitudes are expressed as peak percent increase (ppi). Numbers of effects in A, B, C & D are the same as in Figure 4. G) N=263. H) N=395.

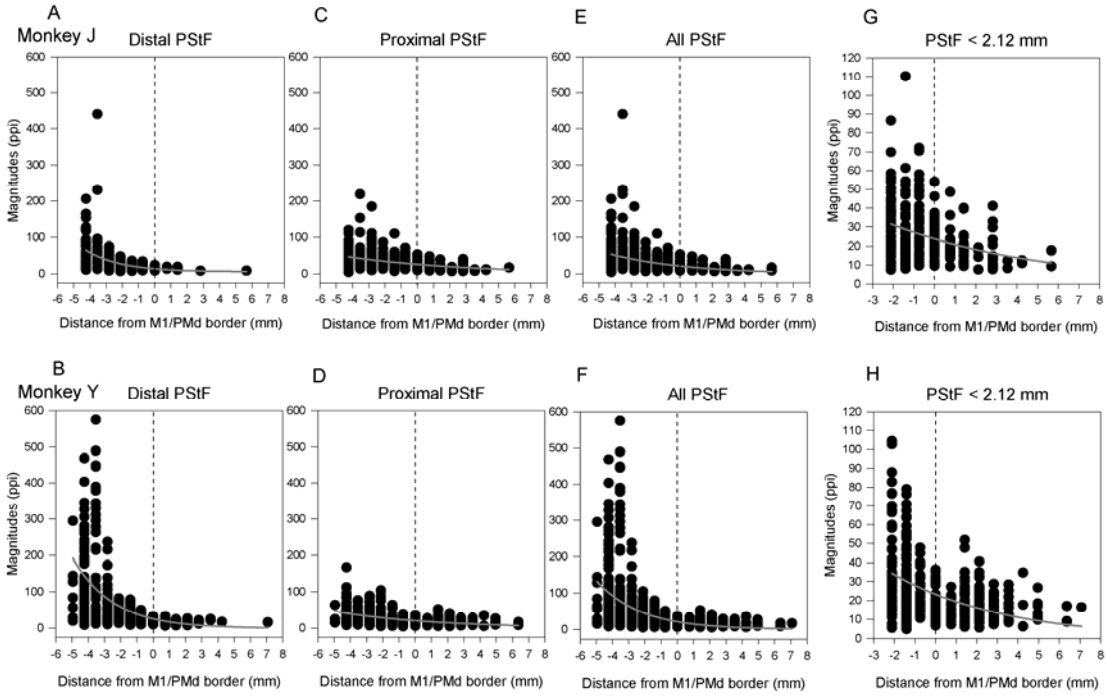
A
Monkey J
Distal PStF
C
Proximal PStF
E
All PStF
G
PStF < 2.12 mm
B
Monkey Y
Distal PStF
D
Proximal PStF
F
All PStF
H
PStF < 2.12 mm
Magnitudes (ppi)
Distance from M1/PMd border (mm)

Figure 6. Increased latencies (A & B) and decreased magnitudes (C & D) of suppression effects from sites in M1 moving rostrally to sites in PMd in two monkeys. A) Linear regression, f = 12.1034 + 0.42x, $P < 0.0005$. B) Linear regression, f = 16.8268+ 1.01x, $P < 0.0005$. C) Linear regression, f = -17.2333 + 1.04x, $P < 0.0005$. D) Linear regression, f = -17.9177 + 1.70x, $P < 0.0005$. Magnitudes are expressed as peak percent decrease (ppd). N=208 for monkey J and N=117 for monkey Y.

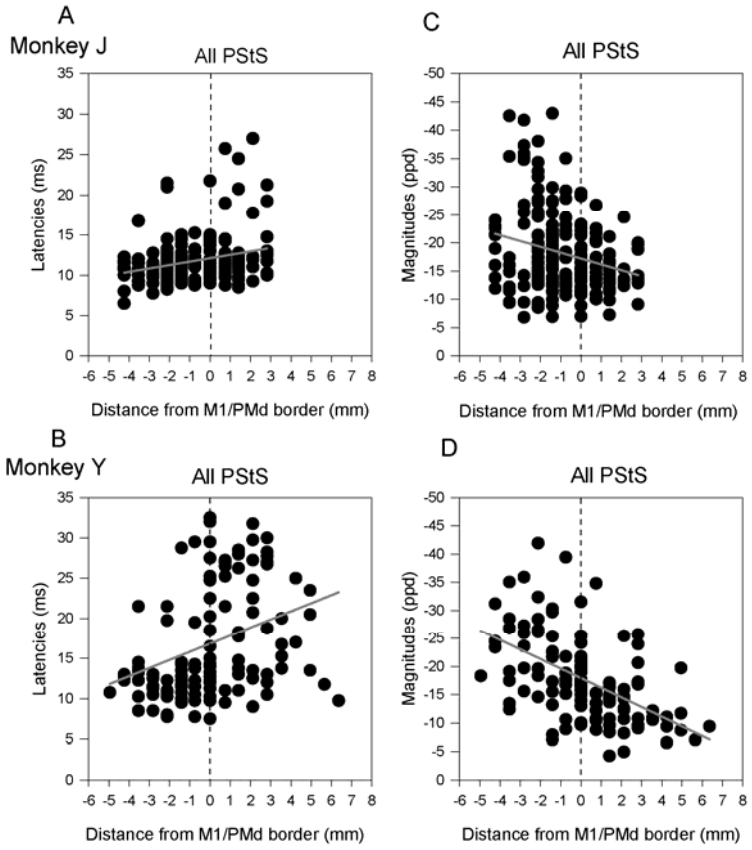
A
Monkey J
All PStS
Latencies (ms)
Distance from M1/PMd border (mm)
C
All PStS
Magnitudes (ppd)
Distance from M1/PMd border (mm)
B
Monkey Y
All PStS
Latencies (ms)
Distance from M1/PMd border (mm)
D
All PStS
Magnitudes (ppd)
Distance from M1/PMd border (mm)

Figure 7. Stimulus-triggered averages (StTA) of forelimb muscles from one site in PMd and one site in PMv at a stimulation intensity of 60 μA, and one M1 site at two different intensities, 15 and 60 μA. Time zero corresponds to the stimulus trigger event used in compiling the average. Poststimulus facilitation (PStF) effects were observed in muscles shown in bold and records with no poststimulus effects are shown in lighter gray. The range of number of trigger events for different channels is given in parenthesis.

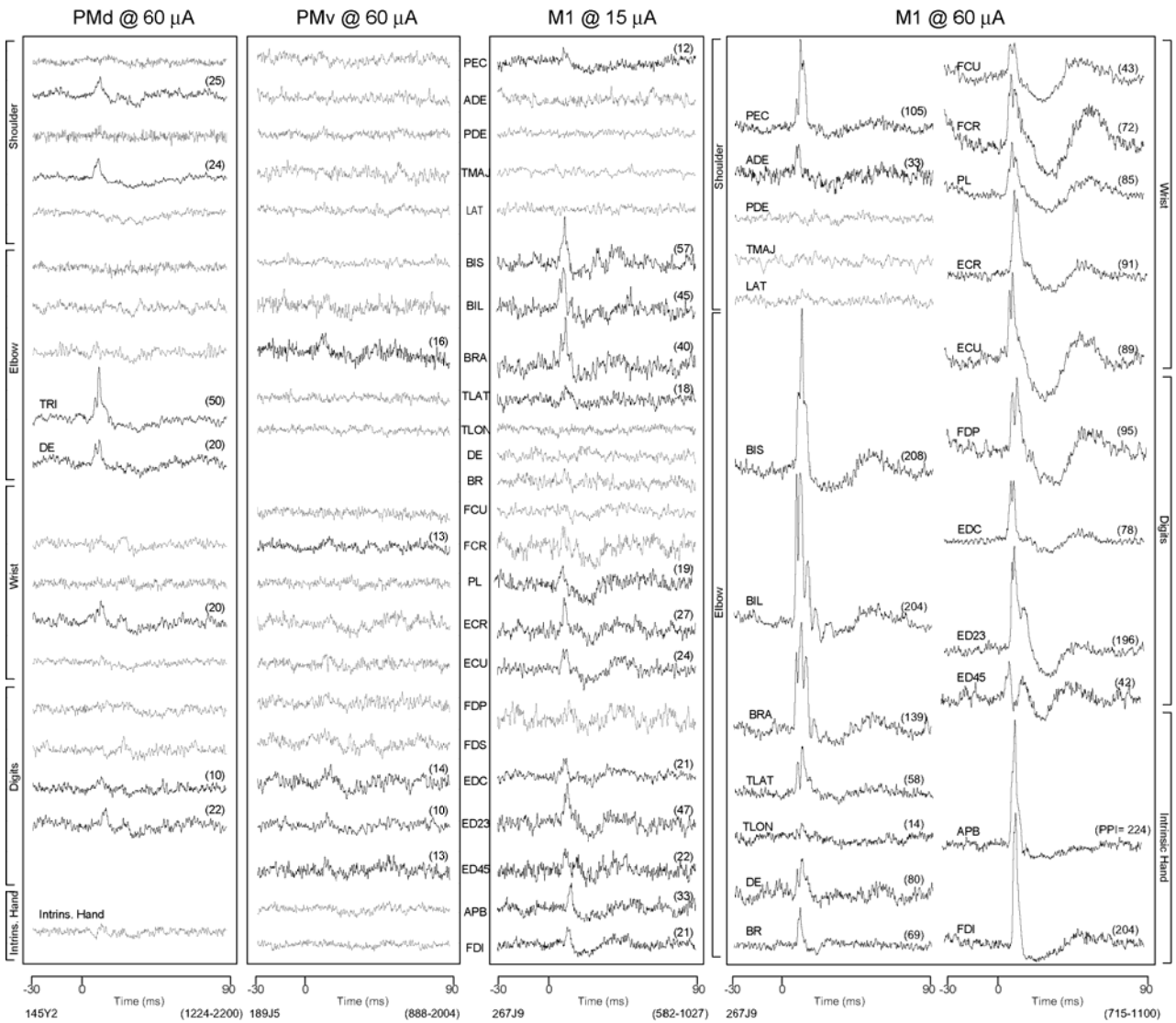
PMd @ 60 µA
PMv @ 60 µA
M1 @ 15 µA
M1 @ 60 µA
Shoulder
Elbow
Wrist
Digits
Intrins. Hand
PEC
ADE
PDE
TMAJ
LAT
BIS
BIL
BRA
TLAT
TLON
DE
BR
FCU
FCR
PL
ECR
ECU
FDP
FDS
EDC
ED23
ED45
APB
FDI
TRI
Intrins. Hand
Time (ms)
-30
0
90
145Y2
(1224-2200)
189J5
(888-2004)
267J9
(582-1027)
267J9
(715-1100)
(PPI= 224)

Figure 8. Stimulus-triggered averages (StTA) of forelimb muscles from three sites located 1-3 mm anterior to the boundary between M1 and PMd stimulated at an intensity of 60 μA. Time zero corresponds to the stimulus trigger event used for compiling the average. Poststimulus suppression (PStS) effects were observed in muscles shown in bold, poststimulus facilitation (PStF) effects were observed in muscles with an asterisk (*), and no poststimulus effects were observed in the light gray records. The range in number of trigger events for different channels is given in parenthesis.

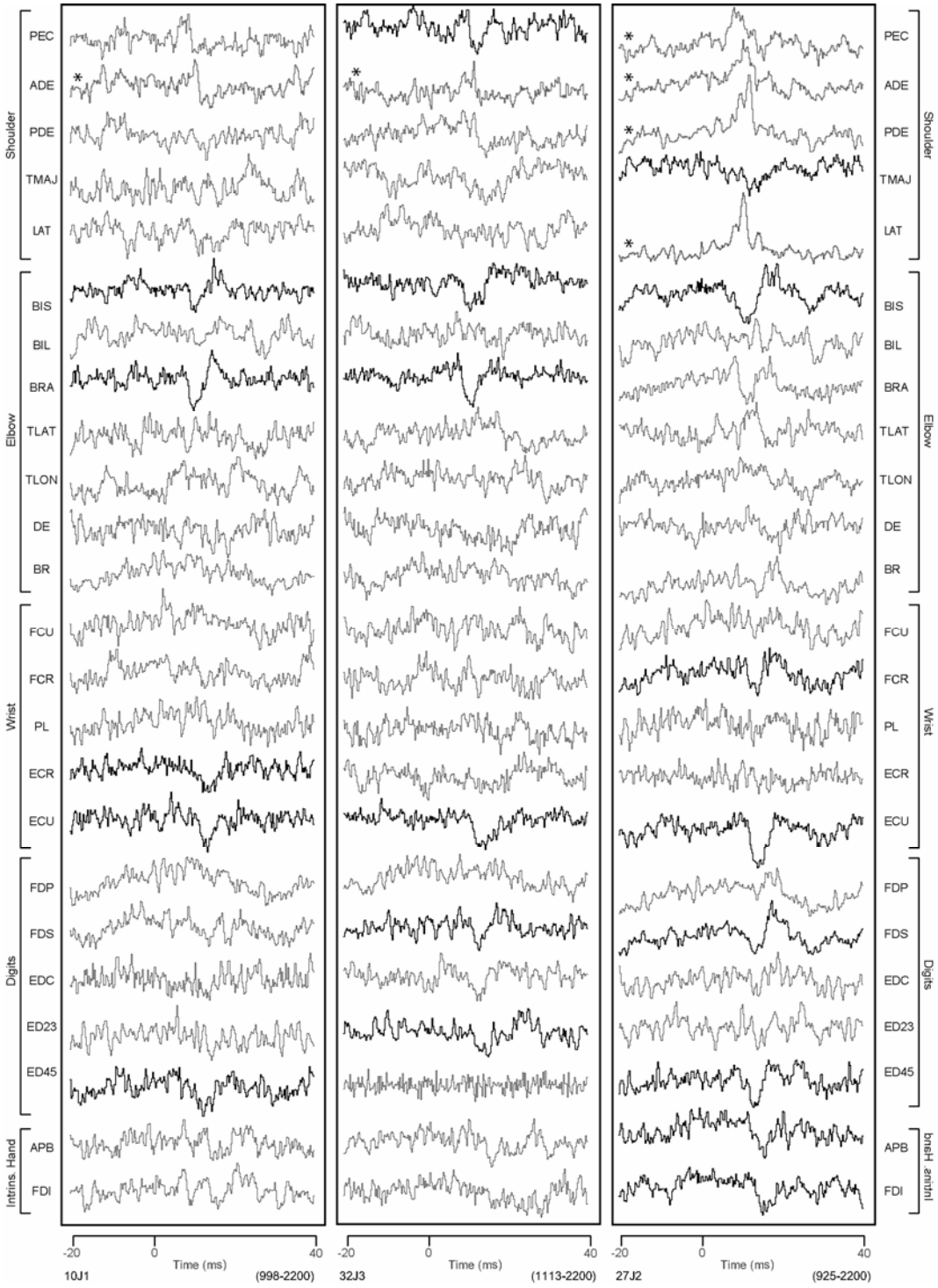
Shoulder
PEC
ADE
PDE
TMAJ
LAT
Elbow
BIS
BIL
BRA
TLAT
TLON
DE
BR
Wrist
FCU
FCR
PL
ECR
ECU
Digits
FDP
FDS
EDC
ED23
ED45
Intrins. Hand
APB
FDI
-20
0
40
Time (ms)
10J1
(998-2200)
32J3
(1113-2200)
27J2
(925-2200)

Figure 9. Distribution of PStF (right) and PStS (left) obtained from 19-23 muscles of the forelimb for A) PMd & B) PMv. The dotted lines separate muscles belonging to different joints. The asterisks (*) on muscles FCU and ED 4, 5 indicates effects from monkey J only. Because of the combination of muscles formed for triceps (TRI) and the intrinsic hand muscles (Intrins.) in monkey Y, the total number of effects in these muscles was divided by two and distributed equally in muscles in TLON and TLAT and in muscles FDI and APB respectively. Pectoralis major (PEC), anterior deltoid (ADE), posterior deltoid (PDE), teres major (TMAJ) and latissimus dorsi (LAT), biceps short head (BIS), biceps long head (BIL), brachialis (BRA), triceps long head (TLON), triceps lateral head (TLAT) and dorso-epitrochlearis (DE), extensor carpi radialis (ECR), extensor carpi ulnaris (ECU), flexor carpi radialis (FCR), flexor carpi ulnaris (FCU) and palmaris longus (PL), extensor digitorum communis (EDC), extensor digitorum 2 and 3 (ED 2, 3), extensor digitorum 4 and 5 (ED 4, 5), flexor digitorum superficialis (FDS) and flexor digitorum profundus (FDP), abductor pollicis brevis (APB) and first dorsal interosseus (FDI).

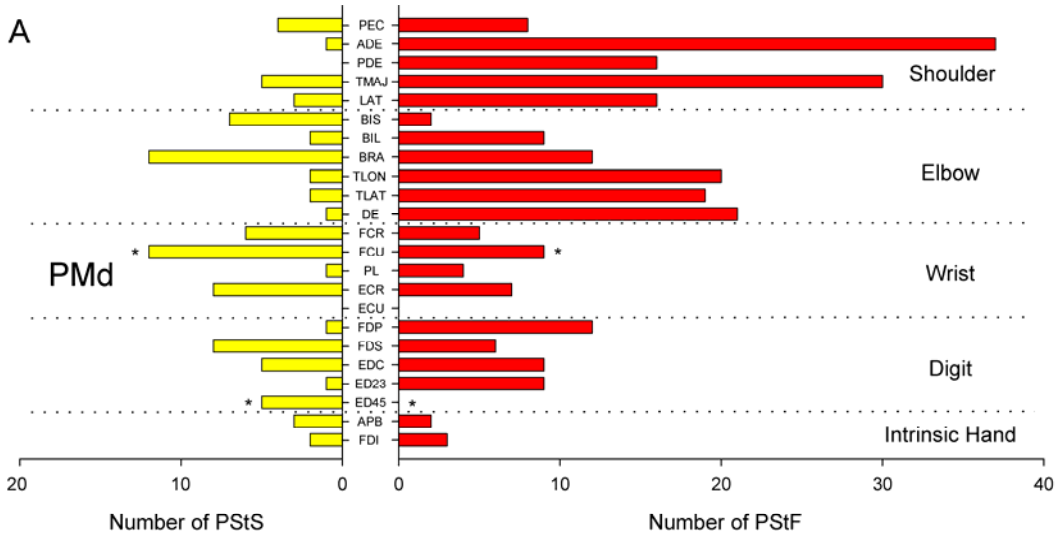
A
PMd
PEC
ADE
PDE
TMAJ
LAT
BIS
BIL
BRA
TLON
TLAT
DE
FCR
FCU
PL
ECR
ECU
FDP
FDS
EDC
ED23
ED45
APB
FDI
Shoulder
Elbow
Wrist
Digit
Intrinsic Hand
20
10
0
0
10
20
30
40
Number of PStS
Number of PStF

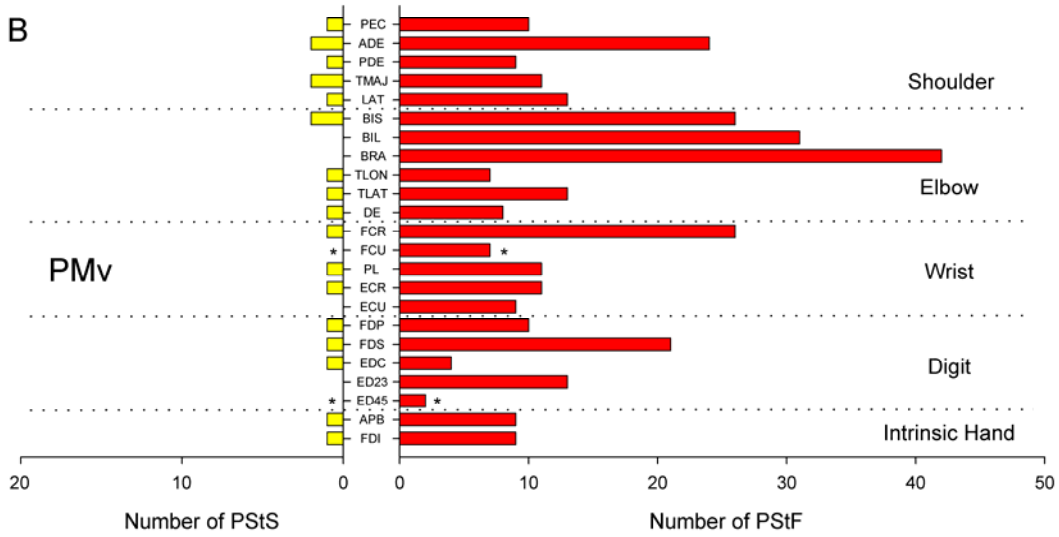
B
PMv
PEC
ADE
PDE
TMAJ
LAT
BIS
BIL
BRA
TLON
TLAT
DE
FCR
FCU
PL
ECR
ECU
FDP
FDS
EDC
ED23
ED45
APB
FDI
Shoulder
Elbow
Wrist
Digit
Intrinsic Hand
20
10
0
0
10
20
30
40
50
Number of PStS
Number of PStF

Figure 10. Muscle output maps for PMd, PMv and M1 obtained from two monkeys based on poststimulus effects in joint, shoulder, elbow, wrist, digit and intrinsic hand muscles. PStF and PStS effects (yellow dots) are shown in separate columns. Red dots correspond to facilitation of shoulder muscles; blue dots correspond to facilitation of elbow muscles; purple dots correspond to facilitation of wrist muscles; pink dots correspond to facilitation of digit muscles; green dots correspond to facilitation of intrinsic hand muscles; yellow dots depict inhibitory effects. The outlined lined regions are the boundaries of PMd, PMv and M1 based on PStEs (Figure 1).

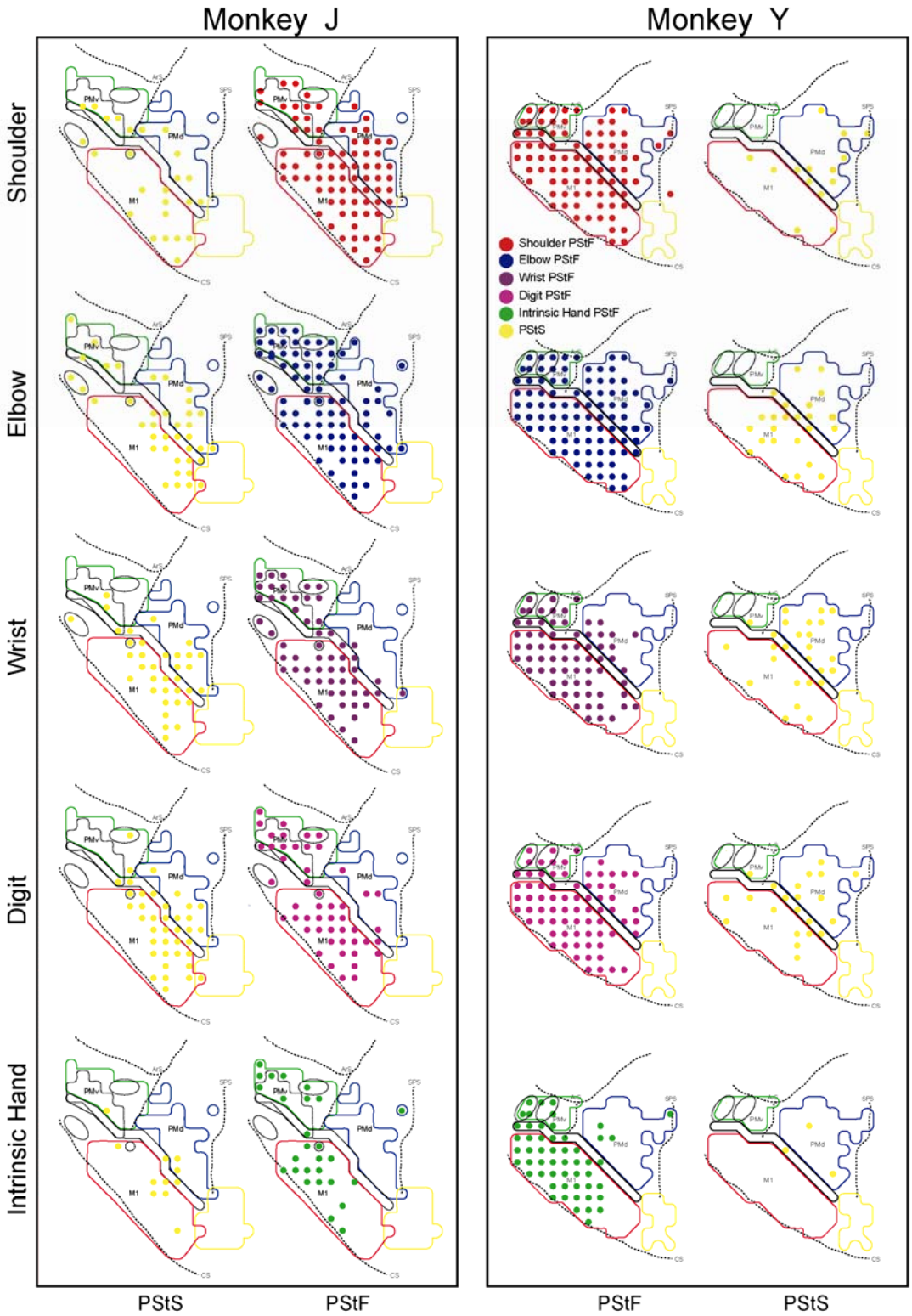
Monkey J
Monkey Y
Shoulder
Elbow
Wrist
Digit
Intrinsic Hand
Shoulder PStF
Elbow PStF
Wrist PStF
Digit PStF
Intrinsic Hand PStF
PStS
PStS
PStF
PStF
PStS

Figure 11. Output maps showing the representation of proximal and distal muscles for PMd, PMv and M1 in two monkeys based on poststimulus effects (PStEs). A) Sites where facilitation and suppression effects were obtained in proximal and distal joints. B) Sites where only proximal or distal effects were present. Red dots correspond to facilitation of proximal muscles (shoulder & elbow); green dots correspond to facilitation of distal muscles (wrist, digit & intrinsic hand muscles); yellow dots correspond to suppression effects. The outlined regions in the background are the boundaries of PMd, PMv and M1 based on PStEs (Figure 1).

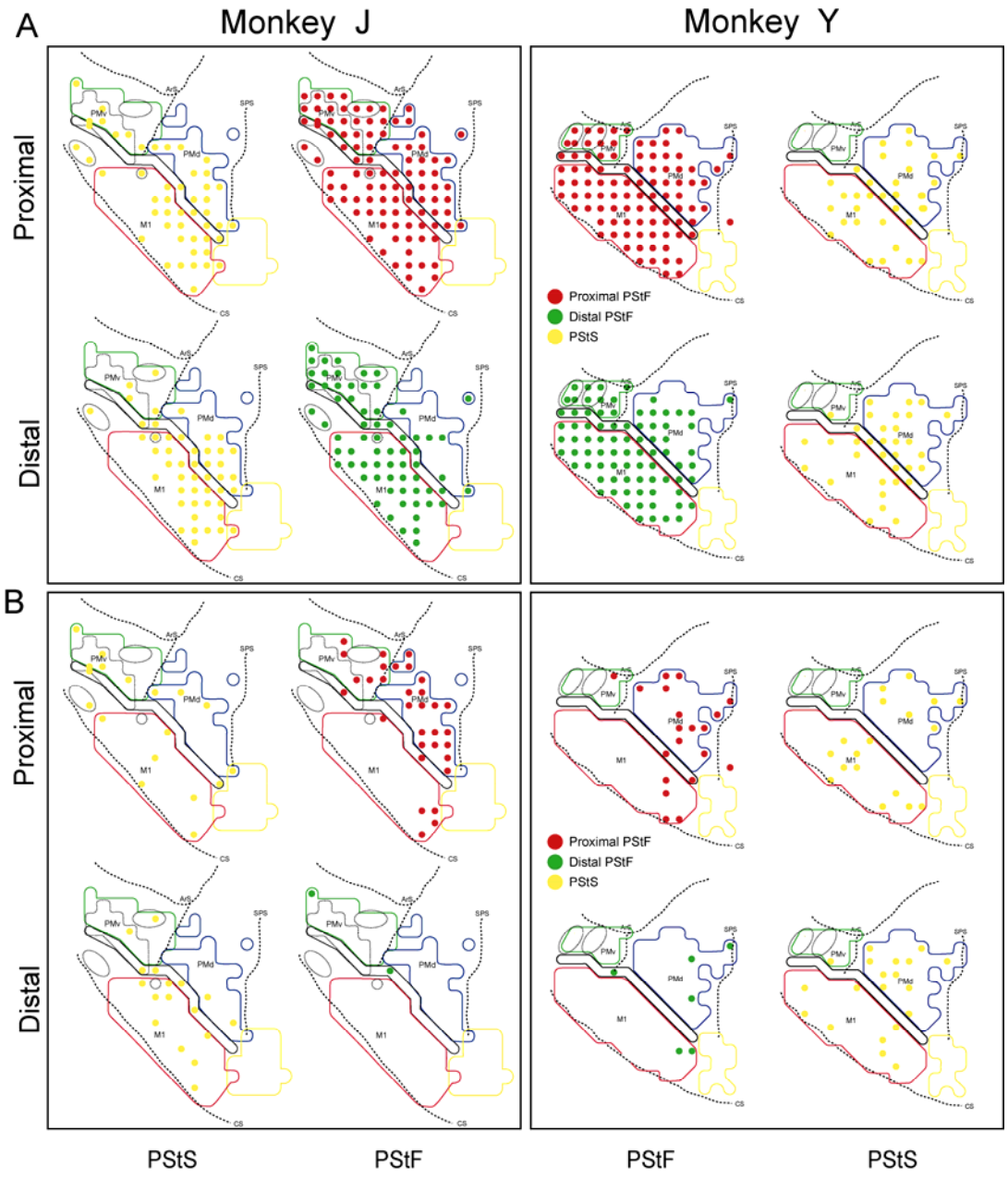
A
Monkey J
Monkey Y
Proximal
Distal
Proximal PStF
Distal PStF
PStS
B
Proximal
Distal
Proximal PStF
Distal PStF
PStS
PStS
PStF
PStF
PStS

Figure 12. Individual muscle representations for monkey J based on PStF and PStS effects obtained from PMd, PMv and M1. Red dots correspond to facilitation of shoulder muscles; blue dots correspond to facilitation of elbow muscles; purple dots correspond to facilitation of wrist muscles; pink dots correspond to facilitation of digit muscles; green dots correspond to facilitation of intrinsic hand muscles; yellow dots depict inhibitory effects. The pink squares in the FDS map came from sites recorded with an EMG implant that showed 25% cross-talk with FCR and PL. Although these sites were not included in our quantitative analysis, we show them here because FDS accounted for most of the EMG signal. The outlined regions in the background are the boundaries of PMd, PMv and M1 based on PStEs (Figure 1).

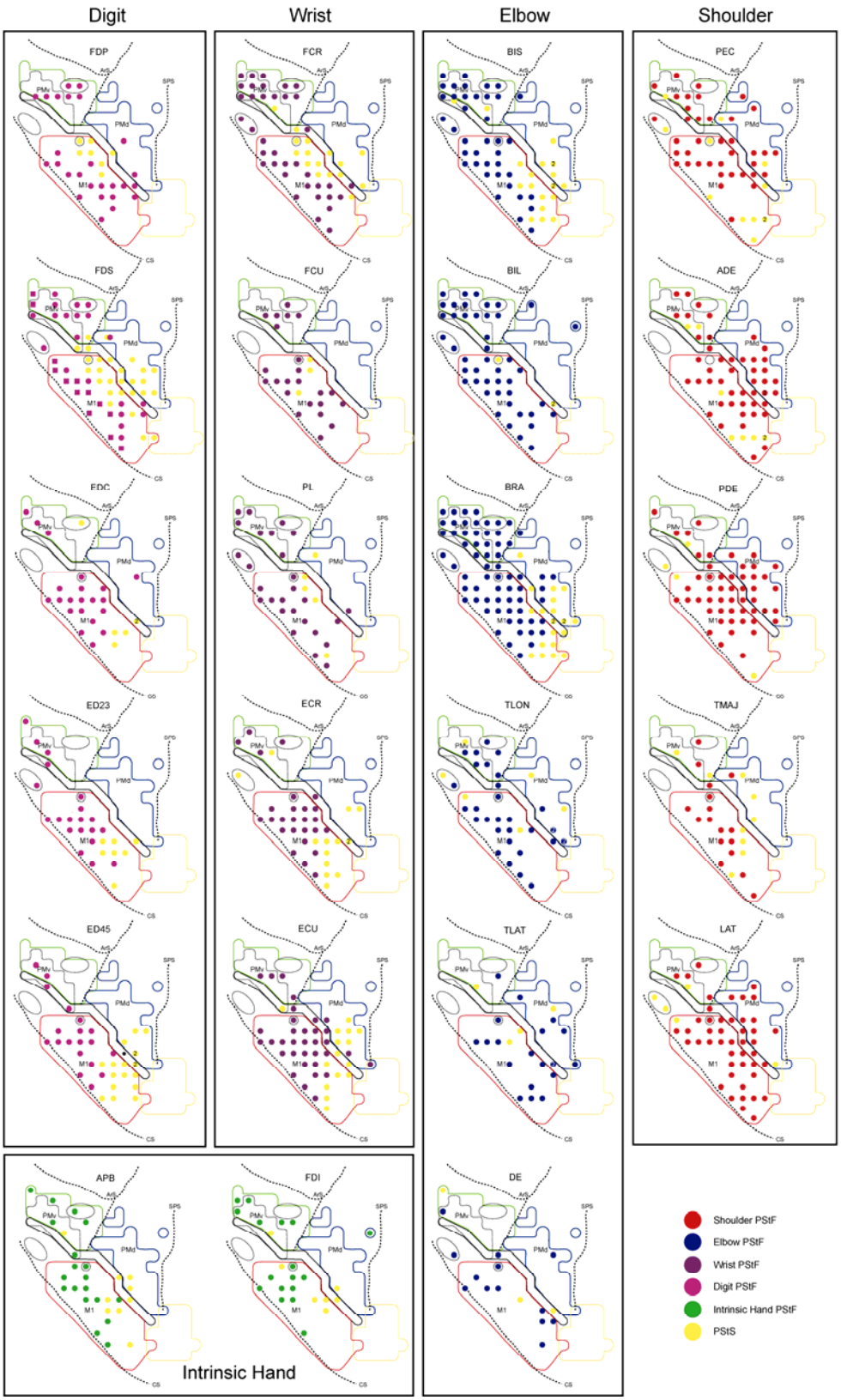
Digit
Wrist
Elbow
Shoulder
FDP
FCR
BIS
PEC
FDS
FCU
BIL
ADE
EDC
PL
BRA
PDE
ED23
ECR
TLON
TMAJ
ED45
ECU
TLAT
LAT
APB
FDI
DE
Intrinsic Hand
Shoulder PStF
Elbow PStF
Wrist PStF
Digit PStF
Intrinsic Hand PStF
PStS

Figure 13. Individual muscle representations for monkey Y based on PStF and PStS effects obtained from PMd, PMv and M1. Red dots correspond to facilitation of shoulder muscles; blue dots correspond to facilitation of elbow muscles; purple dots correspond to facilitation of wrist muscles; pink dots correspond to facilitation of digit muscles; green dots correspond to facilitation of intrinsic hand muscles; yellow dots depict inhibitory effects. The outlined regions in the background are the boundaries of PMd, PMv and M1 based on PStEs (Figure 1).

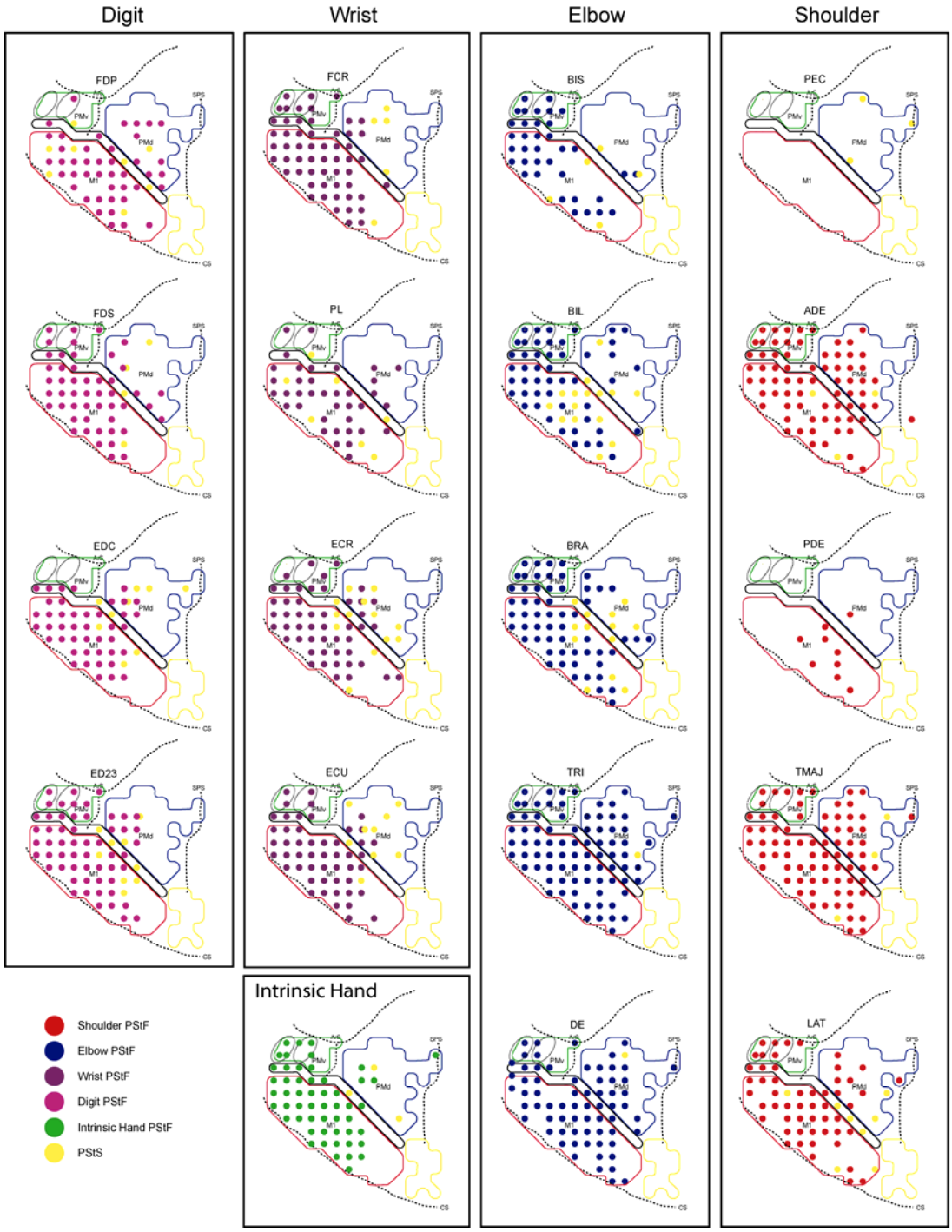
Digit
Wrist
Elbow
Shoulder
FDP
FCR
BIS
PEC
FDS
PL
BIL
ADE
EDC
ECR
BRA
PDE
ED23
ECU
TRI
TMAJ
Intrinsic Hand
DE
LAT
PMv
PMd
M1
SPS
CS
Shoulder PStF
Elbow PStF
Wrist PStF
Digit PStF
Intrinsic Hand PStF
PStS

REFERENCES

Asanuma H, Rosen I (1972) Functional role of afferent inputs to the monkey motor cortex. Brain Res 40:3-5.

Boudrias MH, Belhaj-Saif A, Park MC, Cheney PD (2006) Contrasting properties of motor output from the supplementary motor area and primary motor cortex in rhesus macaques. Cereb Cortex 16:632-638.

Brodmann K (1909) *Vergleichende Lokalisationslehre der Grosshirnrinde*. Leipzig, Germany Barth.

Cerri G, Shimazu H, Maier MA, Lemon RN (2003) Facilitation from ventral premotor cortex of primary motor cortex outputs to macaque hand muscles. J Neurophysiol 90:832-842.

Cheney PD, Fetz EE (1980) Functional classes of primate corticomotoneuronal cells and their relation to active force. J Neurophysiol 44:773-791.

Dancause N, Barbay S, Frost SB, Plautz EJ, Stowe AM, Friel KM, Nudo RJ (2006) Ipsilateral connections of the ventral premotor cortex in a new world primate. J Comp Neurol 495:374-390.

Davare M, Andres M, Cosnard G, Thonnard JL, Olivier E (2006) Dissociating the role of ventral and dorsal premotor cortex in precision grasping. J Neurosci 26:2260-2268.

Dum RP, Strick PL (1991) The origin of corticospinal projections from the premotor areas in the frontal lobe. J Neurosci 11:667-689.

Dum RP, Strick PL (2005) Frontal lobe inputs to the digit representations of the motor areas on the lateral surface of the hemisphere. J Neurosci 25:1375-1386.

Galea MP, Darian-Smith I (1994) Multiple corticospinal neuron populations in the macaque monkey are specified by their unique cortical origins, spinal terminations, and connections. Cereb Cortex 4:166-194.

Gentilucci M, Fogassi L, Luppino G, Matelli M, Camarda R, Rizzolatti G (1988) Functional organization of inferior area 6 in the macaque monkey. I. Somatotopy and the control of proximal movements. Exp Brain Res 71:475-490.

Godschalk M, Lemon RN, Kuypers HG, Ronday HK (1984) Cortical afferents and efferents of monkey postarcuate area: an anatomical and electrophysiological study. Exp Brain Res 56:410-424.

Godschalk M, Mitz AR, van Duin B, van der Burg H (1995) Somatotopy of monkey premotor cortex examined with microstimulation. Neurosci Res 23:269-279.

Graziano MS, Taylor CS, Moore T (2002) Complex movements evoked by microstimulation of precentral cortex. Neuron 34:841-851.

He SQ, Dum RP, Strick PL (1993) Topographic organization of corticospinal projections from the frontal lobe: motor areas on the lateral surface of the hemisphere. J Neurosci 13:952-980.

He SQ, Dum RP, Strick PL (1995) Topographic organization of corticospinal projections from the frontal lobe: motor areas on the medial surface of the hemisphere. J Neurosci 15:3284-3306.

Hoshi E, Tanji J (2006) Differential involvement of neurons in the dorsal and ventral premotor cortex during processing of visual signals for action planning. J Neurophysiol 95:3596-3616.

Jeannerod M, Arbib MA, Rizzolatti G, Sakata H (1995) Grasping objects: the cortical mechanisms of visuomotor transformation. Trends Neurosci 18:314-320.

Kurata K, Hoffman DS (1994) Differential effects of muscimol microinjection into dorsal and ventral aspects of the premotor cortex of monkeys. J Neurophysiol 71:1151-1164.

Kuypers HG, Brinkman J (1970) Precentral projections to different parts of the spinal intermediate zone in therhesus monkey. Brain Res 24:29-48.

Luppino G, Rizzolatti G (2000) The Organization of the Frontal Motor Cortex. News Physiol Sci 15:219-224.

Maier MA, Armand J, Kirkwood PA, Yang HW, Davis JN, Lemon RN (2002) Differences in the corticospinal projection from primary motor cortex and supplementary motor area to macaque upper limb motoneurons: an anatomical and electrophysiological study. Cereb Cortex 12:281-296.

Muakkassa KF, Strick PL (1979) Frontal lobe inputs to primate motor cortex: evidence for four somatotopically organized 'premotor' areas. Brain Res 177:176-182.

Park MC, Belhaj-Saif A, Cheney PD (2000) Chronic recording of EMG activity from large numbers of forelimb muscles in awake macaque monkeys. J Neurosci Methods 96:153-160.

Park MC, Belhaj-Saif A, Cheney PD (2004) Properties of primary motor cortex output to forelimb muscles in rhesus macaques. J Neurophysiol 92:2968-2984.

Park MC, Belhaj-Saif A, Gordon M, Cheney PD (2001) Consistent features in the forelimb representation of primary motor cortex in rhesus macaques. J Neurosci 21:2784-2792.

Porter R, Lemon RN (1993) Corticospinal function and voluntary movement. Oxford: Clarendon Press.

Raos V, Franchi G, Gallese V, Fogassi L (2003) Somatotopic organization of the lateral part of area F2 (dorsal premotor cortex) of the macaque monkey. J Neurophysiol 89:1503-1518.

Raos V, Umilta MA, Gallese V, Fogassi L (2004) Functional properties of grasping-related neurons in the dorsal premotor area F2 of the macaque monkey. J Neurophysiol 92:1990-2002.

Rathelot JA, Strick PL (2006) Muscle representation in the macaque motor cortex: an anatomical perspective. Proc Natl Acad Sci U S A 103:8257-8262.

Rizzolatti G, Luppino G, Matelli M (1998) The organization of the cortical motor system: new concepts. Electroencephalogr Clin Neurophysiol 106:283-296.

Shimazu H, Maier MA, Cerri G, Kirkwood PA, Lemon RN (2004) Macaque ventral premotor cortex exerts powerful facilitation of motor cortex outputs to upper limb motoneurons. J Neurosci 24:1200-1211.

Stark E, Asher I, Abeles M (2007) Encoding of reach and grasp by single neurons in premotor cortex is independent of recording site. J Neurophysiol 97:3351-3364.

Tokuno H, Nambu A (2000) Organization of nonprimary motor cortical inputs on pyramidal and nonpyramidal tract neurons of primary motor cortex: An electrophysiological study in the macaque monkey. Cereb Cortex 10:58-68.

Weinrich M, Wise SP (1982) The premotor cortex of the monkey. J Neurosci 2:1329-1345.

Weinrich M, Wise SP, Mauritz KH (1984) A neurophysiological study of the premotor cortex in the rhesus monkey. Brain 107 (Pt 2):385-414.

CHAPTER 5

CONCLUSION

Stimulus-triggered averaging (StTA) of electromyography (EMG) activity was used to map the cortical forelimb representation and characterize the output properties of SMA, CMAd, PMd, PMv, and M1. Poststimulus effects (PStEs) were obtained by applying 60 μA stimuli to motor areas while the monkey performed a reach-to-grasp task. Twenty-four muscles of the forelimb distributed in proximal and distal joints were implanted with EMG electrodes. Motor output to body regions, other than the forelimb (e.g., face, trunk & hindlimb), were identified using repetitive intracortical microstimulation to evoke movements. The output properties from the secondary motor areas and the organization of their forelimb representations were compared to those from M1 to investigate whether their functional properties parallel those of M1 for the generation of voluntary movements.

Our results demonstrate that the corticospinal neurons originating from secondary motor areas have vastly weaker effects on muscle activity, 7 to 10-fold less, when compared to the powerful effects produced by M1 corticospinal neurons (Figure 1). Additionally, the facilitation effects from SMA, CMAd, PMd and PMv do not show an increase in magnitude for each muscle group, going from the most proximal to the most distal muscles, as occurs for M1 (Park *et al*., 2004). Moreover, our results reveal that PStEs from SMA, CMAd, PMd, and PMV have longer latencies (2 to 12 ms) than those from M1, suggesting a less direct coupling on the motoneurons and/or

the presence of additional synapses in the anatomical pathway for their actions on motoneurons (Figure 3).

Our results also show that the forelimb representations of proximal and distal muscles in SMA, CMAd, PMd, and PMv are not as discretely organized as that for M1 (Park *et al*., 2001). Specific features are found for each of the motor areas: 1) facilitation effects from SMA and CMAd are largely distributed to distal muscles; 2) latencies of PStEs effects from CMAd and SMA are longer and show a broader distribution of facilitation and suppression effects than those observed for PMv and PMd; 3) proximal muscles area more prominently represented in PMd and PMv; 4) PMv has the strongest magnitude of effects among all the secondary motor areas, particularly for the elbow muscles; 5) segregated areas producing suppression effects were found along the medial portion of PMd and adjacent M1 ; 6) the transition of PStEs, in moving from sites in M1 toward sites in PMd, show a gradual decrease in the magnitude and a gradual increase in the latency; and 7) the changes in magnitude and latency of PStEs from M1 to PMd correlate with changes in the number of large pyramidal cells. Our findings also demonstrate patterns of preferential muscle activation specific to each motor area, supporting potential unique roles for each area in the production of forelimb movements (Figure 2).

Compared to the secondary motor areas, connections of M1 with other cortical structures are sparse and come from fewer structures (Rizzolatti *et*

al., 1998). In fact, largest fraction of M1 input arises from the secondary motor areas (Muakkassa and Strick, 1979; Luppino *et al*., 1993; Tokuno and Tanji, 1993; Dum and Strick, 2005; Dancause *et al*., 2006b; Dancause *et al*., 2006a). On the other hand, predominant connections of the secondary motor areas arise from more specific functional circuits, suggesting a sensorimotor transformation for action, unique to each area. Along with this view, various inputs communicated to the secondary motor areas, including visual and somatosensory information, are used to coordinate output at the level of M1 (Figure 1). The effects from PMv on muscular activity are thought to be mainly achieved through this mechanism as its shows many characteristics consistent with a role in coordinating motor output from M1 for accurate visual grasping of objects (Matelli *et al*., 1998; Cerri *et al*., 2003; Shimazu *et al*., 2004; Dum and Strick, 2005; Dancause *et al*., 2006a). PMv shows preferential activation of flexor muscles in elbow, wrist, digit and intrinsic hand muscles. Moreover, it receives strong visual inputs from parietal cortices and it has one of the largest projections of cortico-cortical fibers to M1 among all the secondary motor areas.

The output properties of the secondary motor areas reported in our studies, including PStEs with longer latencies and vastly weaker magnitudes in comparison to those from M1, raise doubts about a prominent role of their corticospinal neurons in the direct control of forelimb motoneurons. Our results suggest that the effects of corticospinal neurons in PMd, SMA and

CMAd are achieved more indirectly on muscular activity, most likely through connections to the intermediate zone of the spinal cord, where they may be involved in modulating the excitability of the motoneurons through connections with spinal interneurons (Figure 3) (Kuypers and Brinkman, 1970; Dum and Strick, 1996, 2002; Maier *et al*., 2002; Rathelot and Strick, 2006). In contrast, M1 contains 79% of the total number of the large corticospinal neurons originating from the frontal lobe. These neurons were shown to be, almost exclusively, the ones making direct monosynaptic linkages to digit motoneurons (Dum and Strick, 1991; Rathelot and Strick, 2006).

The contribution of the secondary motor areas to recovery of function following stroke has been stressed in a variety of studies. After an M1 lesion, extensive reorganization of ipsilesional PMv has been demonstrated in squirrel monkeys, with the enlargement of the hand area and the appearance of new connections with spared pools on corticospinal neurons in the somatosensory cortex (Frost *et al*., 2003; Dancause *et al*., 2005). A transcranial magnetic stimulation (TMS) study inducing temporary disruption of PMd reported slowed reaction-time of finger movements in the affected hand of stroke patients compared to control (Johansen-Berg *et al*., 2002). The slowing of movements with ipsilateral PMd inactivation was correlated with the degree of motor impairment in the patients. Imaging studies have further supported this observation with reports that the secondary motor areas show

greater activation in both hemispheres after a stroke (Ward and Cohen, 2004). The increased movement-related activation of the secondary motor areas was shown to be modulated with the integrity of the corticospinal system; the patients with greater impairment showing greater activation of the secondary motor areas (Ward *et al*., 2006). Thus, reorganization and/or shifts in the activation of the secondary motor areas suggest that they have taken on some of the movement execution properties of M1.

The extent to which movement-related increased activation of secondary motor areas occurring after stroke contributes to motor recovery is still not fully understood. It could reflect an attempt to generate greater motor output from residual M1 corticospinal neurons through their cortico-cortical connections. Additionally, it could be the result of a greater involvement of the corticospinal neurons of secondary cortical areas in the preparation and modulation of intrinsic spinal circuitry, resulting in greater efficiency in driving the motoneurons to their threshold level (Prut and Fetz, 1999; Bizzi *et al*., 2000). In turn, this could increase the firing probability of motoneurons and potentially, indirectly, increase the gain of motor output of spared M1 corticospinal neurons. Motor-related over-activation of the secondary motor areas may also reflect an increased role of corticospinal neurons in these areas, especially those making direct synaptic connections with motoneurons (Dum and Strick, 1996; Rouiller *et al*., 1996). A variety of neuronal plastic events have been shown to occur post-infarct including dendritic

arborizations, formation of new synapses, axonal sprouting, and increased spine densities (Nudo, 2003). The extent to which plastic events take place during motor recovery will require further research but it strongly suggests that intact secondary cortical motor areas undergo adaptive changes to compensate for damaged or disconnected motor regions.

In conclusion, understanding the contribution of the secondary motor areas to the control of muscle activity is potentially highly relevant to enhancing motor recovery in patients suffering from brain injury. The advances of many therapeutic approaches including neuroprosthetic devices, pharmaceutical tools, electrophysiological treatment and specific rehabilitating physical programs targeting the restoration of motor skills specific to the roles played by the spared motor areas, will bring the concept of optimization of motor recovery closer to reality. Our results confirm that corticospinal neurons from the secondary motor areas are poised to contribute to the production of forelimb movements. Furthermore, the studies mentioned above suggest that after stroke, they undergo plastic changes that in part, take over the major roles played by M1 corticospinal neurons in motor execution. The extent to which the properties of secondary cortical motor areas reported in this study might change with injury to primary motor cortex remains for future investigation.

Figure 1. Resume of poststimulus effects recorded in SMA, CMAd, PMd, PMv & M1. A) Latencies and magnitudes of PStF effects. B) Latencies and magnitudes of PStS effects. Magnitudes are expressed in peak percentage increase (ppi) above baseline for PStF effects and peak percentage decrease (ppd) below baseline for PStS effects. The bars represent the standard deviations.

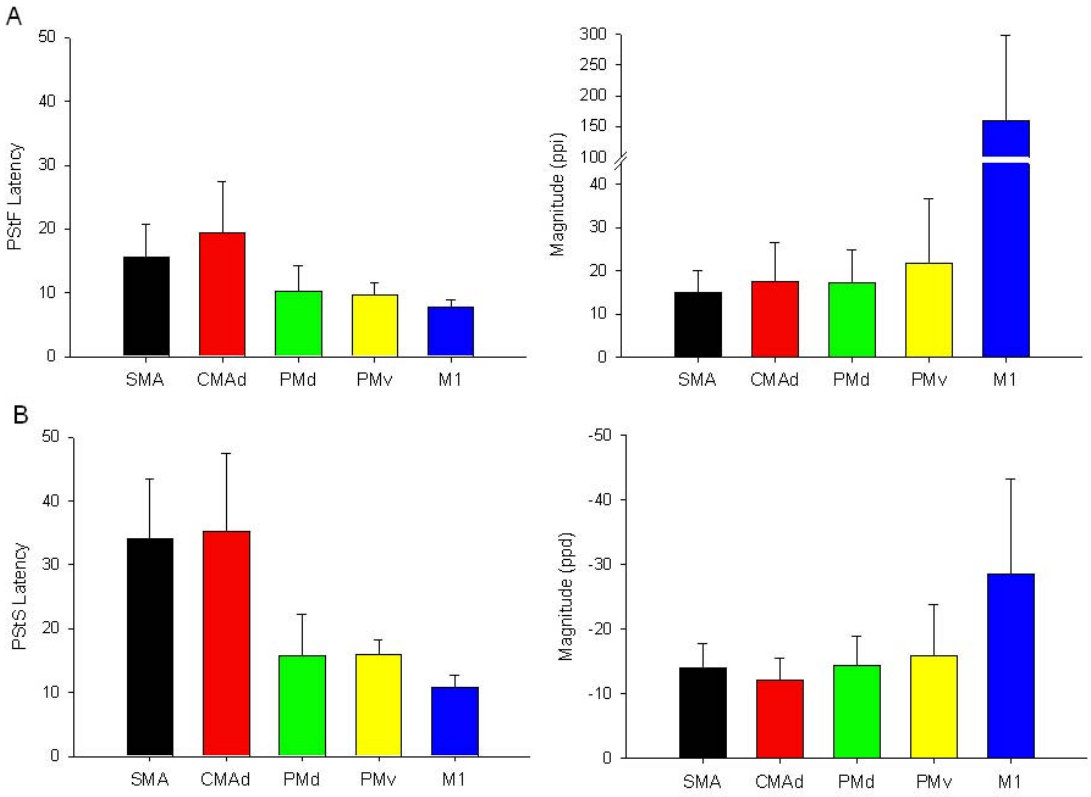
A
PStF Latency
50
40
30
20
10
0
SMA
CMAd
PMd
PMv
M1
Magnitude (ppi)
300
250
200
150
100
40
30
20
10
0
SMA
CMAd
PMd
PMv
M1
B
PStS Latency
50
40
30
20
10
0
SMA
CMAd
PMd
PMv
M1
Magnitude (ppd)
-50
-40
-30
-20
-10
0
SMA
CMAd
PMd
PMv
M1

Figure 2. Distribution of PStF and PStF effects in proximal and distal joints for SMA, CMAd, PMd, PMv & M1. The bars are expressed in percentage (%).

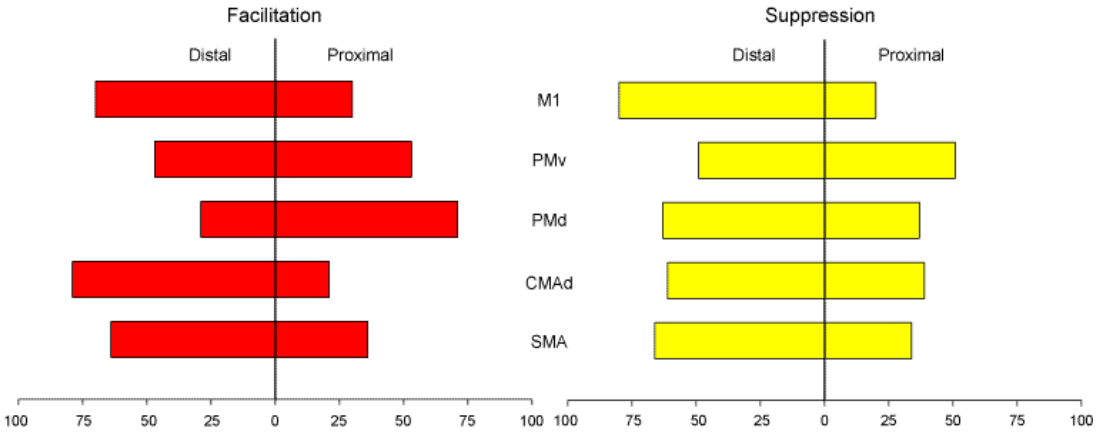
Facilitation
Distal
Proximal
Suppression
Distal
Proximal
M1
PMv
PMd
CMAd
SMA
100
75
50
25
0
25
50
75
100
100
75
50
25
0
25
50
75
100

Figure 3. Pathways by which the motor areas can modulate muscle activity. A) Indirect pathway for PMd and SMA (and CMAd, not shown) corticospinal neurons through an interneuron in the spinal cord and/or cortico-cortical projections to M1. B) Direct pathway for M1 corticospinal neurons by a monosynaptical connection on a motoneuron. C) Indirect pathway for PMv neurons by cortico-cortical projections on M1 corticospinal neurons.

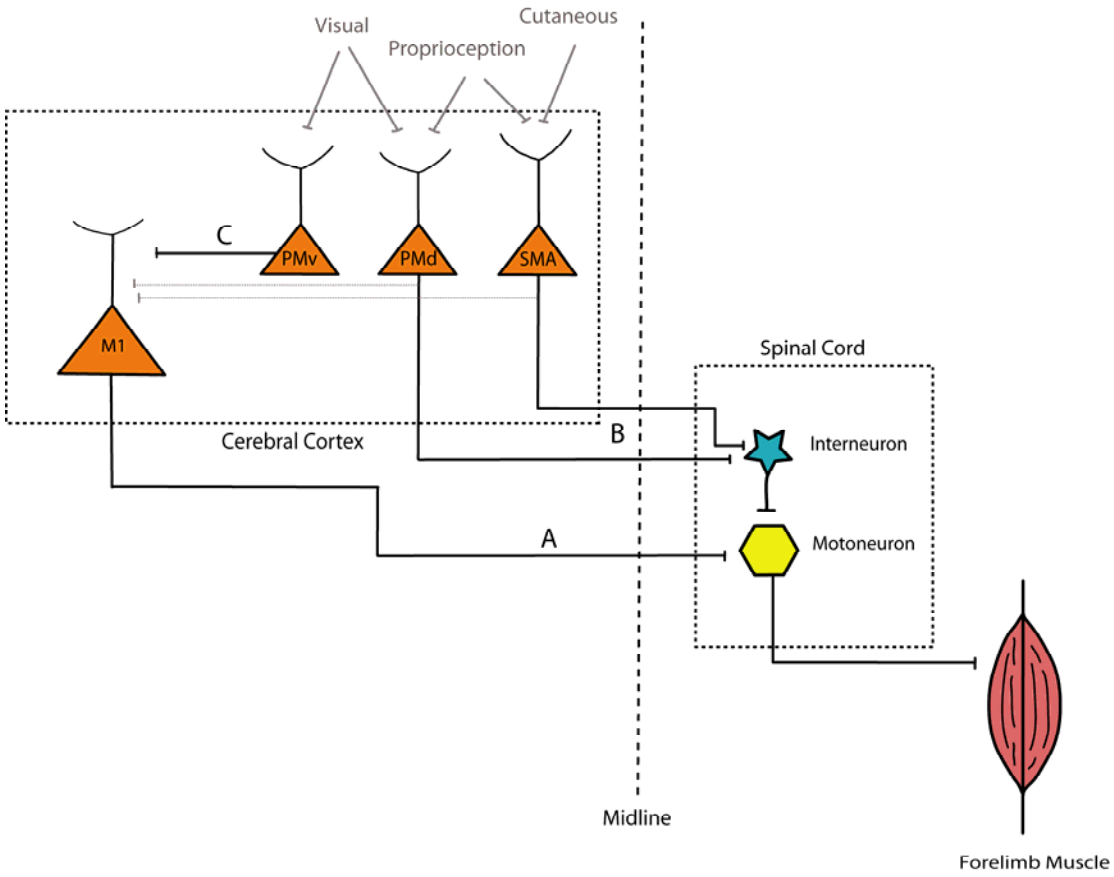
Visual
Proprioception
Cutaneous
C
PMv
PMd
SMA
M1
Cerebral Cortex
B
Spinal Cord
Interneuron
Motoneuron
A
Midline
Forelimb Muscle

REFERENCES

Bizzi E, Tresch MC, Saltiel P, d'Avella A (2000) New perspectives on spinal motor systems. Nat Rev Neurosci 1:101-108.

Cerri G, Shimazu H, Maier MA, Lemon RN (2003) Facilitation from ventral premotor cortex of primary motor cortex outputs to macaque hand muscles. J Neurophysiol 90:832-842.

Dancause N, Barbay S, Frost SB, Plautz EJ, Stowe AM, Friel KM, Nudo RJ (2006a) Ipsilateral connections of the ventral premotor cortex in a new world primate. J Comp Neurol 495:374-390.

Dancause N, Barbay S, Frost SB, Plautz EJ, Chen D, Zoubina EV, Stowe AM, Nudo RJ (2005) Extensive cortical rewiring after brain injury. J Neurosci 25:10167-10179.

Dancause N, Barbay S, Frost SB, Plautz EJ, Popescu M, Dixon PM, Stowe AM, Friel KM, Nudo RJ (2006b) Topographically divergent and convergent connectivity between premotor and primary motor cortex. Cereb Cortex 16:1057-1068.

Dum RP, Strick PL (1991) The origin of corticospinal projections from the premotor areas in the frontal lobe. J Neurosci 11:667-689.

Dum RP, Strick PL (1996) Spinal cord terminations of the medial wall motor areas in macaque monkeys. J Neurosci 16:6513-6525.

Dum RP, Strick PL (2002) Motor areas in the frontal lobe of the primate. Physiol Behav 77:677-682.

Dum RP, Strick PL (2005) Frontal lobe inputs to the digit representations of the motor areas on the lateral surface of the hemisphere. J Neurosci 25:1375-1386.

Frost SB, Barbay S, Friel KM, Plautz EJ, Nudo RJ (2003) Reorganization of remote cortical regions after ischemic brain injury: a potential substrate for stroke recovery. J Neurophysiol 89:3205-3214.

Johansen-Berg H, Rushworth MF, Bogdanovic MD, Kischka U, Wimalaratna S, Matthews PM (2002) The role of ipsilateral premotor cortex in hand movement after stroke. Proc Natl Acad Sci U S A 99:14518-14523.

Kuypers HG, Brinkman J (1970) Precentral projections to different parts of the spinal intermediate zone in the rhesus monkey. Brain Res 24:29-48.

Luppino G, Matelli M, Camarda R, Rizzolatti G (1993) Cortico-cortical connections of area F3 (SMA-proper) and area F6 (pre-SMA) in the macaque monkey. J Comp Neurol 338:114-140.

Maier MA, Armand J, Kirkwood PA, Yang HW, Davis JN, Lemon RN (2002) Differences in the corticospinal projection from primary motor cortex and supplementary motor area to macaque upper limb motoneurons: an anatomical and electrophysiological study. Cereb Cortex 12:281-296.

Matelli M, Govoni P, Galletti C, Kutz DF, Luppino G (1998) Superior area 6 afferents from the superior parietal lobule in the macaque monkey. J Comp Neurol 402:327-352.

Muakkassa KF, Strick PL (1979) Frontal lobe inputs to primate motor cortex: evidence for four somatotopically organized 'premotor' areas. Brain Res 177:176-182.

Nudo RJ (2003) Functional and structural plasticity in motor cortex: implications for stroke recovery. Phys Med Rehabil Clin N Am 14:S57-76.

Park MC, Belhaj-Saif A, Cheney PD (2004) Properties of primary motor cortex output to forelimb muscles in rhesus macaques. J Neurophysiol 92:2968-2984.

Park MC, Belhaj-Saif A, Gordon M, Cheney PD (2001) Consistent features in the forelimb representation of primary motor cortex in rhesus macaques. J Neurosci 21:2784-2792.

Porter R, Lemon RN (1993) Corticospinal function and voluntary movement. Oxford: Clarendon Press.

Prut Y, Fetz EE (1999) Primate spinal interneurons show pre-movement instructed delay activity. Nature 401:590-594.

Rathelot JA, Strick PL (2006) Muscle representation in the macaque motor cortex: an anatomical perspective. Proc Natl Acad Sci U S A 103:8257-8262.

Rizzolatti G, Luppino G, Matelli M (1998) The organization of the cortical motor system: new concepts. Electroencephalogr Clin Neurophysiol 106:283-296.

Rouiller EM, Moret V, Tanne J, Boussaoud D (1996) Evidence for direct connections between the hand region of the supplementary motor area and cervical motoneurons in the macaque monkey. Eur J Neurosci 8:1055-1059.

Shimazu H, Maier MA, Cerri G, Kirkwood PA, Lemon RN (2004) Macaque ventral premotor cortex exerts powerful facilitation of motor cortex outputs to upper limb motoneurons. J Neurosci 24:1200-1211.

Tokuno H, Tanji J (1993) Input organization of distal and proximal forelimb areas in the monkey primary motor cortex: a retrograde double labeling study. J Comp Neurol 333:199-209.

Ward NS, Cohen LG (2004) Mechanisms underlying recovery of motor function after stroke. Arch Neurol 61:1844-1848.

Ward NS, Newton JM, Swayne OB, Lee L, Thompson AJ, Greenwood RJ, Rothwell JC, Frackowiak RS (2006) Motor system activation after subcortical stroke depends on corticospinal system integrity. Brain 129:809-819.